



# HHS Public Access

Author manuscript

*ACS Nano*. Author manuscript; available in PMC 2022 September 29.

Published in final edited form as:

*ACS Nano*. 2021 February 23; 15(2): 2099–2142. doi:10.1021/acsnano.0c09382.

## Hybrid Nanosystems for Biomedical Applications

Joshua Seaberg<sup>1,#</sup>, Hossein Montazerian<sup>3,4,5,#</sup>, Md Nazir Hossen<sup>1,2,#</sup>, Resham Bhattacharya<sup>6</sup>, Ali Khademhosseini<sup>5,\*</sup>, Priyabrata Mukherjee<sup>1,2,\*</sup>

<sup>1</sup>Department of Pathology, University of Oklahoma Health Science Center, Oklahoma City, Oklahoma 73104, USA.

<sup>2</sup>Peggy and Charles Stephenson Cancer Center, University of Oklahoma Health Sciences Center, Oklahoma City, Oklahoma 73104, USA.

<sup>3</sup>Department of Bioengineering, University of California-Los Angeles, Los Angeles, CA 90095, USA

<sup>4</sup>Center for Minimally Invasive Therapeutics (C-MIT), University of California-Los Angeles, Los Angeles, CA 90095, USA

<sup>5</sup>Terasaki Institute for Biomedical Innovation (TIBI), Los Angeles, CA 90024, USA

<sup>6</sup>Department of Obstetrics and Gynecology, University of Oklahoma Health Science Center, Oklahoma City, OK 73104, USA

### Abstract

Inorganic/organic hybrid nanosystems have been increasingly developed for their versatility and efficacy at overcoming obstacles not readily surmounted by non-hybridized counterparts. Currently, hybrid nanosystems are implemented for gene therapy, drug delivery, and phototherapy in addition to tissue regeneration, vaccines, antibacterials, biomolecule detection, imaging probes, and theranostics. Though diverse, these nanosystems can be classified according to foundational inorganic/organic components, accessory moieties, and architecture of hybridization. Within this review, we begin by providing a historical context for the development of biomedical hybrid nanosystems before describing the properties, synthesis, and characterization of their component building blocks. Afterward, we introduce the architectures of hybridization and highlight recent biomedical nanosystem developments by area of application, emphasizing hybrids of distinctive utility and innovation. Finally, we draw attention to ongoing clinical trials before recapping our discussion of hybrid nanosystems and providing a perspective on the future of the field.

### Graphical Abstract

---

\*Correspondence to: Priyabrata Mukherjee, Professor of Pathology, Priyabrata-Mukherjee@ouhsc.edu; Phone: 405-271-1133; Ali Khademhosseini, Professor and Director, Khademh@terasaki.org.

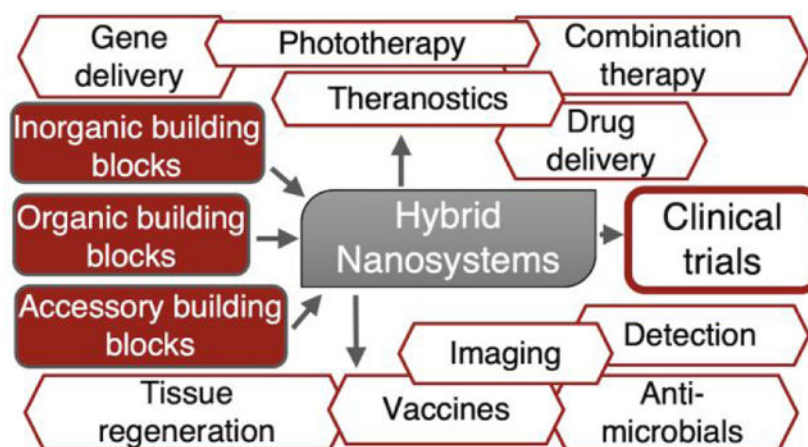
#Equal contribution

Author contributions

PM conceived the concept for the manuscript. JS and HM compiled and analyzed the literature. JS created the figures. JS, MNH, HM, and PM contributed to discussion and perspectives. JS, MNH, HM, RB, AK, and PM contributed to the editing process.

Competing interests

The authors have no conflict of interest to report.



## Keywords

hybrid nanosystem; hybrid nanoparticle; nanomaterials; gene therapy; drug delivery; phototherapy; theranostics; biomolecular sensors; inorganic/organic hybridization; biomedical nanosystems

Inorganic/organic hybrid nanosystems present attractive solutions to current challenges in drug and gene delivery, tissue regeneration, phototherapy, vaccine development, biosensing and detection, and theranostics. Although the development of such nanosystems has occurred only recently, the term “hybrid” appeared in the English lexicon in the 17<sup>th</sup> Century and is derived from the Latin “hybrida,” the offspring of a domesticated sow and a wild boar. The scientific study of hybridization exploded when Gregor Mendel published *Experiments in Plant Hybridization* (1865), in which he described how progeny inherit and express characteristics of their progenitors.<sup>1</sup> The term shed its biological restraints over time and was increasingly used to describe something derived from two or more distinct sources. Under this broader definition, hybrid systems stepped into the public spotlight in 1997 with the release of the Toyota Prius hybrid electric vehicle.<sup>2</sup>

The earliest mention of a hybrid nanosystem in the biomedical field occurred the same year, with Elghanian *et al.* publishing a colorimetric polynucleotide detection system using nucleotide-hybridized gold nanoparticles (AuNPs) in *Science*.<sup>3</sup> True hybrid nanosystems containing inorganic and organic structural components were introduced in 1998 when Caruso *et al.* reported a synthesis of nanoscale silica-polymer hybrid spheres.<sup>4</sup> Around the turn of the 21<sup>st</sup> Century, the development of hybrid nanosystems expanded greatly through the hybridization of silica with micelles,<sup>5</sup> liposomes,<sup>6</sup> and polymers<sup>7</sup> along with the introduction of polymer-functionalized metallic nanoparticles.<sup>8, 9</sup> By 2003, interest in these systems was rapidly growing, and review articles started to appear.<sup>10</sup> This growth has continued steadily over the past two decades, with the search “hybrid nanoparticle” producing nearly 2,000 matches in the National Library of Medicine last year in comparison to only 42 in 2003 (Figure 1).

Here, we give an overview of recent reports of inorganic/organic hybrid nanosystems in the biomedical field. As it was impossible to include all relevant contributions within this

article, we instead report findings of diverse applications and distinct utility and reference reviews for more general topics. Furthermore, we focus on “true” hybrid nanosystems incorporating organics and inorganics as structural components rather than as therapeutics or accessory moieties. As such, we hope that this paper may provide broad information on biomedical hybrid nanosystems that the interested reader can utilize as a starting point for a more thorough investigation.

We start by introducing the primary inorganic and organic building blocks utilized by hybrid nanosystem architects, with emphasis placed on biomedically-relevant properties, synthesis, and characterization. Once each building block has been discussed, standard architectures are presented to provide a framework for understanding hybrid nanosystem design. Afterward, we present select hybrid nanosystems by application, starting with gene and drug delivery before discussing phototherapy, tissue regeneration, antimicrobials, vaccine development, detection and imaging, and theranostics. Finally, we mention the active clinical trials utilizing hybrid nanosystems before concluding with a discussion of the state of the field and providing a perspective on the continued development of hybrid nanosystems.

## Characterization of hybrid nanosystems

Hybrid nanosystems are composed of inorganic and organic building blocks, each displaying distinct properties that determine practical applications and characterization methods (Figure 2). Widely-utilized inorganic building blocks include metals such as gold and iron oxide nanoparticles (AuNPs and IONPs, respectively), inorganic compounds including zinc oxide (ZnO) nanoparticles (ZONPs) and calcium phosphate (CaP) nanoparticles (CPNPs), and porous structures like mesoporous silica nanoparticles (MSNs) and metal-organic frameworks (MOFs). Organic building blocks include polymers and copolymers, lipids, dendrimers, and isolated cell membranes. Carbon derivatives such as graphene oxide (GO), fullerene (C60), carbon nanotubes (CNTs), and graphene quantum dots (GQDs) can display properties similar to both organic and inorganic systems; consequently, we have included carbon-based materials as inorganic building blocks even though they can also function as organic building blocks. From these materials, nearly limitless hybrid nanosystems have been designed to overcome challenges in the biomedical field.

### Inorganic building blocks

**Gold nanoparticles (AuNPs)**—Nanoscale gold is the most frequently-utilized inorganic building block due to its biocompatibility, ease of synthesis, low polydispersity, self-therapeutic properties, and tunable plasmonic properties.<sup>11</sup> Several of these properties are geometry-dependent; consequently, AuNPs,<sup>12</sup> gold nanorods (AuNRs),<sup>13</sup> gold nanoshells (AuNSs),<sup>14, 15</sup> gold nanoclusters (AuNCs),<sup>16</sup> and nanocages<sup>17</sup> are all observed in the literature. Variation of nanoscale gold geometry has been shown to affect its optical properties, the available surface area, and transport properties.<sup>18</sup> Gold nanostructures display self-therapeutic properties to fight cancers, including inhibition of tumoral angiogenesis,<sup>19, 20</sup> inhibition of MAPK-signaling to reverse epithelial-mesenchymal transition in cancer,<sup>21</sup> and alteration of non-viral gene delivery uptake pathways to avoid

lysosomal degradation.<sup>22</sup> Alternatively, nanoscale gold is readily modified by electrostatic interactions or gold-thiol (Au-S) bonds, allowing facile functionalization with a variety of therapeutics, polymers, and targeting ligands.<sup>23</sup> While Au-S bonds are relatively strong (30–40 kJ/mol), the weaker interactions between gold and nucleic acids allow adsorption and release for gene delivery applications.<sup>22</sup> Electrostatic interactions can also facilitate the coating of anionic AuNPs with cationic polymers to promote cellular transfection and provide hybrid systems with simple conjugation chemistries.<sup>24</sup> Through these functionalization techniques, AuNPs can be adapted for use as either a core or surface-adjacent structure in hybrid nanosystems.

The optical properties of gold nanostructures include localized surface plasmon resonance (LSPR), in which incident light induces a collective oscillation in the surface electrons of a nanomaterial.<sup>25</sup> This oscillation can be exploited in several ways: plasmon generation and decay can increase the nanoparticle temperature for hyperthermal therapy, promote electrons to antibonding orbitals for photocatalysis, produce acoustic waves for photoacoustic imaging, or fluoresce by scattering differentially energized photons.<sup>26</sup> LSPR can be tuned *via* geometry variation,<sup>27</sup> *i.e.*, AuNRs may be tuned by varying the aspect ratio, allowing AuNRs to specifically absorb and scatter light within the biological windows for photodynamic/photothermal therapy and photo-triggered therapeutic release.<sup>28–30</sup> Additionally, the size, geometry, and concentration of nanoscale gold alters its absorbance in solution, resulting in color variation.<sup>27</sup> Spectrophotometric characterization has been utilized in biodetection systems by coupling aggregation to the presence of a target molecule in solution.<sup>31,32</sup>

Gold nanostructures have been synthesized through several physical, chemical, and biological methods, though chemical methods are standard for hybrid nanosystems.<sup>33</sup> Chemical synthesis of gold nanostructures requires a source of oxidized gold, a reducing agent, and a capping or stabilizing surfactant to prevent irreversible nanoparticle aggregation; variation in the identity and concentrations of these reagents will affect the size and morphology of the final nanostructure.<sup>34</sup> AuNPs have been synthesized through the reduction of chloroauric acid (HAuCl<sub>4</sub>) with citric acid as a stabilizing and reducing agent where the gold-to-citrate ratio controls nanoparticle size.<sup>35</sup> AuNPs can also be formed through top-down processes such as laser ablation<sup>36</sup> or through “green” syntheses utilizing plant-derived reducing agents.<sup>37</sup> Hollow AuNSs can be synthesized by reducing gold ions on the surface of cobalt nanoparticles while simultaneously oxidizing the core to cobalt oxide.<sup>38</sup> AuNRs can be synthesized from AuNP seeds incubated with silver nitrate (AgNO<sub>3</sub>), while other non-spherical geometries utilized in hybrid nanosystems have been synthesized through seed-growth approaches utilizing sodium borohydride (NaBH<sub>4</sub>) and zwitterionic surfactants,<sup>39</sup> acetic acid and AgNO<sub>3</sub>,<sup>40</sup> and dilute peptide solutions.<sup>16, 29</sup> As such, geometry and synthesis method can be selected on an application-specific basis.

AuNPs can be characterized by several methods. Dynamic light scattering (DLS) and electrophoretic light scattering (ELS) provide information on AuNP size, polydispersity index (PDI), and  $\zeta$ -potential. Scanning electron microscopy (SEM), transmission electron microscopy (TEM), and atomic force microscopy (AFM) show AuNP size, morphology, size distribution, surface properties, and position within a hybrid nanosystem. Fourier transform

infrared (FTIR) and UV-Vis spectroscopy (UV-Vis) measure AuNP optical properties, and surface plasmon spectroscopy allows the characterization of LSPR. Finally, X-ray diffraction (XRD) can describe the structure of the AuNP on an atomic scale and inductively coupled plasma-mass spectrometry (ICP-MS) allows detection of elemental gold at low concentrations.<sup>41</sup> Figure 3 displays geometries and properties of AuNPs in addition to synthesis and characterization techniques. For further reading, we recommend reviews by Yeh *et al.*, Elahi *et al.*, and Dreaden *et al.* on general biomedical applications for AuNPs,<sup>11, 27, 35</sup> Grzelczak *et al.* on shape control in nanoscale gold,<sup>42</sup> Pérez-Juste *et al.* and Cao *et al.* on AuNRs,<sup>43, 44</sup> Amendola *et al.* on AuNP LSPR,<sup>25</sup> and Vines *et al.* on AuNPs in photothermal cancer therapy.<sup>45</sup> Due to the aforementioned characteristics, nanoscale gold is utilized in nearly every biomedical application of hybrid nanosystems.

**Iron oxide nanoparticles (IONPs)**—IONPs are another common inorganic material in hybrid nanosystems. Both forms of IONPs (maghemite ( $\gamma\text{-Fe}_2\text{O}_3$ ) and magnetite ( $\text{Fe}_3\text{O}_4$ )) are attractive in biomedical applications for their biocompatibility and low toxicity.<sup>47</sup> IONPs have been synthesized in many geometries including spheres, hexes, triangular prisms, cubes, stars, rings, clusters, and shells.<sup>48</sup> IONP geometry is related to available surface area, carrying capacity, and interactions with electromagnetic radiation. For example, varying geometries of IONP have shown similar biocompatibility despite varying SA/V ratios, while hollow IONPs can act as drug carriers and IONP rings absorb microwave radiation.<sup>48</sup> Notably, 10–20 nm IONPs exhibit superparamagnetism, making them responsive to an applied magnetic field while otherwise displaying non-magnetic properties.<sup>47</sup> Superparamagnetic IONPs can confer magnetic targeting properties to nanotherapeutics, act as contrast agents for magnetic resonance imaging (MRI), and be utilized for magnetic hyperthermal therapy.<sup>49–51</sup> Biomedical application of IONPs is further expanded by their ability to induce ferroptosis in cancer cells,<sup>52</sup> and additional studies have shown that IONPs exhibit antibacterial activity<sup>53</sup> as well as photoluminescence.<sup>54</sup> As such, this breadth of properties makes IONPs attractive as nanosystem building blocks.

Chemical, physical, and biological methods have been employed in IONP synthesis, with chemical methods being most popular in hybrid nanosystems.<sup>47</sup> IONPs display facile synthesis through basic coprecipitation of iron salts, with variations in particle size being attained through pH control.<sup>50</sup> Alternatively, IONPs can be synthesized through a microemulsion technique in which iron salts combine to form IONPs within a surfactant-stabilized oil and water mixture.<sup>47</sup> Like AuNPs, IONPs are frequently characterized by DLS, ELS, UV-Vis, FTIR, ICP-MS, XRD, and electron microscopy.<sup>55</sup> Ansari *et al.* and Ali *et al.* provide more complete reviews of IONPs for the interested reader.<sup>55, 56</sup> IONPs are the second-most widely employed inorganic building blocks and are used primarily for their superparamagnetic properties.

**Other metallic components**—Other metallic nanoparticles have also been incorporated into hybrid nanosystems for therapeutic effect. Platinum nanoparticles (PtNPs) kill cancer cells through ion leaching,<sup>57</sup> while silver nanoparticles (AgNPs) and copper nanoparticles (CuNPs) are recognized along with PtNPs for their antibacterial properties and are commonly incorporated into systems for treatment or prevention of bacterial infection.<sup>58, 59</sup>

PtNPs exhibit a variety of geometries including spherical, baton, and cubic. They are constructed through chemical processes such as chemical vapor deposition, physical methods including laser ablation, and biological methods utilizing yeast and bacteria.<sup>60</sup> Similarly, AgNPs display distinctive physical and optical properties in addition to strong antimicrobial properties that have been exploited for drug delivery, tissue regeneration, imaging, and diagnostic applications.<sup>61</sup> As with other metallic nanoparticles, AgNPs may be formed *via* top-down methodologies to break down silver (Ag) macrostructures or through bottom-up chemical and biological methods.<sup>61</sup> Finally, CuNPs exhibit properties similar to AgNPs, though their propensity to oxidation makes them less biocompatible than the noble metals.<sup>62</sup> Each of these nanoparticles has been shown to exhibit some form of fluorescence/photoluminescence, plasmonic properties, and catalytic activity. As with the other metallic nanoparticles, PtNPs, AgNPs, and CuNPs are characterized by DLS, ELS, UV-Vis, FTIR, ICP-MS, XRD, SEM, TEM, AFM, and/or x-ray absorption spectroscopy.<sup>60–62</sup> Sim *et al.* and Lee *et al.* provide thorough reviews on AgNPs in biomedical applications,<sup>61, 63</sup> while Jeyaraj *et al.* reviewed the synthesis, characterization, and biomedical use of PtNPs<sup>60</sup> and Al-Hakkani recently published a review of CuNPs of value to the curious reader.<sup>64</sup> These building blocks are less prevalent in the literature than their AuNP and IONP counterparts, but they are commonly utilized in antimicrobial applications along with sporadic use throughout other areas.

**Inorganic compounds**—Several inorganic compounds have been used in hybrid nanosystems. CPNPs exhibit low toxicity and high stability in a range of geometries, including rods, spheres, and needles, and the crystallinity of the structure may be tuned to accommodate specific loading and release profile requirements.<sup>65</sup> Moreover, CPNPs have shown antibacterial effects and fluorescence/photoluminescence in addition to pH-responsive properties for enhanced lysosomal escape.<sup>66, 67</sup> CPNPs are most frequently formed through chemical precipitation processes that can be tuned for use in hybrid nanosystems.<sup>65</sup> For example, therapeutic-loaded CPNPs can be synthesized by coprecipitation from calcium nitrate and diammonium hydrogen phosphate in the presence of a therapeutic.<sup>65, 68</sup> CPNPs can be characterized by DLS, UV-Vis, ICP-MS, XRD, nitrogen adsorption/desorption isotherms, thermogravimetric analysis (TGA), differential scanning calorimetry (DSC), FTIR, and electron microscopy.<sup>65, 69</sup> Though already heavily referenced, the review by Levingstone *et al.* further describes methods for synthesis and characterization of therapeutic CPNPs.<sup>65</sup> CPNPs are most commonly used in gene delivery applications.

Similarly, ZONPs have been employed in biomedical applications for their antibacterial and antifungal activity. Moreover, ZONPs exhibit anti-cancer self-therapeutic properties which have been attributed to the release of zinc ions and the catalytic accumulation of reactive oxygen species (ROS).<sup>70</sup> ZONPs have been synthesized through physical, chemical, and biological mechanisms and demonstrate distinctive optical and semiconducting properties that have led to their use in bioimaging,<sup>71</sup> antimicrobial food packaging,<sup>72</sup> and sunscreen.<sup>71</sup> Furthermore, ZONPs show anti-inflammatory effects that have been harnessed in wound dressings and plasmonic properties that have been optimized for photocatalysis.<sup>73</sup> Wurtzite, which contains zinc and oxygen atoms arranged in tetrahedral formation, is the most stable zinc oxide structure and is consequently the most prevalent form in hybrid nanosystems.<sup>74</sup>

ZONPs can be characterized by DLS, ELS, FTIR, UV-Vis, TEM, SEM, XRD, ICP-MS, TGA, and DSC.<sup>70</sup> Further understanding of ZONPs can be obtained from relevant reviews by Sirelkhatim *et al.*<sup>75</sup> and Jiang, Pi, & Cai.<sup>73</sup> Based on the aforementioned properties, ZONPs find use in several applications, including combination therapy, antimicrobials, detection and imaging, and vaccines.

**Mesoporous nanostructures**—Mesoporous nanostructures are attractive building blocks primarily for their biomolecule adsorption/desorption capabilities.<sup>76</sup> Mesoporous silica has been incorporated into hybrid nanosystems as MSNs or coatings. MSNs introduced in 1968 were noticed for their high surface area and tunable pore size.<sup>77, 78</sup> Current sol-gel synthesis processes utilize polymers and surfactants that are later removed *via* solvent extraction to control pore size and orientation.<sup>79</sup> MSN pore size ranges from 2 to 50 nm and is frequently gated to retain encapsulated therapeutics until a stimulus triggers gate opening.<sup>77, 80</sup> Hollow MSNs are synthesized through soft templating around micelles or by hard templating around the polymer or metallic nanoparticles, with the mesoporous shell conforming to the surface of the degradable template.<sup>79</sup> Mesoporous silica can also coat a core nanoparticle or form a loose outer shell surrounding a cluster of inner core nanoparticles in a “rattle-type” system.<sup>81</sup> MSNs can be characterized by methods similar to other inorganic building blocks, including DLS, ELS, UV-Vis, FTIR, XRD, and TEM. Additional reading on MSN synthesis and advances can be obtained from Wu *et al.* and Narayan *et al.*<sup>77, 79</sup> MSNs are found in hybrid nanosystems throughout the biomedical field, with widespread use in gene/drug delivery and combination therapy as well as in nanovaccines and theranostics.

MOFs form similarly porous structures of metal ions surrounded by organic ligands. Whereas MSNs display few intrinsic therapeutic properties, MOFs can exhibit antibacterial properties along with fluorescence/photoluminescence, pH-responsivity, and catalytic activity. MOFs are regularly synthesized through solvothermal processes featuring a metal salt and organic linker in a poorly volatile solvent, though alternative electrochemical, mechanochemical, and sonochemical processes also exist.<sup>82</sup> Following synthesis, MOFs are activated by removing excess linkers and solvent.<sup>83</sup> Characterization techniques include powder XRD, nitrogen adsorption/desorption, TGA, SEM, ICP-MS, optical emission spectroscopy, nuclear magnetic resonance (NMR), and FTIR, which provide information on the crystallinity, stability, porosity, symmetry, and morphology of MOFs.<sup>82</sup> Zeolitic imidazolate frameworks (ZIFs) are MOFs containing transition metals connected by imidazolate linkers and are attractive for their loading capacity and stimulus-responsive degradation.<sup>84</sup> Moreover, MOFs can acquire additional therapeutic properties by incorporating alternative metal nanoparticles through replacement reactions,<sup>58</sup> and polymer hybridization can improve MOF surface characteristics.<sup>85</sup> Reviews of MOFs by Safaei *et al.*,<sup>83</sup> and Wang, Zheng, & Xie provide content not covered in this overview.<sup>86</sup> MOFs are ubiquitous in hybrid nanosystem applications throughout the biomedical field.

**Nanoclays**—Nanoclays are layered silicates that originate from the clay minerals constituting sedimentary rocks and soils.<sup>87</sup> The general chemical formula of  $(Ca, Na, H)(Al, Mg, Fe, Zn)_2(Si, Al)_4O_{10}(OH)_2$  characterize these clay aluminosilicates.<sup>88</sup> Nanoclays are

primarily formed of the repeated units of alternating octahedral  $\text{AlO}_6$  and tetrahedral  $\text{SiO}_2$  sheets with different  $\text{AlO}_6:\text{SiO}_2$  ratios where the metallic cations are substituted in between the silicate layers.<sup>89</sup> Clay nanomaterials are often available in the form of synthetic and natural platelets that may rearrange structurally to develop few-nanometer-scale nanotubes and nanofibers.<sup>90</sup> The biocompatibility of nanoclays has made them suitable for a wide range of biomedical applications. Among the different nanoclay types, montmorillonite (MMT),<sup>91</sup> Laponite,<sup>92</sup> and whitlockite<sup>93</sup> are some of the most frequently used fillers in biopolymer matrices to enable different functions. Nanoclays such as halloysite have been used as mechanical reinforcements for bone cements in polymer composites. Other examples such as MMT have been served as crosslinking points to endow toughness to hydrogels matrices.<sup>94</sup> Tissue engineering applications have taken advantage of the ability of nanoclays to promote cell adhesion and proliferation. This effect is shown in multiple material compositions, *e.g.*, a gellan/manuka honey-based hydrogel incorporated with MSNs and bentonite clays where the scaffolds supported chondrogenesis and controlled immune response.<sup>95</sup> Nanoclays have been further utilized for immobilizing enzymes particularly in biosensor devices for monitoring biomolecules such as glyphosate.<sup>96</sup> As such, the potential for drug delivery applications have been demonstrated.<sup>97</sup> The antimicrobial protein lysozyme incorporated into the halloysite nanotubes as an example, resulted in poly(lactic acid) (PLA)-based hybrid composites for the delivery of lysozyme.<sup>98</sup> The strong negative charges on the surface of Laponite and its water uptake capability has enabled their use in hemostatic agents for rapid coagulation and control of hemorrhage.<sup>99</sup> Many studies have confirmed promoted wound healing by using nanoclays such as nontronite.<sup>100</sup> The rheological effects of nanoclays in aqueous solutions have opened up their application to injectable shear-thinning biomaterials<sup>101</sup> *e.g.*, for treating aneurysms or delivering biomolecules in the body.<sup>102</sup> Further developments are still in progress as the different aspects of nanoclay-based composites are uncovered.

The natural formation of clay occurs under geologic conditions, most frequently where rocks are in contact with water or air and form sedimentations. Synthetic approaches, however, involve low- and high-temperature techniques through hydrothermal techniques. Nanoclay characterization techniques include but are not limited to powder XRD, small-angle neutron scattering (SANS), TGA, FTIR, DLS, UV-Vis, and TEM.<sup>103</sup> Further readings are available in the literature on synthesis and application of nanoclay-based nanocomposites by Gup *et al.*<sup>104</sup> Rafiee *et al.*<sup>105</sup> have reviewed the mechanical properties of the nanoclay-based nanocomposites. A detailed overview of the nanoclays biomedical applications was also presented by Peña-Parás *et al.*<sup>106</sup> The current trends show that nanoclays hold a tremendous promise for future developments in functional materials.

**Carbon-based materials**—Carbon has been introduced into hybrid nanosystems as GO,<sup>107</sup> GQDs (semiconductor particles <100 nm in diameter),<sup>108</sup> CNTs,<sup>109</sup> C60,<sup>110</sup> and diamond nanocrystals.<sup>111</sup> Carbon building blocks exhibit biocompatibility and are widely utilized in phototheranostics for their tunable photoluminescence<sup>112</sup> and ability to couple with metallic nanoparticles for enhanced imaging contrast.<sup>107, 113</sup> The geometry and conductivity of carbon materials lend them additional functionality for use in biosensors,<sup>114, 115</sup> as exemplified by Lee *et al.*'s nanosystem for DNA detection through



measurement of conductivity changes between AuNPs, iron nanoparticles (FeNPs), and CNTs.<sup>109</sup> As such, nanoscale carbon can confer distinct properties to hybrid nanosystems for diverse applications.

The breadth of existing carbon nanostructures requires an equally-exhaustive set of synthesis and characterization processes. Nanoscale graphene (sheets of sp<sup>2</sup>-hybridized carbon) can be formed from either atomic carbon in bottom-up approaches or through top-down approaches starting from macro-scale graphite.<sup>116</sup> Graphene is oxidized to GO in protonated solvents, and the presence of oxygen-based functional groups provides enhanced versatility to GO nanocomposites and GQDs.<sup>116</sup> C60 can be synthesized through graphite vaporization *via* laser pulsation in helium flow,<sup>117</sup> while CNTs are produced through chemical vapor deposition, laser ablation, or carbon arc-discharge techniques.<sup>118</sup> These nanostructures can be characterized by TEM, SEM, DLS, UV-Vis, mass spectrometry, XRD, DSC, and adsorption/desorption isotherms, in addition to X-ray photoemission spectroscopy, Raman spectroscopy, flow field flow fractionation, near-edge X-ray absorption fine structure, and electron energy loss spectroscopy.<sup>117, 119</sup> For further reading, Dasari Shareena *et al.* expound upon graphene-based nanomaterials in the biomedical field,<sup>120</sup> Astefanei *et al.* provide insight on C60 characterization,<sup>117</sup> Tian *et al.* summarize the synthesis and some applications of GQDs,<sup>121</sup> and Anzar *et al.* and Eatemadi *et al.* further explain the properties and biomedical applications of CNTs.<sup>118, 122</sup> Carbon-based materials are especially suited for use in nanosystems designed for detection and monitoring, phototheranostics, and combination therapy, and consequently, show up disproportionately in those areas of application. Figure 4 displays the inorganic building blocks of hybrid nanosystems along with their characteristics and methods of characterization.

### Organic building blocks

**Lipids/liposomes**—Liposomes, spherical bilayers of lipids encapsulating an inner aqueous space, represent the predominant organic building block of hybrid nanosystems. Lipid-based nanosystems exhibit biocompatibility, self-assembly, facile synthesis, high loading capacity, and trans-membrane delivery capability.<sup>123</sup> Liposomes are frequently constructed from a combination of lipids for  $\zeta$ -potential (surface charge) control, with cationic liposomes displaying enhanced cellular uptake but poor serum stability and neutral/anionic liposomes displaying poor uptake and varying serum stability.<sup>22</sup> Cationic lipids like *N*-[1-(2,3-dioleoyloxy)propyl]-*N,N,N*-trimethylammonium (DOTAP) can be combined with anionic lipids, cholesterol, or zwitterionic lipids to tune the liposome  $\zeta$ -potential to 20–25 mV.<sup>124, 125</sup> Furthermore, lipids are occasionally conjugated with hydrophilic polymers such as polyethylene glycol (PEG) or zwitterionic polymers to reduce *in vivo* clearance.<sup>126</sup> Finally, lipids can be functionalized with targeting ligands to improve specific accumulation of liposomes in targeted environments.<sup>127</sup>

Liposome construction requires both synthesis/isolation of constituent lipids and the formation of liposomal structure. Natural lipids and cholesterol can be isolated from biological systems, whereas other lipids are synthesized *de novo* from chemical building blocks.<sup>128, 129</sup> Liposome formation can be accomplished in several ways. In thin-film rehydration, lipids dissolved in an organic solvent or organic/aqueous emulsion form a

film through lyophilization or evaporation that is subsequently rehydrated and formed into liposomes through vortexing, extrusion, or sonication.<sup>130</sup> Alternatively, liposomes can be formed through solvent vaporization, ethanol injection, or reverse-phase evaporation.<sup>131</sup> Liposomes are characterized *via* DLS, ELS, TEM, UV-Vis, FTIR, high-performance liquid chromatography (HPLC), and gel filtration.<sup>132, 133</sup> Has and Sunthar provide a comprehensive review on liposomal preparation,<sup>134</sup> while reviews from Akbarzadeh *et al.* explain liposome classification and preparation<sup>131</sup> and Pattni, Chupin & Torchilin review liposomal drug delivery systems.<sup>135</sup> Liposomes are prevalent throughout the biomedical field with exception of the areas of antimicrobials and vaccines.

**Polymers**—Polymers form the second class of organic building blocks. Cationic polymers such as chitosan, poly(ethylene imine) (PEI), and poly(L-lysine) (PLL) enhance cellular uptake through electrostatic interactions with anionic cell membranes. These polymers facilitate electrostatic loading of nucleic acids and conjugation with stimulus-responsive and/or active targeting ligands.<sup>24, 38, 136, 137</sup> Alternatively, stimulus-responsive polymers display conformational changes in response to exogenous or endogenous stimuli, including temperature,<sup>138</sup> redox,<sup>139</sup> and pH.<sup>140</sup> Some polymers such as polydopamine (PDA) convert incident light into thermal energy, allowing them to be used as LSPR-independent photoabsorbers.<sup>141</sup> Regularly, two or more polymers are combined into the block or grafted copolymers like poly(lactic-co-glycolic acid) (PLGA) to combine the functionalities of constituent polymers and introduce previously unrealized functionality.<sup>142</sup>

The method of polymer synthesis for a hybrid nanosystem is both material and system dependent. For example, the natural polymer chitosan is isolated from the shells of crustaceans,<sup>143</sup> whereas synthetic polymers such as PEI are formed through addition or condensation reactions.<sup>144</sup> Poly-amino acids can be synthesized by polymerization initiation in the presence of monomer, with the degree of polymerization controlled by tuning the initiator, reactant concentrations, and reaction conditions.<sup>145</sup> In contrast, PDA can be synthesized through dopamine oxidation followed by cyclization and polymerization.<sup>146</sup> Copolymer grafting can be accomplished by *n*-hydroxysuccinimide (NHS) or maleimide chemistries,<sup>147</sup> whereas block copolymers are typically synthesized through sequential polymerization reactions.<sup>148</sup> Polymer characterization can be accomplished *via* NMR, FTIR, UV-Vis, XRD, SANS, DSC, Raman spectroscopy, and matrix-assisted laser desorption ionization time-of-flight mass spectroscopy, whereas characterization of polymer nanoparticles is commonly accomplished by DLS, ELS, SEM, TEM and AFM.<sup>149</sup> Several relevant reviews exist on biomedical applications of PEI<sup>150–152</sup> as well as PLL,<sup>153</sup> PLGA,<sup>154</sup> poly(*N*-isopropylacrylamide) (PNIPAM),<sup>155</sup> and poly(methyl methacrylate) (PMMA).<sup>156</sup> Polymer building blocks are pervasive and can be found in hybrid nanosystems in every area of biomedical application.

**Dendrimers**—The third organic building blocks are dendrimers, which are branching, radially-symmetric star-shaped biomolecules made up of repetitive units dispersing from an origin.<sup>157</sup> Dendrimers are especially suited for biomedical applications because of their monodispersity, non-toxicity, solubility, self-assembly, and stability.<sup>157</sup> Polyamidoamine (PAMAM) is the standard dendrimer used in hybrid nanosystems and has been useful for

gene delivery,<sup>158</sup> chemotherapy,<sup>159</sup> and *in vivo* imaging.<sup>160</sup> Ligand-functionalized PAMAM has shown active targeting capabilities,<sup>158, 161</sup> while selective dendrimer crosslinking can control the release profile of an entrapped therapeutic.<sup>159</sup>

Dendrimer synthesis can take several forms. Divergent PAMAM synthesis is carried out by sequential addition of methyl acrylate and ethylene diamine branching away from a functional core. Each pair of reactions adds a new layer (generation) to the dendrimer, and the extent of the reaction may be monitored spectrophotometrically *via* copper sulfate chelation reactions.<sup>162</sup> Alternatively, convergent synthesis involves the creation of the branches before final connection to a core structure, and some have experimented with combined divergent/convergent processes in which branches and microbranched cores are formed separately before combination.<sup>163</sup> Several notable biomedical hybrid nanosystems utilize divergently-synthesized fifth-generation (G5) PAMAM.<sup>158, 164, 165</sup> Dendrimer can be characterized through gel permeation chromatography (GPC), HPLC, potentiometric titration, and electrospray ionization mass spectroscopy (EI-MS) in addition to SEM, FTIR, UV-Vis, ELS, and DLS.<sup>166–168</sup> Reviews by de Araújo *et al.*<sup>169</sup> and Abbasi *et al.*<sup>157</sup> provide additional insight into the biomedical application of dendrimers. As with liposomes, dendrimers are found in all areas of the biomedical field inhabited by hybrid nanosystems except antimicrobials and vaccines.

**Cell membranes**—Several groups have begun coopting the membranes from cells to encapsulate nanoparticles. These cell membranes provide high serum stability in addition to cell-specific properties. The membranes of several types of cells have been incorporated into nanotherapeutics, including platelets, red blood cells (RBCs), white blood cells (WBCs), cancer cells, mesenchymal stem cells (MSCs), and bacteria.<sup>170</sup> Cell selection heavily influences the properties of membrane-bound nanosystems. For instance, nanoparticles coated in cancer cell membranes can present antigens to activate anticancer immunity,<sup>171</sup> whereas RBC membranes promote long circulation and trans-epithelial transport, MSC membranes target cancers, and platelet membranes target damaged blood vessels and pathogens.<sup>170, 172</sup> Cell membranes have encapsulated organic materials such as polymer nanoparticles,<sup>171</sup> gelatin, liposomes, and proteins,<sup>172</sup> and inorganics including MOFs,<sup>173</sup> MSNs,<sup>174</sup> gold nanocages,<sup>175</sup> upconversion nanoparticles,<sup>176</sup> IONPs,<sup>177</sup> and quantum dots.<sup>178</sup> These hybrids have been applied for purposes ranging from targeted delivery of small interfering RNA (siRNA) and chemotherapeutics<sup>173, 179</sup> to imaging-guided phototherapy<sup>180</sup> and vaccine development.<sup>174</sup>

The formation of membrane-based nanosystems requires initial membrane isolation followed by encapsulation of a desired core. Organelles can be separated from membrane components through sonication, extrusion, freeze/thaw cycling, hypotonic lysis buffer, or Dounce homogenization followed by differential ultracentrifugation.<sup>172</sup> The isolated membrane can then encapsulate nanoparticles *via* coincubation in conjunction with sonication, extrusion, electroporation, or microfluidic techniques.<sup>170, 172</sup> The resultant nanohybrids are commonly characterized by DLS, ELS, TEM, SEM, and UV-Vis.<sup>171, 174, 175</sup> Several recent reviews from Xuan, Shao & Li<sup>170</sup> and Vijayan, Uthaman, & Park<sup>172</sup> provide useful supplementary information on synthesis, characterization, and application of cell membrane-based biomedical nanosystems. Cell membrane building blocks are found in

hybrid nanosystems used in gene and drug delivery, phototherapy, combination therapy, vaccines, and theranostics.

**Accessory building blocks**—Along with the aforementioned inorganic and organic building blocks, accessory building blocks are often included in hybrid architectures. Accessory building blocks are chemical groups or molecules included in the structure of the hybrid nanosystem that confer additional properties to the system without contributing as a major structural component. The major accessory building blocks include hydrophilic polymers, targeting ligands, and stimulus-responsive moieties (Figure 5E). Hydrophilic polymers such as PEG or zwitterionic polymers confer stealth properties to a nanosystem by forming a hydration shell.<sup>39, 181</sup> This hydration shell creates an energy barrier that must be overcome to contact the polymer, thus reducing non-specific protein interactions and extending circulation time *in vivo*.<sup>182</sup> Furthermore, PEG can selectively adsorb proteins that improve nanosystem retention, whereas select zwitterionic polymers have shown complete elimination of the protein corona.<sup>181, 183, 184</sup> As serum stability and low *in vivo* clearance are prerequisites for many nanotherapeutic applications, hydrophilic polymers are included in a notable portion of hybrid nanosystems. For additional information, we recommend several reviews on PEG hydrogels<sup>185–187</sup> as well as Erfani *et al.* on zwitterionic moieties.<sup>181</sup> Hydrophilic polymers can be expected to be found throughout the biomedical field.

Active targeting moieties such as antibodies and ligands for upregulated receptors can enhance the accumulation of a hybrid nanosystem to a specific environment. The tumor microenvironment of several cancers has been reported to disproportionately express folate receptors, CD44 receptors, and integrins  $\alpha 5\beta 3$  and  $\alpha v\beta 3$ , which can be actively targeted by folic acid (FA), hyaluronic acid (HA), and arginine-glycine-aspartic (RGD) peptides respectively.<sup>14, 24, 188</sup> Cyclic targeting ligand iRGD utilizes a two-step process to sequentially target  $\alpha v$  integrins and neuropilin-1 *via* a CendR interaction following proteolytic cleavage.<sup>189</sup> Finally, nanosystems can be modified with redox/pH-sensitive moieties, crosslinked to control therapeutic loading and release profiles, or functionalized to alter nucleic acid condensation.<sup>142, 190</sup> Reviews on active targeting in biomedical nanosystems can be obtained from Muhamad, Plengsuriyakarn, & Na-Banchang<sup>191</sup> and Bazak *et al.*<sup>192</sup> Targeting ligands and antibodies have been included in hybrid nanosystems throughout the biomedical field. Figure 5 describes the organic and accessory building blocks for hybrid nanosystems.

**Hybrid architectures**—Hybrid nanosystems consistently take one of several forms. Hybridization of inorganic nanoparticles with lipids creates nanoparticle-functionalized liposomes boasting liposomal loading and delivery along with nanoparticle targeting, transfection, transport, and/or plasmonic properties (Figure 6A).<sup>125, 193–195</sup> Similarly, cell membrane-encapsulated nanoparticles combine the properties of the inorganic core with serum stability and biospecific targeting (Figure 6B). Alternatively, metal nanoparticles can be bound to the surface of liposomes for stimulus-responsive release of encapsulated components (Figure 6C).<sup>28</sup> Utilizing polymers or dendrimers instead of lipids allows inorganic nanoparticles to be encased in a shell to create core/shell nanosystems (Figure 6D,E,F);<sup>196, 197</sup> inversely, polymer nanoparticles can also be functionalized with

surface-associated inorganic components (Figure 6G).<sup>198</sup> The layer-by-layer architecture involves sequential coating of metallic nanoparticles by polymer and therapeutic to create nanosystems with tunable release profiles (Figure 6H).<sup>199</sup> Finally, the rattle-type architecture consists of a solid core nanoparticle surrounded by an unattached porous shell (Figure 6I).<sup>200</sup> The hybrid architectures in the mixtures and dispersions of nanoparticles in polymer networks and prepolymers are governed by the surface energies and the molecular interactions between media and the nanoparticles. For instance, shear-thinning gelation in the aqueous solutions of Laponite-based hybrid nanoclays stems from the synergistic contribution of negative and positive charges present on the Laponite nanoplatelets which is responsible for the so-called “house of cards” hybrid architectures.<sup>201</sup> These architectures play an important role in determining the physical properties of the hybrid nanosystems and explains gelation in the absence of shear forces (shear-thinning property). Though not every biomedical hybrid nanosystem will fit these classifications, they can be used as a reference for architectures present in the field.

## Biomedical applications

Having discussed their components and architectures, we will now describe current hybrid nanosystems in various biomedical applications. Gene and drug delivery commonly utilize hybridization to marry the carrying capacity of organic materials with the self-therapeutic, biocompatible, and imaging properties inherent to inorganic materials. Hybridization in phototherapy alone and in combination with gene and/or drug delivery offers coupling of photo-responsive properties with carrying capacity, stimulus-responsivity, and targeted therapeutic delivery. In tissue engineering, hybridization confers additional properties over pure organic or inorganic systems, including improved wound healing, enhanced cellular adhesion and remodeling, and reduced inflammation. In the context of antimicrobials, hybrid nanosystems offer the opportunity to selectively eliminate bacterial targets, reverse antibiotic resistance, and couple antibacterial properties with phototherapy. Hybrid vaccines have shown improved thermostability over non-hybridized counterparts. For imaging and detection applications, hybrid nanosystems offer altered imaging/visual properties based on the local microenvironment detectable through changes in conductivity, absorption, fluorescence, and/or T<sub>1</sub> relaxation time. Finally, theranostics integrate imaging properties with gene delivery, drug delivery, and/or phototherapy, a task better suited for hybrid nanosystems in comparison to non-hybridized parallels. As such, hybrid nanosystems offer advantages over non-hybridized systems in each of these applications.

## Gene delivery

Some of the most notable advances in hybrid nanosystem technologies have come in the field of gene therapy, which seeks to treat disease through the transfer of genetic material to enhance, augment, or inhibit gene expression. Current gene delivery strategies include viral and non-viral techniques, the former utilizing the natural transduction efficacy of viral particles while the latter relies upon the transfection properties of engineered vectors. Some challenges facing viral gene delivery efforts include reduced carrying capacity, tropism, and inflammation, while non-viral vectors show better carrying capacity but face major challenges in transfection efficiency and gene modulation efficacy.<sup>207</sup> Hybrid inorganic/

organic vectors offer enhanced transfection efficacy over either material alone, which has resulted in notable growth in hybrid vector development in recent years.

### Liposome hybridizations for gene delivery

Liposomes offer effective gene transfection exemplified by commercial liposome-based transfection reagents such as Lipofectamine™ and HiPerfect™. Liposomal systems overcome gene transfection challenges by providing a positive surface charge and lipid shell to prevent charge repulsion and allow membrane fusion for gene delivery. Nevertheless, several studies have shown that liposome transfection is improved through AuNP hybridization, as nucleic acids can be adsorbed to the AuNP surface and subsequently loaded into liposomes (Figure 6A). Gold-functionalized liposomes have been synthesized to deliver siRNA, with the uptake pathway determined by the AuNP-liposome composition.<sup>208</sup> Similarly, we recently reported the development of an AuNP-liposome siRNA delivery system that significantly improved knockdown of a glycolytic switch in ovarian cancer by shifting the uptake pathway to avoid lysosomal degradation.<sup>22</sup> These findings suggest that AuNP-hybridized liposome delivery systems can provide dramatic improvements to non-hybridized vectors.<sup>22</sup>

AuNP-liposomal delivery of siRNA can be enhanced by active targeting. Du *et al.* presented an AuNP-liposome containing FA that showed improved transfection efficiency in folate-receptor positive cells.<sup>209</sup> Moreover, active targeting combined with liposome-AuNP hybridization can permit delivery to traditionally hard-to-treat locations.<sup>210</sup> AuNP-liposomes can also deliver a combined gene/protein payload such as that required for CRISPR/Cas9 therapy. The Jiang lab reported that a gold/lipid-based vector successfully knocked down PIK1 expression in A375 cells *in vitro* through the delivery of Cas9 protein and sgRNA.<sup>211</sup> A follow-up study showed that the plasmonic properties of AuNPs allowed for the targeted release of Cas9-sgPlk-1 plasmids in response to laser radiation to better control gene-editing practices *in vivo*.<sup>212</sup> As such, AuNP-liposome hybrids appear poised to deliver next-generation gene-editing technologies in upcoming years.

### Polymer hybridizations for gene delivery

Polymer nanosystems commonly utilize a cationic polymer to complex with nucleic acids and overcome charge repulsion from anionic cell membranes in conjunction with a metal nanoparticle containing self-therapeutic or magnetic properties. The combination of AuNPs and biocompatible polymers as gene vectors typically take one of two forms: the core-shell morphology includes an AuNP within a functionalized shell of polymer and therapeutic,<sup>196</sup> while the “layer-by-layer” approach consists of an AuNP sequentially coated in cationic polymer and nucleic acid.<sup>199</sup> In core-shell architectures, AuNPs have been functionalized with PEI to deliver DNA and RNA for pre-clinical treatment of prostate cancer,<sup>24, 213</sup> breast cancer,<sup>214</sup> liver cancer,<sup>215</sup> melanoma,<sup>216</sup> and glioblastoma.<sup>217</sup> Furthermore, AuNPs enhance the permeability of lipid bilayers, which has been exploited by AuNP-PEI hybrids in transdermal gene delivery.<sup>216</sup> AuNP-PEI vectors have also been functionalized with FA and other ligands to improve their target-specific transfection efficiency.<sup>213, 218</sup> Lastly, gold-PEI vectors can display photo-responsive delivery properties through absorption of near-infrared (NIR) radiation.<sup>38</sup> Like PEI, PLL is a cationic polymer effective for gene transfection, and

gold-PLL vectors have been developed to deliver RNA to treat breast cancer<sup>39, 219, 220</sup> and liver cancer *via* the RNA interference (RNAi) regulatory system.<sup>40</sup> Others have applied AuNP-chitosan hybrids in applications from liver and breast cancer treatment to iontophoretic melanoma therapy and osseointegration of dental implants.<sup>137, 221, 222</sup> Gold-polymer vectors can also display redox-responsivity, allowing them to selectively release nucleic acids in environments of elevated glutathione.<sup>198, 223</sup> This evidence suggests that gold-polymer nanosystems present an effective hybridization for gene delivery applications.

Other inorganic building blocks applied in hybrid polymer gene vectors include IONPs and mesoporous structures. IONP-cationic polymer nanosystems have been employed to deliver siRNA and plasmid DNA and have shown enhanced transfection over non-magnetic vectors.<sup>224, 225</sup> Alternatively, Salah *et al.* used nanozeolite MOF-polymer nanosystems to deliver miR-34a to hepatocellular carcinoma,<sup>226</sup> and polyelectrolyte-conjugated MSNs have served as siRNA vectors for the treatment of H1N1.<sup>227</sup> Finally, CaP and PEI have been hybridized to deliver mcDNA to T-cells for cancer immunotherapy, resulting in rapid T-cell-induced apoptosis of hepG2 cells.<sup>228</sup> As such, inorganic-polymer vectors show breadth in application, with an emphasis on cancer therapy and versatility to treat viral disease.

### Dendrimer and cell membrane hybridizations for gene delivery

Thirdly, inorganic-dendrimer nanosystems have been investigated as non-viral vectors. As with cationic polymers, dendrimers conjugated to inorganics overcomes charge repulsion with cell membranes and facilitates delivery of nucleic acids. The Shi lab among others has published several recent articles on PAMAM-entrapped AuNP nanosystems as non-viral vectors, where AuNPs confer biocompatibility and structural integrity while PAMAM conveys enhanced loading and transfection capabilities.<sup>164</sup> Furthermore, AuNP-PAMAM hybrids have been functionalized with an array of surface moieties ranging from zwitterions for stealth to  $\beta$ -cyclodextrin for improved nucleic acid condensation,<sup>158, 164, 190</sup> and FA, HA, or RGD-peptides augment gene delivery efficacy for inhibition of tumor growth.<sup>158, 161, 165</sup> Consequently, AuNP-PAMAM hybridization shows notable potential for gene delivery. Alternatively, cell membranes can encapsulate inorganic nanoparticles loaded with siRNA to create biocompatible nanovectors; these nanovectors offer distinct advantages over other organic components in that they more closely replicate the endogenous tissues. For example, Zhuang *et al.* incorporated an siRNA-loaded ZIF-8 MOF into a platelet cell membrane for targeted gene silencing in mammary adenocarcinoma.<sup>173</sup> These approaches signify the diversity and effect of hybrid nonviral vectors.

The building blocks and architectures utilized in gene delivery applications allow us to make several observations about hybrid vectors. Unsurprisingly, nanoscale gold is the most utilized building block for its myriad beneficial properties, including biocompatibility, cell membrane destabilization, nucleic acid adsorption/desorption, self-therapeutic properties, and ease of synthesis. AuNPs hybridized with liposomes, polymers, or dendrimers form the largest group of hybrid gene delivery systems, and the organic building blocks seem to represent comparable alternatives with minimal differences observed in the efficacy of one over another. Intriguingly, few of these systems display magnetic targeting or photoresponsive gene release, though this is likely due to vectors with those properties

also displaying phototherapeutic or imaging properties. As such, hybrid gene vectors with nanoscale gold are among the most promising and effective non-viral vectors for future gene therapies.

## Drug delivery

Drug delivery systems (DDSs) seek to increase the local concentration of a drug in a specified environment to reduce side effects and improve efficiency, and hybrid nanosystems show potential to overcome drug delivery barriers like rapid *in vivo* clearance and selective drug encapsulation/release.<sup>229</sup> In the following section, we summarize notable strides made by hybrid DDSs within recent years.

### Liposome hybridizations for drug delivery

Inorganic-liposome hybridizations are distinctively suited for small molecule drug delivery applications. The lipid bilayer of liposomes is practical for drug loading and can isolate encapsulated therapeutics from the surroundings, while inorganic components may provide magnetic targeting, imaging, biocompatibility, and photothermal drug release capabilities. Chemotherapeutic agents such as doxorubicin (DOX) and paclitaxel (PTX) have been widely encapsulated within gold-liposome hybrids for drug delivery applications.<sup>230, 231</sup> NIR-triggered DOX release has been achieved by coating liposomes in gold shells or nanocages that rupture the lipid bilayer *via* thermal decay or CO<sub>2</sub> bubble generation.<sup>14, 17, 28</sup> Other gold-liposome DDSs respond to endogenous stimuli; *e.g.* several AuNP-liposome hybrids have been designed to degrade in the mildly acidic tumor microenvironment.<sup>193, 232</sup>

The superparamagnetic properties of IONPs provide active drug targeting capabilities to liposomes by application of an external magnetic field, and these “magnetoliposomes” are widely successful as DDSs.<sup>126</sup> Magnetic targeting improves magnetoliposomal DOX delivery efficacy in comparison to both liposomal and free DOX.<sup>233–235</sup> Magnetoliposomes have also been utilized to delivered curcumin, docetaxel, gemcitabine, cisplatin, and cuphen, and have been reported effective for radical scavenging as well as treatment of diverse cancers.<sup>202, 236–238</sup> Magnetoliposome-mediated chemotherapy can be further enhanced through active targeting ligands and moieties with endogenous stimulus sensitivity.<sup>127, 194, 239, 240</sup> Finally, one report describes a IONP/liposome-based docetaxel delivery system that displayed drug release in response to both an external magnetic field as well as NIR.<sup>241</sup> As such, the development of magnetoliposomes has been a boon for targeted drug delivery.

Aside from AuNPs and IONPs, few inorganic materials have been hybridized in liposomal DDSs. Liposome-encapsulated MOFs can codeliver several drugs simultaneously<sup>195</sup> and display self-therapeutic properties against cancer through ion leaching.<sup>242</sup> Si-O-Si networks have been incorporated into thermosensitive liposomes to improve their stability for room temperature storage,<sup>243</sup> and nickel-bis(dithiolene) display gold-like NIR absorption properties to induce drug release under NIR.<sup>244</sup> Finally, incorporation of AgNPs into liposomes has been shown to alter the loading capability and partition coefficient of encapsulated curcumin, suggesting that metal nanoparticles can relocate hydrophobic drugs



closer to the liposome surface.<sup>245</sup> As such, liposome-encapsulated metal nanoparticles form effective platforms for the delivery of small molecule drugs to a variety of targets.

### Polymer hybridizations for drug delivery

Inorganic-polymer DDSs have been investigated with less intensity as have inorganic-liposome hybrids. The biocompatibility of AuNPs has been applied in conjunction with chitosan, polyvinylpyrrolidone (PVP), and polypeptides to deliver drugs including 5-fluorouracil, DOX, curcumin, and sunitinib malate.<sup>21, 246, 247</sup> Moreover, polymers conjugated to AuNP DDS hybrids can be readily modified with pH-responsive moieties and targeting ligands.<sup>197</sup> Additionally, inorganic compounds and MSNs can form the core of hybrid polymer DDSs, while others have designed systems including ZIFs, and PtNPs to release chemotherapeutics in response to reduced pH.<sup>57, 85, 248</sup> For example, Dong *et al.* utilized a CaP shell around a phosphatidylserine-PEG core to confer pH-responsivity to co-delivery of verapamil and novantrone to treat multidrug-resistant breast cancer.<sup>66</sup> Finally, inclusion of AgNPs can confer hybrid polymer DDSs with antibacterial properties, allowing them to be used in combination antibacterial/chemotherapeutic capacity.<sup>249</sup>

### Alternative hybridizations for drug delivery

Inorganic-dendrimer hybrids are also effective for chemotherapeutic delivery.<sup>159</sup> In one example, Parlanti *et al.* designed an IONP-PAMAM nanosystem exhibiting magnetic targeting and pH-responsive DOX release for the treatment of pancreatic cancer.<sup>250</sup> This system is noteworthy for its uptake mechanism in which the dendrimer is cleaved and taken into the cell while the inorganic core remains outside.<sup>250</sup> Alternatively, ruthenium-modified carbosilane dendrimers exhibit low toxicity to non-cancerous cells while inhibiting leukemia cell viability.<sup>251</sup> Membrane-coated inorganics show potential as DDSs as well. MSC and RBC membranes have been used to encapsulate MOFs for targeted protein delivery,<sup>252</sup> while DOX has been delivered *via* AuNCs encapsulated within 4T1 breast cancer cell membranes,<sup>175</sup> and therapeutic antibodies have been delivered with platelet membrane-coated IONPs.<sup>253</sup> Conversely, some DDSs have utilized nucleic acids for structural purposes. Wang *et al.* developed a fascinating system for the delivery of anticancer drugs by encapsulating ZONPs in DNAzyme (a short catalytic sequence of DNA)-substrate scaffolds. When the ZONPs responded to reduced pH by producing  $Zn^{2+}$ , a DNAzyme cofactor, the DNAzyme broke down the scaffold for therapeutic release.<sup>67</sup> Finally, several forms of carbon have been utilized as pseudo-organic components in hybrid DDSs. Cyclic carbon (C18) has been employed as a shell surrounding IONPs for benzamide loading. The hybrid nanosystem prevented biofilm generation by *C. albicans* while exhibiting biocompatibility, suggesting potential for infection treatment.<sup>254</sup> Lastly, MSNs conjugated with GO and functionalized with aspartic acid show low cytotoxicity alone but enhanced cell death and apoptosis in MCF-7 cells when loaded with curcumin.<sup>255</sup> Though the building blocks may vary, hybridization offers a distinct and effective approach to constructing DDSs.

Hybrid DDSs take advantage of the carrying capacity of liposome, polymer, dendrimer, and cell membrane components to deliver a variety of small molecule therapeutics to diverse targets. AuNP- and IONP-liposome hybridizations are among the most effective systems due to their ability to carry both hydrophilic and hydrophobic drugs in an isolated

environment and respond to exogenous stimuli, which allows selective delivery and release of encapsulated therapeutics. Aside from these popular architectures, the diversity expressed by hybrid DDSs is astounding. Porous materials allow facile adsorption/desorption of small molecules, which are ideal properties for DDSs, and hybridization within organic building blocks facilitates tuning of the release profile. Drug delivery is also where we initially encounter carbon-based materials, and they make a minor but not insignificant contribution to our understanding of hybrid DDSs. All considered, hybrid nanosystems represent a noticeable improvement over nonhybridized DDSs by allowing drug delivery to correspond with external targeting and photo-responsive drug release.

## Phototherapy

Phototherapy harnesses external radiation for therapeutic purposes. The first NIR window (wavelength 700–1000 nm, NIR-I) is characterized by reduced absorption by biological tissues, allowing deep its penetration into the body.<sup>256</sup> A second biological window (NIR-II) has been reported above 1000 nm, and some sources indicate that a third biological window exists above 1500 nm, though others have designated it a subset of NIR-II.<sup>257, 258</sup> Semantics aside, compounds incorporated into nanosystems that absorb in these biological windows can allow NIR activation of therapeutics. Phototherapy can be split into two categories. Photothermal therapy (PTT) harnesses the increase in temperature experienced by photoabsorbing nanoparticles to kill adjacent cells,<sup>259</sup> whereas photodynamic therapy (PDT) utilizes electrons excited by photons interacting with photosensitizers to generate active therapeutics such as singlet oxygen ( $^1\text{O}_2$ ) and other ROS.<sup>260</sup> Several recent advances in the application of hybrid nanosystems to phototherapy are outlined in the following section (Figure 7).

The absorption spectra of photothermal nanosystems are heavily influenced by the material and geometry of the inorganic component. AuNRs and AuNPs can be engineered to exhibit an absorption peak within the NIR range (See Figure 3). Additionally, absorptive LSPR decay is readily employed for hyperthermic therapy, and as a result, several groups have developed gold-based hybrid nanosystems for PTT.<sup>45</sup> AuNPs have been incorporated into liposomes to improve tumor targeting and deep phototherapy by exploiting the NIR-II window.<sup>261, 262</sup> As with gene and drug delivery, these AuNP-liposome systems can be modified with ligands and magnetic components to allow both endogenous and exogenous targeting.<sup>262, 263</sup> Similarly, AuNRs have been utilized as the core of NIR-I-responsive core-shell poly(o-methoxyaniline) hybrids displaying morphology control through polymer concentration variation.<sup>13</sup> In one geometry, gold-capped polymer janus particles encapsulated in cell membranes exhibited photothermal effects resulting in enhanced motile behavior along with PTT.<sup>204, 264</sup> As a gold alternative, aniline-based polymers have been applied to PTT in coordination with lanthanide-based upconversion nanoparticles (which absorb two photons at low energy and emit a single photon at higher energy). This nanosystem was shown to effectively photoablate tumors *in vivo* with NIR radiation but to be non-toxic in its absence.<sup>265</sup> While most photothermal hybrid nanosystems are developed for cancer treatment, other applications exist. For instance, Zhou *et al.* designed a nanocomposite capable of PTT simultaneously displaying non-NIR-coupled effectivity against bacterial infection and applications in wound healing,<sup>141</sup> which

exemplifies how photothermal hybrid nanosystems can be designed for several applications simultaneously.

Unlike PTT, PDT harnesses incident light to initiate a chemical reaction. In these systems, metal nanoparticles are frequently included for their non-optical properties, and additional photosensitizers are included to facilitate the therapeutic process. For example, liposomes carrying the photosensitizer chlorin e6 (Ce6) were modified with AuNCs, where the AuNCs inhibited thioredoxin reductase to improve the efficacy of  $^1\text{O}_2$  produced by Ce6.<sup>16</sup> Liposomes have also been modified with IONPs to provide magnetic targeting capabilities for protoporphyrin delivery.<sup>266</sup> Likewise, MOFs have been conjugated with photosensitizers and nanozymes for two-step PDT in which the nanozymes generate  $\text{O}_2$  from  $\text{H}_2\text{O}_2$  before photosensitizer radiation converts  $\text{O}_2$  to  $^1\text{O}_2$ , overcoming the PDT limiting factor of tumor hypoxia.<sup>267</sup> A similar approach to alleviate tumor hypoxia prior to PDT was exploited by Zuo *et al.* in constructing a platelet membrane-encapsulated  $\text{W}_{18}\text{O}_{49}$  and metformin nanosystem.<sup>268</sup> Other membrane-based PDT nanosystems have employed platelet membranes in conjunction with photodynamic cores to improve PDT efficacy and reduce skin damage,<sup>269</sup> and macrophage membrane-encased IONPs for magnetic responsivity.<sup>203</sup> Additional PDT hybridizations have utilized  $\text{TiO}_2$ ,  $\text{SiO}_2$ , phosphorus quantum dots, iridium nanocrystals, PtNPs, and AgNPs along with photosensitizers to kill cancers and bacteria.<sup>270–273</sup>

Though both PTT and PDT exploit the biological windows for therapeutic purposes, differences in exploitation mechanisms highlight a distinction between them in hybrid nanosystem building block selection. Those employing PTT commonly utilize inorganic nanoparticles for photoabsorption while organic components are included for biodistribution, targeting, and stability purposes. Consequently, PTT *via* hybrid nanosystems allows for improved efficacy over non-hybridized systems through improved accumulation in the desired environment and reduced *in vivo* clearance. In contrast, transferring the onus of PDT to a photosensitizer allows for the selection of inorganic building blocks based on non-optical properties, which provides versatility to overcome common PDT obstacles such as tumor hypoxia and photosensitizer loading/delivery. As such, hybrid nanosystems offer advantages over current therapies for both PTT and PDT through differing means.

## Combination therapy

While the aforementioned examples show the benefits of hybridization in gene and drug delivery as well as phototherapy, hybrid nanosystems excel in combination therapies utilizing multiple strategies (*i.e.* combined chemo/phototherapy, gene/drug codelivery, *etc.*) to more effectively treat malignancies. In the following section, we summarize the current work in combination therapy using hybrid nanosystems. From an architecture perspective, gold-functionalized liposomes are well-suited for chemo-phototherapy and co-delivery of genes and small molecule drugs, as this combines the loading capacity and transfection of liposomes with the optical and self-therapeutic properties of nanoscale gold. Polymer-functionalized gold of varying geometries has been proven effective for gene/drug codelivery, gene-PTT, and chemo-phototherapy, with cationic polymers enhancing transfection capability and facilitating drug loading while gold cores provide tunable optical

and self-therapeutic properties. Moreover, as the majority of these systems discussed thus far have been cancer therapies, Table 1 displays notable hybrid nanosystems developed for cancer treatment.

### Gene and drug codelivery

Codelivery of nucleic acids and small molecule drugs have the potential to exceed the most effective monotherapies. Through careful drug and gene selection, the therapeutic effect of one can enhance the efficacy of the other. For example, interfering RNA (RNAi) therapy can downregulate nonspecific cellular efflux pumps responsible for clearing the cytoplasm of chemotherapeutics, improving the efficacy of drugs co-delivered by the hybrid system.<sup>274, 275</sup> One popular hybridization for gene/drug codelivery is nanoscale gold and liposomes, and these systems have been further modified for magnetic targeting and photo-triggered release of encapsulated therapeutics.<sup>276, 277</sup> Alternatively, Han *et al.* developed an AuNP-PEI nanosystem capable of re-educating stellate cells in pancreatic ductal adenocarcinoma through the co-delivery of all-trans retinoic acid and siRNA to knockdown heat shock protein 47.<sup>278</sup> AuNRs have been combined with PEI to co-deliver DOX and short hairpin RNA (shRNA) to metastatic breast cancer (MBC) and inhibited tumor growth and metastasis.<sup>279</sup> Another MBC therapy was developed from AuNPs incorporated into hydrogels for co-delivery of miRNA and cisplatin.<sup>280</sup> AuNPs have also been decorated with DOX and siRNA-loaded proteins for ovarian cancer therapy,<sup>281</sup> conjugated with DNazymes, and ZnO quantum dots for miR-21 and DOX delivery,<sup>282</sup> and even trapped within a dendrimer for ultrasound-triggerable release of miR-21 and gemcitabine.<sup>283</sup> Finally, MSN-ZIFs have been designed for the pH-responsive delivery of DOX, DNA, and CRISPR-Cas9 components *via* subretinal injection *in vivo*.<sup>205</sup> As such, hybrid nanosystems make up an effective strategy for co-delivery of nucleic acids and small molecules.

### Gene delivery and photothermal therapy

The biocompatible and self-therapeutic properties of nanoscale gold combined with tunable absorption properties make it unparalleled in combination gene-PTT. AuNPs, AuNRs, AuNSs, and gold nanoprisms have been combined with biocompatible polymers to create nanosystems to treat lung cancer, breast cancer, and gastric cancer.<sup>29, 284-286</sup> As with gene/drug codelivery, careful selection of therapeutics can produce synergistic effects. Liu *et al.* used a gold nanoflower-based hybrid to delivered siRNA to knock down heat-shock proteins prior to PTT.<sup>287</sup> Mesoporous PDA nanoparticles also display effective photothermal conversion. PDA has been coated with CaP to produce pH-responsive nanosystems exhibiting effective siRNA knockdown and PTT.<sup>288</sup> As such, gold and PDA provide effective means for harvesting NIR and converting it to thermal energy for PTT in combination with gene delivery.

### Combination chemo-phototherapy

Chemo-phototherapy has recently emerged as a next-generation cancer treatment in which gold nanostructures are regularly employed to harvest NIR radiation and convert it to thermal energy. AuNS-coated liposomes containing chemotherapeutics can couple laser-activated drug release with PTT.<sup>289, 290</sup> In a similar approach, gold-coated MnFe<sub>2</sub>O<sub>4</sub> nanoparticles have been encapsulated within liposomes to create photoresponsive and

superparamagnetic DDSs,<sup>291</sup> and Au nanocages have been encapsulated within cancer cell membranes to deliver DOX for selective combination chemo-PTT.<sup>175</sup> One study compared the efficacy of AuNPs and AuNSs within a thermo-responsive liposomal coating and determined that AuNSs displayed better LSPR tunability, allowing for more efficient absorption of NIR for PTT and drug release.<sup>292, 293</sup> Nevertheless, even less efficient AuNPs have displayed photoinduced PTX release and photothermal hypothermia when conjugated with PLL and loaded with PTX.<sup>294</sup>

Gold has also been hybridized with structural nucleic acids and mesoporous semiconductors for chemo-phototherapy. Song *et al.* developed AuNR-DNA nanostructures loaded with DOX through base-pair intercalation that showed increased cellular uptake of both the DOX and AuNRs.<sup>295</sup> Another AuNR-DNA nanoplatform was developed to release DOX in response to NIR through the photoacoustic effect in addition to mRNA-triggered release.<sup>296</sup> Finally, a rattle-type chemo-phototherapy hybrid nanosystem was constructed from Au@Cu<sub>2</sub>-xS mesoporous nanocrystals that exploited metal-semiconductor hybridization to deliver DOX with NIR activation and detect the presence of oncogenic RNA through adsorption of miRNA gene probes to the nanocrystal surface.<sup>297</sup>

Carbon-based inorganic building blocks find special use in chemo-phototherapy. Wang *et al.* detailed an intricate nanosystem containing a hollow, IONP-functionalized carbon core surrounded by a redox-responsive MnO<sub>2</sub> shell coated in PEI and RGD targeting peptides. Upon exposure to glutathione, the MnO<sub>2</sub> shell degraded and activated a ROS-generating chemodynamic drug that showed greater than 99% tumor suppression when coupled with NIR.<sup>298</sup> Furthermore, GO-polymer nanosystems have been designed to actively target tumors for methotrexate delivery in combination with PTT,<sup>299</sup> and chitosan-reduced GO can deliver DOX in conjunction with photodynamic <sup>1</sup>O<sub>2</sub> generation.<sup>300</sup> Thus, hybrid nanosystems can readily combine delivery of small molecule therapeutics with phototherapy in addition to NIR-responsive drug release.

### Gene and drug co-delivery in combination with phototherapy

As combination therapies have shown improvement over monotherapies, gene and drug co-delivery in coordination with phototherapy offers even greater opportunity for enhanced therapeutic efficacy. As such, Deng *et al.* designed an AuNP-liposome hybrid capable of X-ray-triggered gene and drug release. Moreover, the photosensitizer verteporfin was incorporated within the liposome to generate <sup>1</sup>O<sub>2</sub> upon X-ray irradiation.<sup>301</sup> Similarly, AuNR-silica nanocapsules have been designed to deliver sorafenib and p53 to malignant hepatocellular carcinoma; this nanosystem displayed both NIR-triggered release of the encapsulated gene/drug and PTT from the AuNRs.<sup>200</sup> From these examples, we can conclude that hybridization provides a method by which nanosystems can effectively approach the challenges of combination therapies.

Hybridization in the context of combination therapy provides opportunities for synergy, with drugs, genes, and phototherapies selected to amplify the efficacy of the cotherapies of a given nanosystem. Though it is possible for synergistic effects to be observed in non-hybridized systems, hybridization offers improved methods for their inclusion in a single system. Based on this evidence, polymer-functionalized gold nanosystems are the

preeminent architecture in combination therapy applications. For alternatives to gold, carbon-based building blocks have shown promise in delivering chemotherapeutics in combination with both PDT and PTT, and PDA is also an effective photoabsorber. Table 1 displays recent hybrid nanosystems for gene, chemo, and phototherapy for cancer treatment.

## Tissue regeneration and remodeling

Tissue engineering aims to recapitulate native tissue characteristics to develop biological substitutes for replacing damaged tissues.<sup>311, 312</sup> Hybrid nanosystems have led to significant advances in fabricating biomimetic tissue constructs. Both inorganic and organic building blocks have shown promise *via* regulating cell growth and differentiation as well as tuning the material properties of the extracellular matrices (ECM). These improvements are demonstrated for regeneration of the tissue types such as skin, bone and cartilage, nerve, cardiac, and vascular tissues. In the following sections, the recent advances made by hybrid nanosystems in tissue healing and regenerative areas are summarized.

## Wound management

Hybrid nanosystems have facilitated wound healing in different capacities. In particular, metal nanoparticles incorporated with injectables and wound dressing patches can promote wound healing efficacy. This improvement stems from the active tissue regenerative and antimicrobial function of nanoparticle components during the stages of wound healing. AgNPs are one of the most widely used compounds for treating chronic ulcers and tissue burn infections.<sup>313</sup> The non-specific release of AgNPs which initially raised toxicity concerns was circumvented in the recent silver-based products such as Acticoat Flex 3 wound dressings.<sup>313</sup> AgNPs can facilitate wound epithelialization according to a study on human anorectal surgery wounds treated with AgNPs extracted from the *Delonix elata* leaf in which the wound fully disappeared after 17 days post-procedure.<sup>314</sup> AuNPs can accelerate wound healing in polymer-based hybrids because of their antioxidant and antimicrobial properties. AuNPs aid hemostasis and inflammatory phases of wound healing.<sup>315</sup> Skin wound healing capability of biopolymers such as collagen<sup>316</sup> and chitosan,<sup>317</sup> increased with the addition of AuNPs. One attractive feature of AuNPs is the possibility of surface functionalization through which their wound healing efficacy can be further enhanced. Cyclic lipopeptide surfactin functionalization of AuNPs further improved wound healing capability in AuNPs incorporated polymer as confirmed in a rodent wound model.<sup>318</sup> The plasmonic properties of AuNPs can also enable their wound healing capability, as the emitted heat in response to NIR light is known to reconfigure and interdigitate the tissues locally at the wound site.<sup>319</sup> Among the metal nanoparticles, CuNPs play a pivotal role in wound healing by inducing angiogenesis through enhancing the release of vascular endothelial growth factor (VEGF), upregulating the expression of integrin, and stabilizing the ECM proteins. A wound-healing agent based on chitosan and CuNPs studied by Gopal *et al.*<sup>320</sup> demonstrated a decrease in tumor necrosis factor- $\alpha$  (TNF- $\alpha$ ) and an increase in interleukin-10 (IL-10) in the rat models.

ZONPs have also proved their excellent potential for wound healing applications. The addition of ZONPs to polymer matrices is associated with an increase in re-epithelialization,

tissue granulation, keratinocyte migration, as well as collagen deposition. The ZONPs synthesized from the *Trianthema portulacastrum* Linn. exhibited anti-inflammatory, antibacterial, and antioxidant properties based on which the wound healing characteristics are stemmed from.<sup>321</sup> The planar structure of GO sheets also enables grafting bio-functionalities required for wound healing. Recently, a reduced graphene oxide (rGO) embedded in isabgol was utilized for treating diabetic wounds.<sup>322</sup> Addition of rGO was associated with accelerated wound healing in Wistar rats. The rGO can favor re-epithelialization, promote the collagen concentration, as well as angiogenesis in the wound area. The use of silica in wound dressings can enhance the proliferation and migration of fibroblast cells.<sup>323</sup> The positively charged silica nanoparticles (SiNPs) can be dissolved in the wound media and thereby generate the silicic acid that has been shown to stimulate wound healing in dressings. Wound healing was escalated with the addition of SiNPs to the PVP polymers due to the sustained delivery of SiNPs at the wound site. Nanoparticles of titanium dioxide (TiNPs) also demonstrated enhance in burn wound model *in vivo* which results in re-epithelialization, angiogenesis, and fibroblast migration.<sup>324</sup> Hybrid nanosystems led to a significant impact on the wound healing efficacy of the polymeric matrices.

In addition to the tissue regenerative properties, hybrid nanosystems have advanced wound management techniques by due to their hemostatic effects which facilitates blood coagulation in case of hemorrhage. The hemostatic properties in nanoparticles originate from their large surface charges and water absorbing capability. SiNPs coated with PDA is one example of additives that could shorten the time to hemostasis (by 150 seconds compared to a commercial Celox hemostatic agent).<sup>325</sup> The hemostatic effect was due to the activation of the extrinsic coagulation cascade by SiNPs and promoting platelet and erythrocytes aggregation. Nanoclays such as nanokaolin in combination with tannic acid was shown to act as FXII factor activator to trigger hemostasis in an adhesive hydrogel platform.<sup>326</sup> Laponite, the synthetic nanosilicate formed of nontoxic components ( $\text{Na}^+$ ,  $\text{Mg}^{2+}$ ,  $\text{Si}(\text{OH})_4$ ,  $\text{Li}^+$ ) is known for its hemostatic properties due to its strong surface charges. Addition of Laponite to gelatin leads to a shear-thinning injectable biomaterial which can reduced the clotting time by ~50% (at 2 wt.% Laponite) by activating the intrinsic coagulation pathway through Factor XII.<sup>99, 327</sup> MMT can induce coagulation in blood. MMT particles were incorporated in a GO crosslinked composite could stop bleeding in a rabbit artery wound model within 84 seconds.<sup>328</sup> Rapid plasma absorption is an established mechanism of hemostasis in MMT based composites. The release of  $\text{Ca}^{2+}$ ,  $\text{Mg}^{2+}$ , and  $\text{PO}_4^{3-}$  ions from nanowhitlockites ( $\text{Ca}_{18}\text{Mg}_2(\text{HPO}_4)_2(\text{PO}_4)_{12}$ ) have accelerated activation of coagulation cascade and reduced bleeding time *in vitro* and blood loss *in vivo* by ~50% compared to a sham control.<sup>93</sup>

### Bone and cartilage tissue engineering

Bone damage causes a large financial burden on the health care system. The lack of sufficient osteointegration in bone implants limits their lifetime and leads to revision surgeries that are often more costly and associated with more severe complications. Hybrid nanosystems have shown potential to enable nanoscale engineering of bone implants for more robust integration with the surrounding tissue. It is important to note that nanocrystalline hydroxyapatite (nHA), *i.e.*,  $\text{Ca}_{10}(\text{PO}_4)_6(\text{OH})_2$ , forms the majority of the

bone matrix. Nano-phase ceramics, therefore, have received attention to address challenges at the bone-implant interface. Nanoscale nHA (e.g., 67 nm grain size of nHA) provide a high surface fraction enhancing osteoblast activity due to the larger vitronectin adsorption.<sup>329</sup> Similarly, the ZONPs and titania, with 23 and 32 nm sizes, respectively, were reported to enhance calcium and collagen deposition. They also increased alkaline phosphatase activity compared to their microscale counterparts.<sup>330</sup> Self-assembly of organic helical rosette nanotubes based on DNA pairs in aqueous solution was characterized with osteogenic properties due to the structure of their peptide side chains (e.g., RGD, KRSR for osteoblast adhesion, and lysine).<sup>331</sup> The nanostructured self-assemblies of peptides based on KLD-12 and Lys-Leu-Asp was proposed for cartilage repair application.<sup>332</sup> The hydrogels promoted chondrocyte differentiation and facilitated the deposition of the cartilage-like ECM.

Another rosette nanotube functionalized with lysine was reported for improvement in chondrogenic differentiation of adipose-derived mesenchymal stem cells (ADSCs).<sup>333</sup> The nanotubes were integrated with gelatin methacryloyl (GelMA) and poly(ethylene glycol) diacrylate (PEGDA) polymer matrices and 3D printed using a stereolithography printer. The addition of the nanotubes was associated with 34% increase in the ADSCs population. Carbon-based inorganic nanoparticles and their induced electrical conductivity have been frequently demonstrated to enhance osteogenic activities for bone tissue engineering applications. For instance, the incorporation of CNTs in polymers has increased the volume of bone formation by four times.<sup>334</sup>

Organic assemblies engineered in nanoscale such as nanofibrous polymers processed through electrospinning, particulate leaching, as well as phase separation are among the potential methods for bone tissue regeneration. Stem cell differentiation can be regulated by the organic hybrid nanosystems based on electrospun poly ( $\epsilon$ -caprolactone) (PCL).<sup>335</sup> The electrospun nanofibers comprised of PLGA-tussah silk fibroin doped with GO aided MSC differentiation, accelerated the osteoblast differentiation as well as new bone formation.<sup>336</sup> Hybrid 3D porous scaffolds based on rGO and nHA was developed to fill in bone defects *in vivo* for circular calvarial defects in rabbit models.<sup>337</sup> Nanosphere metals, their oxides, and metallic alloys are three other classes of nanoparticles with osteoconductive properties. Titanium (Ti), the medical-grade titanium alloy (Ti6Al4V) and chrome alloys (CoCrMo) have been studied in their nanophase, and their enhanced osteoblast adhesion behavior was confirmed compared to their conventional solid counterparts.<sup>338</sup> To promote osteogenesis, nanofibers based on Zein PDA were developed to deliver TONPs conjugated with protein-2 (BMP-2). MSNs with cone-like pore shapes were also characterized for BMP-2 delivery.<sup>339</sup> The BMP-2 conjugates resulted in an increased expression of the osteoblast cells and its sustained delivery facilitated cell differentiation and adhesion due to their interconnected nanoscale matrix.<sup>340</sup> A 3D printed PCL scaffold was coated in a layer by layer fashion by PDA and AgNPs.<sup>341</sup> The findings were suggestive of improvement in both antibacterial and bone regeneration and demonstrated excellent performance in treating bone defects *in vivo*. Among other metal-based nanoparticles, the combination of zinc silicate and nHA with collagen has been associated with improved angiogenesis in bone scaffolds through p38 MAPK pathway in activated monocytes.<sup>342</sup> AuNPs in another study was conjugated with siRNA to activate both osteogenic as well as revascularization capabilities of the Ti



implants.<sup>343</sup> Nanoscale components can further improve in terms of their osteoactivity by chemical modifications at their surfaces.

### Vascular tissue engineering

Vascular diseases and disorders due to coronary heart disease, or atherosclerosis have led to a large demand for vascular grafts. The vascular cell function is improved by incorporation of functional nanoscale components *via* preventing thrombosis and inflammation. Cell alignment in vascular cells (*i.e.*, smooth and endothelial muscle cells) play a key role in their function and have been paid particular attention in the literature. In this context, processing methods such as electrospinning have enabled directional deposition of nanofibers from hybrids that are capable of cell alignment. For instance, smooth muscle cell infiltration was reported in the case of nanofibrous scaffolds based on collagen/elastin/PLLA, 21 days post culture.<sup>344</sup> Vascular grafts were obtained by a combination of 3D printing and electrospinning.<sup>345</sup> A triple-layer PCL consisting of 3D printed inner layer-coated with aligned nanofibers were co-electrosprayed to form the third layer. In an *in vivo* study, the longitudinally aligned fibers facilitated migration of endothelial cells. Bilayered vascular grafts involving the inner layer of aligned PCL and collagen nanofibers with an outer layer from a randomly oriented PCL and silica nanofibers were fabricated by co-electrospinning.<sup>346</sup> In this vascular graft, the inner layer aimed to facilitate endothelial cell adhesion and migration while the outer layer provided strong mechanical support and enhanced fibroblast affinity. Shear-thinning biomaterials also have shown a great promise for endovascular embolization.<sup>102, 347</sup> The synthesized hybrids of nanosilicates (Laponite) with gelatin has been introduced an excellent candidate as they provide a biocompatible and injectable material platform as they could occlude blood vessels and promote connective tissue formation in the vessel lumen. Besides, they have shown excellent function for treatment of aneurysms as their injection at the aneurysm site can stop progression of disease and prevent damage to the blood vessels.

### Cardiac tissue engineering

The complexity of the cardiac tissue structure and its regeneration process have led to major challenges in reproducing the cardiac tissue functions. Material selection, surface engineering, processing method (*e.g.*, electrospinning and 3D bioprinting) as well as the electrical coupling between the artificial scaffold and native tissue have been the main subjects in the study of cardiac scaffolds. Cardiac tissues have been enabled by the cell aligning effect of nanofibrous hybrids and the electrical conductivity offered by the carbon and metal-based systems.<sup>348</sup> Cardiac patches are aimed to host living cells (cardiomyocytes, bone marrow-derived stem cells *etc.*) and allow cell cultivation in presence of conductive components. Cardiac patches can be highly aligned in micro- and nanoscales to enhance synchronized contractions for instance, using the highly-aligned CNT sheets.<sup>349</sup> In the CNT-based hybrid systems, cardiomyocytes have shown similar electrical-impulse transmission behavior as the native myocardium and demonstrated lower cell-to-cell and beat-to-beat dispersion of the repolarization in the cultured cells with CNT content.<sup>350</sup> An engineered CNT embedded GelMA was characterized with 85% decrease in excitation threshold and 4 times larger synchronous beating rate due to the nanofibrous network of CNTs.<sup>351</sup> Functionalized CNT with hydrazine in pericardial matrix led to human-induced pluripotent

stem cell (hiPSC)-derived cardiomyocyte maturation. The cells demonstrated larger than 500% maturation on the conductive hydrogels and enhanced connexin 43 expression.<sup>352</sup> AuNPs deposited on decellularized omental matrix was proposed by Shevach *et al.*<sup>353</sup> for cardiac tissue engineering. The fabricated cardiac patches were characterized with Cx43 expression and increased contraction force and resulted in a larger calcium signal propagation. AuNPs incorporated in hydrogels can promote cardiomyogenic differentiation of stem cells. The electrical stimulation on the H9c2 cells in a porous polyurethane (PU)/AuNRs and AuNSs was investigated by Ganju *et al.*<sup>354</sup> The results suggested active expression of Nkx-2.5 antriuretic peptide precursor, and atrial natriuretic peptide. GelMA hydrogels containing AuNRs were also characterized by increased troponin I and sarcomeric actinin (cardiac markers).<sup>355</sup>

### Neural tissue engineering

Hybrid nanosystems have had a notable contribution to improve healing disorders and injuries in the nervous system. The materials for neural tissue engineering are sought to be cytocompatible and should pose mechanical and electrical properties similar to that of native tissue to effectively direct neuron outgrowth and thereby bridge disordered nerve gaps. Nanofibrous electrospun PLLA incorporated in laminin (the protein that is known to promote neurite) was proposed for peripheral nerve repair.<sup>356</sup> A recent work demonstrated the aligned touch-spun PCL nanofibers could enhance neuron-specific class III  $\beta$ -tubulin expression along with bipolar elongation.<sup>357</sup> The excellent electrical properties of the carbon-based nanomaterials have made them an attractive candidate for nerve tissue regeneration. Manipulation of surface charges on the CNTs is an important factor as the neurite length, cone growth density, and branching improved by introducing positive charges.<sup>358</sup> Metallic nanoparticles such as AuNPs have been also able to endow electrical conductivity to the polymer matrices for regulation of neural cell differentiation. Hybrid nanocomposites based on AuNP complexes with polyaniline enabled electrical stimulation.<sup>359</sup> Particularly, microtubule-associated BMP-2 was prominently expressed and the stimulation process led the neurites to grow from the stem cells. Peripheral nerve regeneration can be also enabled by layered electrospun scaffolds based on Fe<sub>3</sub>O<sub>4</sub> magnetic nanoparticles and melatonin.<sup>360</sup> The scaffolds were able to mitigate the oxidative stress and inflammation which eventually resulted in enhanced nerve regeneration performance.

### Antimicrobials

We now direct our discussion towards antimicrobial hybrid nanosystems. Where gold is disproportionately employed in delivery applications, AgNPs are unequally exploited for antibacterial functions. While naked AgNPs are invaluable for disinfection, their shortcomings include cytotoxicity and ecosystem damage.<sup>361</sup> Hybridized AgNPs, in contrast, demonstrate applications ranging from water treatment to delivery of oral antibiotics. For example, silver-based nanosystems produced a 4-log reduction in waterborne *L. pneumophila* and a 6-log reduction in *B. subtilis*, and the inclusion of magnetic components facilitated removal from solution for reduced ecotoxicity.<sup>361</sup> AgNPs can be incorporated into polymers for enhanced bacterial membrane damage,<sup>360, 362</sup> functionalized with photosensitizers for photodynamic antibacterial activity,<sup>363</sup> or incorporated into NIR-

responsive MOFs for photothermal-antibacterial activity.<sup>58</sup> Others have developed magnetic field-responsive antibacterials displaying enhanced penetration of bacterial biofilms through IONP hybridization.<sup>364, 365</sup> Finally, Ag/CuNPs have been conjugated with PDA and shown to exhibit both rapid and extended antibacterial activity through sequential burst/sustained ion release.<sup>59</sup>

AgNP hybridization has also heightened the efficacy of antibiotics. Ullah *et al.* conjugated tobramycin to graphene-coated AgNPs and reported severe cell wall damage among *E. coli*,<sup>366</sup> and Al-Obaidi *et al.* developed hybrid silver-chitosan-ciproflaxin nanoparticles to deliver antibiotics to the alveoli *via* inhalation.<sup>367</sup> AgNPs have also been the foundation for targeted antibiotic nanosystems, with one study reporting that selective wall binding domains allow for specific targeting of *B. anthracis* over *B. subtilis* or *S. aureus*, suggesting the ability to eliminate pathogen without compromising the gut microbiota.<sup>368</sup> As the extent of the influence of the gut microbiota is still poorly understood, the development of targeted antibiotic delivery systems are expected to be a growing area of research in upcoming years.

Though less prevalent than silver-based antimicrobial hybrid nanosystems, AuNPs can also form the basis for nanoparticle-like antibacterials. AuNPs have been conjugated with antimicrobial peptides to vastly improve the disinfection capability of the peptide alone<sup>369</sup> As such, this system utilizes the antimicrobial properties of an organic component with the delivery function of an inorganic component, whereas the previously discussed systems used the antimicrobial properties of AgNPs with delivery conferred by organic materials. AuNP hybrids have also been loaded with conventional antibiotics. Monti *et al.* performed a computational/experimental study and found that gentamicin release from an AuNP-chitosan core-shell nanoparticle can be controlled by varying the polymer to antibiotic ratio and the deposition pattern of the adsorbed layer.<sup>370</sup> An inverse architecture of chitosan-poly(acrylic acid) coated with AuNPs was developed as a photosensitive system capable of disinfection when exposed to NIR.<sup>371</sup> Alternatively, AuNRs have been incorporated into RBC and platelet membranes to create hybrid nanosystems capable of acoustic propulsion and removal of pathogenic bacteria and toxins.<sup>372</sup> Perhaps the most interesting application of gold in antibacterials is in reversing developed antibiotic resistance. When combined with ampicillin and daptomycin, AuNC hybrids have been shown to kill antibiotic-resistant bacteria.<sup>373, 374</sup> With the selection for superbugs a concern, the ability to kill antibiotic-resistant bacteria is an essential development in drug research.

Tertiary to silver and gold, copper has also formed the inorganic portion of antimicrobial hybrid nanosystems. Copper displays antibacterial properties similar to silver; it is thus unsurprising that copper-chitosan hybrids have shown efficacy in killing cariogenic *S. mutans*.<sup>375</sup> In another study, Elfeky *et al.* developed a cellulose nanocrystal loaded with copper/ZnO that displayed effective photo-induced efficacy against bacteria and *A. stephensi* larvae, a known vector for malaria.<sup>376</sup> Finally, atypical inorganic building blocks utilized in antibacterial hybrid nanosystems have included ZnO, cerium oxide, and silica.<sup>377, 378</sup>

Hybrid antimicrobials offer several advantages over their non-hybridized counterparts. AgNPs are highly effective antibacterials whose drawbacks can be negated by hybridization with polymers and other organics. Additionally, hybridization allows for targeted delivery

of antibiotics, which could become crucial as we continue to learn about the effect of the gut microbiota on human health. Furthermore, hybridization allows for combination phototherapy in addition to antimicrobial activity, providing heretofore unrealized control in clinical settings. Finally, the discovery that gold hybrids can reverse antibiotic resistance in bacterial strains could prove essential with current concerns about human selection for superbugs. As such, antimicrobial nanosystems are yet another area where hybridization can offer great strides forward over current practices.

## Vaccines

Vaccines have saved approximately 40,000 lives per birth cohort, making them among the most vital contributions of modern medicine.<sup>379</sup> Despite our advances, we still face challenges in vaccine development such as vaccine efficacy and thermostability that can be addressed by hybrid nanosystems. The improved thermostability of hybrid nanovaccines is notable because vaccine stability greatly affects the efficacy of immunization programs across the world. Metal nanoparticles form the basis of several hybrid vaccines. As the size of a nanoparticle-based vaccine influences its efficacy, the high tunability and low PDI of AuNPs make them especially useful for vaccine hybrids.<sup>380</sup> AuNP-based vaccines have been developed against pathogen ranging from dengue virus to *Burkholderia mallei* and enterohemorrhagic *E. coli*.<sup>381–383</sup> Al-Deen *et al.* developed a DNA-based malaria vaccine from IONPs coated in PEI, claiming magnetic targeting and pH-responsive DNA condensation.<sup>384</sup> Others report that hybridized silica-PEI vaccines show improved thermostability and shelf-life over conventional vaccines<sup>385</sup> and that silica-cationic polymer hybridization can form the basis for oral vaccines.<sup>386</sup> Other mesoporous materials have been shown useful for codelivery of antigen and adjuvant. Yang *et al.* reported a redox-responsive hybrid vaccine based on a MOF (MIL-101-Fe-NH<sub>2</sub>) nanoparticle to deliver antigen and adjuvant simultaneously, which suggests that MOFs can improve immune-response to vaccines through stabilization and co-delivery.<sup>387</sup>

Cancer immunotherapy is another area of rapid vaccine development. Hybrid nanosystems are useful cancer vaccines and have been constructed in a variety of materials and architectures. In one example, hollow MSNs hybridized with PEI have shown improved Th1 antitumor immunity and memory in comparison to hollow MSNs alone.<sup>302</sup> MSNs coated in dextran and encapsulated within cancer cell membranes have shown similar potential for cancer immunotherapy.<sup>174</sup> Others have designed zinc phosphate-lipid hybrids to induce immunity against melanoma<sup>303</sup> and ZnO nanowires complexed with poly-L-lactide microfibers to effectively deliver colorectal cancer antigen to dendritic cells.<sup>304</sup> As such, vaccine efficacy and clinical translation may be improved noticeably by hybrid nanosystems.

Vaccines based on hybridization show several benefits over alternatives. In addition to thermostability, hybrid nanosystems provide versatility to treat and prevent a variety of diseases, and it is here that we see MSNs and MOFs utilized widely for their carrying capacity and delivery capabilities. Interestingly, the range of maladies that can be addressed *via* hybrid nanovaccines is broad, yet the number of publications in this area is smaller than in other areas. Though this could be seen as a mark against hybridization, the success of the

published hybrid vaccines suggest rather that the field is young and that further development should be expected in coming years.

## Detection and imaging

Hybrid nanoarchitectures can dramatically improve the existing technologies employed in biomedical detection and imaging. In these applications, inorganic building blocks typically provide responsivity to external radiation or magnetism while organic components contribute to biodistribution and functionality. As such, the following section provides an overview of current hybrid nanosystems used for MRI and photoimaging in addition to systems developed to detect and monitor specific biomolecules *in vivo*.

### Imaging

MRI functions by aligning the protons in a tissue with magnetic field, knocking them out of alignment with the field *via* radio waves, and recording the image produced as the protons realign with the magnetic field. MRI contrast agents (probes) such as chelated gadolinium or IONPs assist proton realignment and decrease the longitudinal relaxation time ( $T_1$ ), thus improving image clarity.<sup>388</sup> As such, gadolinium has been incorporated into a polymer-liposome system to allow the selective accumulation in the tumor microenvironment *via* the enhanced permeability and retention EPR effect.<sup>389</sup> Another design coated superparamagnetic IONPs with exopolysaccharide and reported dose-dependent  $T_1$  decreases.<sup>390</sup> Where hybrid nanoprobe improve on non-hybrid contrast agents is in stimulus sensitivity. Through rational design, nanoprobe can alter contrast properties in response to endogenous stimuli. Kim *et al.* report a hybridization of an IONP coated in manganese oxide and polysorbate 80 that responds to intracellular glutathione to lower  $T_1$  only in reductive environments.<sup>391</sup> Similarly, the Wang lab developed pH-responsive magnesium oxide/silica core/shell nanoparticle functionalized with FA to actively target the tumor microenvironment. As the manganese oxide was degraded in the acidic tumor,  $Mn^{2+}$  ions acted as  $T_1$  contrast agents. As an additional measure, coumarin-545T was incorporated within the silica shell to allow fluorescence imaging as an alternative cancer visualization tool.<sup>392</sup>

Along with MRI, hybrid nanosystems exhibit advantages in both fluorescence and photoacoustic imaging. When AuNRs were encapsulated within liposomes containing indocyanine green, combination photoacoustic tomography and fluorescence imaging improved the detection and resolution of liver cancer *in vivo* ten-fold.<sup>393</sup> Lipid-encapsulated AuNPs can also improve the detection of biological autoluminescence by penetrating the mitochondrial membrane and enhancing ROS production, greatly improving the utility of biological autoluminescence as a diagnostic tool.<sup>394</sup> Furthermore, dendrimer-entrapped cubic IONPs have been conjugated with HSP90 $\alpha$  mRNA attached to a quenched fluorophore; when the nanoparticles were taken up by cells overexpressing HSP90 $\alpha$ , the fluorescence was recovered allowing their location to be determined with high specificity through both fluorescence imaging and MRI.<sup>160</sup> Finally, RBC membrane-containing upconversion nanoparticles have shown promise for *in vivo* tumor imaging through active targeting and reduced protein corona formation.<sup>176</sup> These functions have only been

performed by inorganic-organic nanosystems, suggesting that hybridization will continue to be relevant to biomedical imaging.

### Detection and monitoring

Hybrid nanosystems have been developed for several detection and monitoring applications, including glucose monitoring,<sup>395</sup> cancer diagnosis,<sup>31</sup>, and detection of viral infections.<sup>396</sup> Gold-based hybridizations are prevalent, as the biocompatibility, optical properties, and ability of gold to adsorb nucleic acids lends it widespread value. AuNPs and AuNCs have been incorporated into liposomes to create nanoscale detection kits: Tang *et al.* designed a liposome-based system for glucose detection through selective dequenching of an AuNP-associated fluorophore,<sup>395</sup> whereas Tao *et al.* used the peroxidase activity of AuNCs in a colorimetric assay to detect HER2-positive breast cancer.<sup>31</sup> By replacing AuNPs with IONPs, NIR- and magnetic field-responsive liposome hybrids have demonstrated capabilities to monitor cellular functions to identify targets for cancer therapies.<sup>397</sup>

Monitoring biomolecules such as glucose has been advanced by hybrid nanosystems. Nanoparticle building blocks act as supports for the immobilization of enzymes or perform as mediators or as signal amplifiers. Carbon-based nanomaterials offer chemical inertness and low background current for glucose monitoring. Paper-based technologies enabled low-cost sensors using human sweat and blood to characterize the amount of blood glucose.<sup>398</sup> In a recent study, a photolithographic screen-printing was used to introduce an aldehyde functionalized along with a reference electrode layer to immobilize glucose oxidase (GOx). A GO-tetraethylene pentamine (rGO-TEPA/PB)-based electrode was used as the electrochemically sensitive electrode for H<sub>2</sub>O<sub>2</sub> detection (the enzyme-catalyzed product).<sup>399</sup> The proposed sensor responded linearly between 0.1 mM and 25 mM with a 25 μM detection threshold. Metallic nanoparticles can also immobilize enzymes in glucose detection biosensors. A non-invasive wireless glucose biosensor was proposed by Kim *et al.* where a hyaluronate-gold nanoparticle/glucose oxidase (HA-AuNP/GOx) complex was prepared by conjugating thiolated HA to AuNPs. The prepared conjugate was capable of physical binding of GOx and characterized with slow water evaporation as well as fast response (5 s) and high sensitivity of 2.37 μA·dL/mg·cm<sup>2</sup>. Hybrid nanosystems for glucose monitoring are not limited to carbon or metal nanoparticles. Metal oxides<sup>400</sup> and SiO<sub>2</sub><sup>401</sup> are among other candidates for biosensor development. Layered fabrication methods to integrate nanoparticles with polymer matrices are critical in the development of next-generation biosensors.

Inorganic nanoparticle-carbon hybrids have also been used to detect small molecule drugs through accelerated electron transfer and photoluminescence. AuNPs coupled with GQDs or GO have formed systems capable of detecting the antibiotic kanamycin,<sup>402, 403</sup> and AuNPs have also been combined with L-cysteine- and penicillinase-functionalized Pt nanowires to detect penicillin and tetracycline as residual antibiotics in food animals.<sup>404</sup> In other carbon hybrids, GO and silver co-deposited on silver-copper alloy fibers have been utilized to detect sulfadiazine and sulfamethoxazole,<sup>405</sup> while copper oxide nanospheres coated with multiwalled CNTs are sensitive to flunitrazepam, a hypnotic drug utilized in anesthesia.<sup>406</sup>

Virus detection is a third area where nanohybridization excels, with nanohybrids having been developed to detect viruses ranging from human papillomavirus (HPV) and influenza to bursal disease. Jimenez *et al.* reported a hybrid nanosystem containing magnetic glass nanoparticles functionalized with a DNA probe coupled to CdTe/ZnSe core/shell quantum dots for the detection of HPV; interestingly, the system was capable of distinguishing between patients with HPV infections that did and did not develop cancer as a result of infection.<sup>407</sup> AuNPs have been linked to peptide nucleic acids for influenza detection, with AuNP aggregation allowing spectrophotometric detection.<sup>32</sup> Alternatively, functionalized AuNP/IONPs conjugated to CNTs demonstrate the ability to detect influenza DNA *via* conductivity changes.<sup>109</sup> Finally, fluorescence resonance energy transfer (FRET) can be utilized to detect the presence of biomolecules, as FRET properties can be altered through substrate binding;<sup>408</sup> FRET was employed in an AuNP-quantum dot-rhodamine hybrid to detect bursal disease virus.<sup>396</sup> As such, hybrid nanosystems are well-situated for applications in detection and imaging.

In detection and imaging, carbon and gold building blocks are especially suited for their combination of conductive and optical properties. Whereas non-hybridized nanosystems may be limited in their capacities to alter their properties when in contact with a target molecule, hybrid systems allow detection through changes in conductivity, absorption, fluorescence, T<sub>1</sub> relaxation time, and FRET. This range of methods techniques available allows hybrid nanosystems to display flexibility and sensitivity in regions that were previously constrained. Table 2 provides an overview of hybrid nanosystems in non-cancer applications.

## Theranostics

To this point, biomedical hybrid nanosystems have been shown effective for targeted delivery, phototherapy, tissue engineering, improved vaccines and antibiotics, and detection of biomolecules; however, we have not yet discussed imaging in concert with therapy. Theranostics is a rapidly growing field in which therapeutic and diagnostic tools are combined for simultaneous imaging and treatment. As expected, hybrid nanosystems are well-situated for theranostic use and have been increasingly employed for such in recent years.

### Drug/gene delivery theranostics

Hybrid drug- and gene-based theranostic systems have been designed in a variety of architectures. Inorganic NP-liposome systems are effective theranostics when constructed from several different building blocks. AuNPs and GQDs have been incorporated into DOX-loaded liposomes that display photosensitive drug release and *in vivo* tumor diagnosis through enhanced contrast and emissivity on X-ray computed tomography (CT).<sup>427</sup> AuNRs and ammonium bicarbonate encapsulated in liposomes have formed thermoresponsive nanosystems that generate bubbles for enhanced ultrasound imaging,<sup>428</sup> and gold nanoshells have been incorporated into bubble-generating, dual ligand-functionalized liposomes displaying increased uptake in MCF-7 cells.<sup>429</sup> Theranostic magnetoliposomes are also employed to improve MRI visualization through T<sub>1</sub> reduction and magnetic targeting.<sup>430</sup>

Several magnetoliposomes have been developed to deliver chemotherapeutics to cancer cells, using targeting ligands and functional moieties to improve delivery to the tumor environment and confer stimulus sensitivity.<sup>110, 431–434</sup> Theranostic magnetoliposomes can also display fluorescent properties and generate bubbles for observation *via* fluorescence and ultrasound imaging in addition to MRI.<sup>433, 435</sup> Similarly, IONPs and siRNA encapsulated within stem cell membranes have formed hybrid nanosystems capable of combination gene therapy and PTT in addition to MRI.<sup>179</sup>

Inorganic NPs conjugated with polymers and dendrimers are also useful theranostic vessels. Au nanostar-PAMAM hybrids have delivered siRNA to tumors in combination with PTT and CT imaging,<sup>436</sup> whereas gold-silver alloy nanoclusters conjugated with PEI show improved fluorescent signal and transfection efficiency over each constituent building block.<sup>437</sup> In another hybridization, AuNR-hydrogels were loaded with therapeutics to create bubble-free theranostic devices for ultrasound imaging.<sup>438</sup> In an especially intriguing combination, a nanohybrid made up of AuNRs, MSNs, quantum dots, and poly(glycidyl methacrylate) delivered nucleic acids and chemotherapeutics along with AuNR-mediated PTT and CT/photoacoustic imaging.<sup>439</sup> MSNs have also been hybridized with thermosensitive polymers to produce nanosystems displaying photoacoustic and fluorescence amplification, NIR-triggered release of SN38, and utility in positron emission tomography (PET) when functionalized with <sup>64</sup>Cu.<sup>440</sup> Additionally, theranostic IONP-polymer nanosystems have been employed in cancer immunotherapy, with one such architecture inducing immune responses against melanoma cells while allowing the vaccine to be tracked *in vivo via* MRI.<sup>441</sup> Finally, a Bi<sub>2</sub>S<sub>3</sub>-PLGA nanocapsule was constructed as an ultrasound contrast and therapeutic for high-intensity focused ultrasound therapy. The system also offered dual functionality by inducing radiosensitivity in prostate cancer cells under X-ray radiation.<sup>442</sup>

Several atypical geometries for hybrid drug/gene theranostics exist. AuNPs have been combined with bovine serum albumin (BSA) and MSNs to co-deliver gemcitabine and doxorubicin while allowing *in vivo* fluorescence imaging.<sup>443</sup> Gold nanocages have also been capped with BSA to enable optoacoustic tomography imaging along with chemotherapy and PTT.<sup>444</sup> In another study, CPNP cores were hybridized with rare earth nanoparticles and targeting DNA to create pH-responsive drug delivery systems with lanthanide luminescence-based imaging and magnetic resonance.<sup>445</sup> Furthermore, core-shell hybrids consisting of carbon-coated IONPs decorated with AgNPs showed efficient DOX release under NIR radiation as well as fluorescence and functionality as an MRI probe.<sup>49</sup> Finally, ZIF-8 has been hybridized around palladium nanosheets, loaded with DOX, and conjugated with PDA to produce a dual-responsive pH- and NIR-triggered drug release in conjunction with photoacoustic imaging.<sup>84</sup> As such, these systems display effectivity in theranostic applications despite not falling in the more common hybrid architecture categories.

### Phototheranostics

Hybrids combining PDT/PTT and imaging have largely exploited carbon-based building blocks such as GQDs, C60, GO, and carbon nitride (CN). CN is a photocatalyst for water decomposition and can generate sustainable levels of oxygen to relieve



tumor hypoxia and facilitate PDT in conjunction with ultrasound and fluorescence imaging.<sup>446</sup> Correspondingly, GQDs exhibit fluorescent properties and have been adapted as photosensitizers.<sup>108</sup> When utilized in conjunction with mesoporous silica, hybrid CN/GQDs displayed ultrasound and fluorescence imaging combined with PDT uninhibited by hypoxic tumor conditions.<sup>446</sup> CN nanosheets also show photodynamic and fluorescent properties that promote effective therapy and imaging when functionalized with DNA hairpin probes.<sup>113</sup> Fullerene is also useful in this application. IONP-C60s display magnetic targeting capabilities in conjunction with MRI contrast, while AuNP-C60s have been used as probes in X-ray cancer diagnosis.<sup>447, 448</sup> Finally, gadolinium nanoparticles on GO have displayed MRI-guided photothermal properties along with DOX loading for combination chemo-phototheranostics.<sup>107</sup>

The nanosystems about to be described draw from all aspects of biomedical hybridization and are among the most impressive developments in the field in recent years. When hybridized with poly(allylamine)-modified black phosphorus quantum dots, AuNPs displayed enhanced PDT/PTT mediated by plasmon-induced resonant energy transfer in conjunction with photoacoustic imaging and MRI.<sup>449</sup> AuNRs incorporated into a functional DNA-origami nanostructure have shown enhanced *in vivo* diagnostic and therapeutic properties through optoacoustic imaging and PTT.<sup>450</sup> Similarly, Song *et al.* utilized ultrasmall AuNRs within PLGA to create vesicles capable of EPR-mediated tumor accumulation, photoacoustic imaging, and rapid excretion upon nanosystem dissociation.<sup>451</sup> Likewise, Huang *et al.* coated AuNRs in mesoporous silica functionalized with upconversion nanoparticles and photosensitizers to create a nanobubble capable of plasmonically-enhanced PTT and PDT in addition to fluorescent imaging and ultrasound.<sup>452</sup> Furthermore, rattle-type MSN-PDA nanoparticles have been loaded with GOx to create nanohybrid theranostics capable of photoacoustic imaging and low-temperature PTT through GOx suppression of heat shock proteins HSP70 and HSP90.<sup>81</sup> IONPs have been encased into cancer cell membranes alone or with Ce6 to produce nanosystems for combination MRI, fluorescence imaging, and PDT/PTT.<sup>177, 180, 453</sup> Finally, mesoporous copper sulfide nanoparticles have been coupled with an amphiphilic copolymer to create a pH/redox responsive DDS/PTT hybrid capable of fluorescence and photoacoustic imaging.<sup>454</sup> Accordingly, theranostic hybrid nanosystems are among the most impressively engineered nanostructures today.

Theranostic application is where biomedical hybridization surpasses all competition. As with delivery applications and combination therapies, AuNPs and IONPs are widely utilized within liposomes and polymers, and these systems provide numerous expected benefits including real-time observation of therapeutic delivery. However, several atypical hybrid architectures have also been proposed, which not only expand the practical functions of hybrids but also introduce paradigms through which we may view theranostic challenges. For example, protein-conjugated nanoparticles appear promising in drug delivery theranostics, while carbon-based building blocks are useful for phototheranostics. Finally, theranostics is where we see the most creative designs for hybrid nanosystems, with each offering one or more methods of detecting, imaging, and treating maladies *in vivo*. We expect that theranostic hybrids will be one of the major areas of nanosystem

development over the next half-decade. Table 3 displays several notable hybrid nanosystems in theranostics, and Figure 8 displays selected hybrid nanosystems discussed thus far.

## Clinical trials

Despite the thoroughly-published efficacy of hybrid nanosystems in pre-clinical evaluations, few have yet entered into clinical trials. Several current clinical trials are investigating AGuIX, a gadolinium-polysiloxane hybrid, for use as an imaging agent in diagnosis, imaging, and treatment of brain metastases and gynecological cancer. Another hybrid of silica, hydrophilic polymers, and targeting peptides is being studied for use in real-time imaging of head and neck melanoma, breast cancer, and colorectal cancer. Finally, in a Phase 1 study targeting Type 1 diabetes, peptide-functionalized AuNPs are being tested to determine their safety and effect in mitigating the body's destruction of insulin-producing cells. Current human trials of hybrid nanosystems are limited, especially when noting that there are over 350,000 ongoing clinical trials worldwide (as per [ClinicalTrials.gov](https://clinicaltrials.gov)). Nevertheless, the recent growth of publications pertaining to hybrid nanosystems suggests that clinical trials incorporating them will expand in the coming years. Table 4 summarizes the active clinical trials involving hybrid nanosystems.

## Concluding remarks and future perspectives

Nanotechnology has made notable contributions to the biomedical field within the past two decades. Nanosystems have vastly improved our ability to selectively deliver therapeutics, noninvasively visualize and diagnose maladies, detect biomolecules of interest, and harness light for therapeutic purposes. Despite this progress, further obstacles remain and researchers are turning increasingly to hybridization as a solution. Hybrid nanosystems have improved the efficacy of monotherapies while simultaneously welcoming combination therapies. Single-component inorganic or organic nanosystems represent an “all-or-nothing” approach in which the utility of the system is intrinsically tied to a single function. Hybrid nanosystems, on the other hand, bring flexibility and versatility to the biomedical research table, with many performing several functions within a single design. In these cases, a system's utility can be based on several tasks rather than just one. This could be advantageous in the coming years, as regulatory agencies are more apt to fast-track therapeutic compounds that have been previously approved for other applications. Additionally, several groups have shown that a broad approach to the treatment of human disease offered through hybridization provides previously unattainable treatment opportunities, an exciting development for medical science.

We anticipate that hybrid nanosystem development will continue to increase in the coming years especially in combination therapy, imaging, and theranostics. Moreover, we expect that clinical trials involving hybrid nanosystems will expand greatly in the next decade just as publications of preclinical investigations have since 2010. For this to occur, however, the incongruence of complexity and translational compatibility must be reconciled. Despite the promise of increasingly complex nanosystems, increased intricacy can also introduce challenges in reproducibility, scale-up/out, and quality control. As a result, translation from the benchtop to the clinic can present a notable hurdle, and

successful developers must keep this in mind throughout the design process. In addition to complexity, therapy cost is a notable concern for hybrid nanosystems. The rising cost of healthcare is a pressing challenge, especially in the United States; as such, the increased material resources and extended synthesis procedures that hybrid nanosystems require over non-hybridized alternatives must be justified in therapeutic efficacy. Moreover, translatable hybrid nanosystems must produce clinically-significant improvements to justify the increase in treatment cost. These realities may be reflected in the relative dearth of ongoing clinical trials featuring hybrid nanosystems in comparison to both the number of systems in development and number of ongoing trials. We expect that the number of hybrid nanosystems in clinical trials will increase as the challenges of complexity, mass production, and cost are addressed.

Hybrid nanosystems possess enormous potential for both bench and bedside applications. It may be used as discovery tools to unravel mysteries of many physiological and pathological conditions such as wound healing, cancer, diabetes, cardiovascular, neurodegenerative diseases to name a few. Understanding biological effects of these nanoparticles, particularly long-term effects and toxicity is essential in order to translate their applications from bench to bedside. On the other hand, understanding how these hybrid nanosystems interacts with biological systems such as cells, tissues, biological fluids and their mechanism of interaction may provide opportunities to design hybrid nanosystems for personalized medicine. Nevertheless, based on the progress summarized in this review we expect that hybrid nanosystems will continue to grow in prevalence and importance in the biomedical field in upcoming years.

## Acknowledgements

This work was supported by 1R01CA253391-01A1, CA213278, 2CA136494 and P30 CA225500 Team Science grants. In addition, this work is also supported by the Peggy and Charles Stephenson Endowed Chair fund and TSET Scholar fund to PM.

## References

1. Mendel G, Experiments in Plant Hybridization (1865). Verhandlungen Des Naturforschenden Vereins Brünn 1996, Accessed 23 July, 2020, <http://old.esp.org/foundations/genetics/classical/gm-65-a.pdf>.
2. Wyczalek FA, Market Mature 1998 Hybrid Electric Vehicles. IEEE Aerosp. Electron. Syst. Mag 1999, 14 (3), 41–44.
3. Elghanian R; Storhoff JJ; Mucic RC; Letsinger RL; Mirkin CA, Selective Colorimetric Detection of Polynucleotides Based on the Distance-Dependent Optical Properties of Gold Nanoparticles. Science 1997, 277 (5329), 1078–81. [PubMed: 9262471]
4. Caruso F; Caruso RA; Mohwald H, Nanoengineering of Inorganic and Hybrid Hollow Spheres by Colloidal Templating. Science 1998, 282 (5391), 1111–1114. [PubMed: 9804547]
5. Das S; Jain TK; Maitra A, Inorganic-Organic Hybrid Nanoparticles from *n*-Octyl Triethoxy Silane. J. Colloid Interface Sci 2002, 252 (1), 82–88. [PubMed: 16290765]
6. Katagiri K; Ariga K; Kikuchi J. i., Preparation of Organic-Inorganic Hybrid Vesicle “Cerasome” Derived from Artificial Lipid with Alkoxysilyl Head. Chem. Lett 1999, 28 (7), 661–662.
7. von Werne T; Patten TE, Atom Transfer Radical Polymerization from Nanoparticles: A Tool for the Preparation of Well-Defined Hybrid Nanostructures and for Understanding the Chemistry of Controlled/“Living” Radical Polymerizations from Surfaces. J. Am. Chem. Soc 2001, 123 (31), 7497–7505. [PubMed: 11480969]

8. Aymonier C; Schlotterbeck U; Antonietti L; Zacharias P; Thomann R; Tiller JC; Mecking S, Hybrids of Silver Nanoparticles with Amphiphilic Hyperbranched Macromolecules Exhibiting Antimicrobial Properties. *Chem. Commun* 2002, 24, 3018–3019.
9. Nuß S; Böttcher H; Wurm H; Hallensleben ML, Gold Nanoparticles with Covalently Attached Polymer Chains. *Angew. Chem. Int. Ed* 2001, 40 (21), 4016–4018.
10. Ruiz-Hitzky E, Functionalizing Inorganic Solids: Towards Organic-Inorganic Nanostructured Materials for Intelligent and Bioinspired Systems. *Chem. Rec* 2003, 3 (2), 88–100. [PubMed: 12731079]
11. Elahi N; Kamali M; Baghersad MH, Recent Biomedical Applications of Gold Nanoparticles: A Review. *Talanta* 2018, 184, 537–556. [PubMed: 29674080]
12. Hamzawy MA; Abo-Youssef AM; Salem HF; Mohammed SA, Antitumor Activity of Intratracheal Inhalation of Temozolomide (TMZ) Loaded into Gold Nanoparticles and/or Liposomes against Urethane-Induced Lung Cancer in BALB/c Mice. *Drug Deliv.* 2017, 24 (1), 599–607. [PubMed: 28240047]
13. Wang J; Zhu C; Han J; Han N; Xi J; Fan L; Guo R, Controllable Synthesis of Gold Nanorod/Conducting Polymer Core/Shell Hybrids toward *in Vitro* and *in Vivo* Near-Infrared Photothermal Therapy. *ACS Appl. Mater. Interfaces* 2018, 10 (15), 12323–12330. [PubMed: 29595952]
14. Jiang J; Zhong X; Zhang H; Wang C, A Novel Corona Core–Shell Nanoparticle for Enhanced Intracellular Drug Delivery. *Mol. Med. Rep* 2020, 21 (4), 1965–1972. [PubMed: 32319626]
15. Morgan E; Wupperfeld D; Morales D; Reich N, Shape Matters: Gold Nanoparticle Shape Impacts the Biological Activity of siRNA Delivery. *Bioconjug. Chem* 2019, 30 (3), 853–860. [PubMed: 30735028]
16. Gao F; Zheng W; Gao L; Cai P; Liu R; Wang Y; Yuan Q; Zhao Y; Gao X, Au Nanoclusters and Photosensitizer Dual Loaded Spatiotemporal Controllable Liposomal Nanocomposites Enhance Tumor Photodynamic Therapy Effect by Inhibiting Thioredoxin Reductase. *Adv. Healthc. Mater* 2017, 6 (7), 1601453, 1–12.
17. Chuang E-Y; Lin C-C; Chen K-J; Wan D-H; Lin K-J; Ho Y-C; Lin P-Y; Sung H-W, A FRET-Guided, NIR-Responsive Bubble-Generating Liposomal System for *in Vivo* Targeted Therapy with Spatially and Temporally Precise Controlled Release. *Biomaterials* 2016, 93 (C), 48–59. [PubMed: 27070992]
18. Arnida; Janát-Amsbury MM; Ray A; Peterson CM; Ghandehari H, Geometry and Surface Characteristics of Gold Nanoparticles Influence Their Biodistribution and Uptake by Macrophages. *Eur. J. Pharm. Biopharm* 2011, 77 (3), 417–423. [PubMed: 21093587]
19. Zhang Y; Xiong X; Huai Y; Dey A; Hossen M; Roy R; Elechalawar C; Rao G; Bhattacharya R; Mukherjee P, Gold Nanoparticles Disrupt Tumor Microenvironment - Endothelial Cell Cross Talk to Inhibit Angiogenic Phenotypes *in Vitro*. *Bioconjug. Chem* 2019, 30 (6), 1724. [PubMed: 31067032]
20. Patra C; Jing Y; Xu Y-H; Bhattacharya R; Mukhopadhyay D; Glockner J; Wang J-P; Mukherjee P, A Core-Shell Nanomaterial with Endogenous Therapeutic and Diagnostic Functions. *Cancer Nanotechnol.* 2010, 1 (1), 13–18. [PubMed: 21318050]
21. Saber MM; Bahrainian S; Dinarvand R; Atyabi F, Targeted Drug Delivery of Sunitinib Malate to Tumor Blood Vessels by cRGD-Chitosan-Gold Nanoparticles. *Int. J. Pharm* 2017, 517 (1–2), 269–278. [PubMed: 27956189]
22. Hossen MN; Wang L; Chinthalapally HR; Robertson JD; Fung K-M; Wilhelm S; Bieniasz M; Bhattacharya R; Mukherjee P, Switching the Intracellular Pathway and Enhancing the Therapeutic Efficacy of Small Interfering RNA by Auroliposome. *Sci. Adv* 2020, 6 (30), eaba5379, 1–16.
23. Kokkin DL; Zhang R; Steimle TC; Wyse IA; Pearlman BW; Varberg TD, Au-S Bonding Revealed from the Characterization of Diatomic Gold Sulfide, AuS. *J. Phys. Chem. A* 2015, 119 (48), 11659–11667. [PubMed: 26535608]
24. Rahme K; Guo J; Holmes JD, Bioconjugated Gold Nanoparticles Enhance siRNA Delivery in Prostate Cancer Cells. *Methods Mol. Biol* 2019, 1974, 291–301. [PubMed: 31099011]
25. Amendola V; Pilot R; Frascioni M; Maragò OM; Iatù MA, Surface Plasmon Resonance in Gold Nanoparticles: A Review. *J. Phys.: Condens. Matter* 2017, 29, 203002, 1–48. [PubMed: 28426435]

26. Yu H; Peng Y; Yang Y; Li Z-Y, Plasmon-Enhanced Light-Matter Interactions and Applications. *npj Comput. Mater* 2019, 5 (1), 45, 1–14.
27. Dreaden EC; Alkilany AM; Huang X; Murphy CJ; El-sayed MA, The Golden Age: Gold Nanoparticles for Biomedicine. *Chem. Soc. Rev* 2012, 41 (7), 2740–2779. [PubMed: 22109657]
28. Knights-Mitchell SS; Romanowski M, Near-Infrared Activated Release of Doxorubicin from Plasmon Resonant Liposomes. *Nanotheranostics* 2018, 2 (4), 295–305. [PubMed: 29977741]
29. Ni Q; Teng Z; Dang M; Tian Y; Zhang Y; Huang P; Su X; Lu N; Yang Z; Tian W; Wang S; Liu W; Tang Y; Lu G; Zhang L, Gold Nanorod Embedded Large-Pore Mesoporous Organosilica Nanospheres for Gene and Photothermal Cooperative Therapy of Triple Negative Breast Cancer. *Nanoscale* 2017, 9 (4), 1466–1474. [PubMed: 28066849]
30. Tsai M-F; Chang S-HG; Cheng F-Y; Shanmugam V; Cheng Y-S; Su C-H; Yeh C-S, Au Nanorod Design as Light-Absorber in the First and Second Biological Near-Infrared Windows for *in Vivo* Photothermal Therapy. *ACS Nano* 2013, 7 (6), 5330–5342. [PubMed: 23651267]
31. Tao Y; Li M; Kim B; Auguste DT, Incorporating Gold Nanoclusters and Target-Directed Liposomes as a Synergistic Amplified Colorimetric Sensor for HER2-Positive Breast Cancer Cell Detection. *Theranostics* 2017, 7 (4), 899–911. [PubMed: 28382162]
32. Kumar N; Bhatia S; Pateriya AK; Sood R; Nagarajan S; Murugkar HV; Kumar S; Singh P; Singh VP, Label-Free Peptide Nucleic Acid Biosensor for Visual Detection of Multiple Strains of Influenza A Virus Suitable for Field Applications. *Anal. Chim. Acta* 2020, 1093, 123–130. [PubMed: 31735205]
33. Freitas de Freitas L; Varca GHC; Dos Santos Batista JG; Benévolo Lugão A, An Overview of the Synthesis of Gold Nanoparticles Using Radiation Technologies. *Nanomaterials* 2018, 8 (11), 939, 1–23.
34. Phan CM; Nguyen HM, Role of Capping Agent in Wet Synthesis of Nanoparticles. *J. Phys. Chem. A* 2017, 121 (17), 3213–3219. [PubMed: 28398756]
35. Yeh Y-C; Creran B; Rotello VM, Gold Nanoparticles: Preparation, Properties, and Applications in Bionanotechnology. *Nanoscale* 2012, 4 (6), 1871–1880. [PubMed: 22076024]
36. Correard F; Maximova K; Estève M-A; Villard C; Roy M; Al-Kattan A; Sentis M; Gingras M; Kabashin AV; Braguer D, Gold Nanoparticles Prepared by Laser Ablation in Aqueous Biocompatible Solutions: Assessment of Safety and Biological Identity for Nanomedicine Applications. *Int. J. Nanomed* 2014, 9, 5415–5430.
37. Pandey S; Goswami GK; Nanda KK, Green Synthesis of Polysaccharide/Gold Nanoparticle Nanocomposite: An Efficient Ammonia Sensor. *Carbohydr. Polym* 2013, 94 (1), 229–234. [PubMed: 23544533]
38. Liu F; Kong FF; Li QP; Yuan H; Du YZ; Hu FQ; Sun JH; You J, Low Molecular Weight Polyethylenimine-Conjugated Gold Nanospheres: A Platform for Selective Gene Therapy Controlled by Near-Infrared Light. *Nanomedicine (London, U. K.)* 2017, 12 (5), 511–534.
39. Sardo C; Bassi B; Craparo EF; Scialabba C; Cabrini E; Dacarro G; D'Agostino A; Taglietti A; Giammona G; Pallavicini P; Cavallaro G, Gold Nanostar-Polymer Hybrids for siRNA Delivery: Polymer Design towards Colloidal Stability and *in Vitro* Studies on Breast Cancer Cells. *Int. J. Pharm* 2017, 519 (1–2), 113–124. [PubMed: 28093325]
40. Zhu H; Liu W; Cheng Z; Yao K; Yang Y; Xu B; Su G, Targeted Delivery of siRNA with pH-Responsive Hybrid Gold Nanostars for Cancer Treatment. *Int. J. Mol. Sci* 2017, 18 (10), 2029, 1–15.
41. Aromal SA; Babu KV; Philip D, Characterization and Catalytic Activity of Gold Nanoparticles Synthesized Using Ayurvedic Arishtams. *Spectrochim. Acta, Part A* 2012, 96, 1025–1030.
42. Grzelczak M; Pérez-Juste J; Mulvaney P; Liz-Marzán LM, Shape Control in Gold Nanoparticle Synthesis. *Chem. Soc. Rev* 2008, 37 (9), 1783–1791. [PubMed: 18762828]
43. Cao J; Sun T; Grattan KTV, Gold Nanorod-Based Localized Surface Plasmon Resonance Biosensors: A Review. *Sens. Actuators, B* 2014, 195 (C), 332–351.
44. Pérez-Juste J; Pastoriza-Santos I; Liz-Marzán LM; Mulvaney P, Gold Nanorods: Synthesis, Characterization and Applications. *Coord. Chem. Rev* 2005, 249 (17), 1870–1901.
45. Vines JB; Yoon J-H; Ryu N-E; Lim D-J; Park H, Gold Nanoparticles for Photothermal Cancer Therapy. *Front. Chem* 2019, 7, 167, 1–16. [PubMed: 31024882]

46. Crut A; Maioli P; Del Fatti N; Valle F, Optical Absorption and Scattering Spectroscopies of Single Nano-Objects. *Chem. Soc. Rev* 2014, 43 (11), 3921–3956. [PubMed: 24724158]
47. Arias LS; Pessan JP; Vieira APM; Lima T. M. T. d.; Delbem ACB; Monteiro DR, Iron Oxide Nanoparticles for Biomedical Applications: A Perspective on Synthesis, Drugs, Antimicrobial Activity, and Toxicity. *Antibiotics* 2018, 7 (2), 46, 1–32.
48. Xie W; Guo Z; Gao F; Gao Q; Wang D; Liaw B-S; Cai Q; Sun X; Wang X; Zhao L, Shape-, Size- and Structure-Controlled Synthesis and Biocompatibility of Iron Oxide Nanoparticles for Magnetic Theranostics. *Theranostics* 2018, 8 (12), 3284–3307. [PubMed: 29930730]
49. Chen J; Guo Z; Wang HB; Gong M; Kong XK; Xia P; Chen QW, Multifunctional Fe<sub>3</sub>O<sub>4</sub>@C@Ag Hybrid Nanoparticles as Dual Modal Imaging Probes and Near-Infrared Light-Responsive Drug Delivery Platform. *Biomaterials* 2013, 34 (2), 571–581. [PubMed: 23092859]
50. Horst MF; Coral DF; Fernández van Raap MB; Alvarez M; Lassalle V, Hybrid Nanomaterials Based on Gum Arabic and Magnetite for Hyperthermia Treatments. *Mater. Sci. Eng., C* 2017, 74, 443–450.
51. Ferreira RV; Martins TM; Goes AM; Fabris JD; Cavalcante LC; Outon LE; Domingues RZ, Thermosensitive Gemcitabine-Magnetoliposomes for Combined Hyperthermia and Chemotherapy. *Nanotechnology* 2016, 27 (8), 085105, 1–8. [PubMed: 26820520]
52. Wang S; Luo J; Zhang Z; Dong D; Shen Y; Fang Y; Hu L; Liu M; Dai C; Peng S; Fang Z; Shang P, Iron and Magnetic: New Research Direction of the Ferroptosis-Based Cancer Therapy. *Am. J. Cancer Res* 2018, 8 (10), 1933–1946. [PubMed: 30416846]
53. Seabra AB; Pelegrino MT; Haddad PS, Chapter 24 - Antimicrobial Applications of Superparamagnetic Iron Oxide Nanoparticles: Perspectives and Challenges. In *Nanostructures for Antimicrobial Therapy*, Ficiari A; Grumezescu AM, Eds. Elsevier: 2017; Vol. 1, pp 531–550.
54. Shi D; Sadat ME; Dunn AW; Mast DB, Photo-Fluorescent and Magnetic Properties of Iron Oxide Nanoparticles for Biomedical Applications. *Nanoscale* 2015, 7 (18), 8209–8232. [PubMed: 25899408]
55. Ali A; Zafar H; Zia M; Ul Haq I; Phull AR; Ali JS; Hussain A, Synthesis, Characterization, Applications, and Challenges of Iron Oxide Nanoparticles. *Nanotechnol., Sci. Appl* 2016, 9, 49–67. [PubMed: 27578966]
56. Ansari SAMK; Ficiarià E; Ruffinatti FA; Stura I; Argenziano M; Abollino O; Cavalli R; Guiot C; D'Agata F, Magnetic Iron Oxide Nanoparticles: Synthesis, Characterization and Functionalization for Biomedical Applications in the Central Nervous System. *Materials* 2019, 12 (3), 465, 1–24.
57. Shi H; Xu M; Zhu J; Li Y; He Z; Zhang Y; Xu Q; Niu Y; Liu Y, Programmed Co-Delivery of Platinum Nanodrugs and Gemcitabine by a Clustered Nanocarrier for Precision Chemotherapy for NCSLC Tumors. *J. Mater. Chem. B* 2020, 8 (2), 332–342. [PubMed: 31825452]
58. Yang Y; Wu X; He C; Huang J; Yin S; Zhou M; Ma L; Zhao W; Qiu L; Cheng C; Zhao C, Metal-Organic Framework/Ag-Based Hybrid Nanoagents for Rapid and Synergistic Bacterial Eradication. *ACS Appl. Mater. Interfaces* 2020, 12 (12), 13698–13708. [PubMed: 32129070]
59. Yeroslavsky G; Lavi R; Alishaev A; Rahimpour S, Sonochemically-Produced Metal-Containing Polydopamine Nanoparticles and Their Antibacterial and Antibiofilm Activity. *Langmuir* 2016, 32 (20), 5201–5212. [PubMed: 27133213]
60. Jeyaraj M; Gurunathan S; Qasim M; Kang M-H; Kim J-H, A Comprehensive Review on the Synthesis, Characterization, and Biomedical Application of Platinum Nanoparticles. *Nanomaterials* 2019, 9 (12), 1719, 1–41.
61. Lee SH; Jun B-H, Silver Nanoparticles: Synthesis and Application for Nanomedicine. *Int. J. Mol. Sci* 2019, 20 (4), 865, 1–24.
62. Mott D; Galkowski J; Wang L; Luo J; Zhong C-J, Synthesis of Size-Controlled and Shaped Copper Nanoparticles. *Langmuir* 2007, 23 (10), 5740–5745. [PubMed: 17407333]
63. Sim W; Barnard RT; Blaskovich MAT; Ziora ZM, Antimicrobial Silver in Medicinal and Consumer Applications: A Patent Review of the Past Decade (2007–2017). *Antibiotics* 2018, 7 (4), 93, 1–15.
64. Al-Hakkani MF, Biogenic Copper Nanoparticles and Their Applications: A Review. *SN Appl. Sci* 2020, 2 (3), 505, 1–20.
65. Levingstone TJ; Herhaj S; Dunne NJ, Calcium Phosphate Nanoparticles for Therapeutic Applications in Bone Regeneration. *Nanomaterials* 2019, 9 (11), 1570, 1–22.

66. Dong Y; Liao H; Yu J; Fu H; Zhao D; Gong K; Wang Q; Duan Y, Incorporation of Drug Efflux Inhibitor and Chemotherapeutic Agent into an Inorganic/Organic Platform for the Effective Treatment of Multidrug Resistant Breast Cancer. *J. Nanobiotechnol* 2019, 17 (1), 125, 1–15.
67. Wang J; Wang H; Wang H; He S; Li R; Deng Z; Liu X; Wang F, Nonviolent Self-Catabolic DNAzyme Nanosponges for Smart Anticancer Drug Delivery. *ACS Nano* 2019, 13 (5), 5852–5863. [PubMed: 31042356]
68. Banik M; Basu T, Calcium Phosphate Nanoparticles: A Study of Their Synthesis, Characterization and Mode of Interaction with Salmon Testis DNA. *Dalton Trans.* 2014, 43 (8), 3244–3259. [PubMed: 24356414]
69. Yan F; Jiang J; Chen X; Tian S; Li K, Synthesis and Characterization of Silica Nanoparticles Preparing by Low-Temperature Vapor-Phase Hydrolysis of SiCl<sub>4</sub>. *Ind. Eng. Chem. Res* 2014, 53 (30), 11884–11890.
70. Król A; Pomastowski P; Rafińska K; Railean-Plugaru V; Buszewski B, Zinc Oxide Nanoparticles: Synthesis, Antiseptic Activity and Toxicity Mechanism. *Adv. Colloid Interface Sci* 2017, 249, 37–52. [PubMed: 28923702]
71. Cross SE; Innes B; Roberts MS; Tsuzuki T; Robertson TA; McCormick P, Human Skin Penetration of Sunscreen Nanoparticles: *in Vitro* Assessment of a Novel Micronized Zinc Oxide Formulation. *Skin Pharmacol. Physiol* 2007, 20 (3), 148–154. [PubMed: 17230054]
72. Marra A; Silvestre C; Duraccio D; Cimmino S, Polylactic Acid/Zinc Oxide Biocomposite Films for Food Packaging Application. *Int. J. Biol. Macromol* 2016, 88, 254–262. [PubMed: 27012896]
73. Jiang J; Pi J; Cai J, The Advancing of Zinc Oxide Nanoparticles for Biomedical Applications. *Bioinorg. Chem. Appl* 2018, 2018, 1–18, 1062562–1062562.
74. Wilson HF; Tang C; Barnard AS, Morphology of Zinc Oxide Nanoparticles and Nanowires: Role of Surface and Edge Energies. *J. Phys. Chem. C* 2016, 120 (17), 9498–9505.
75. Sirelkhatim A; Mahmud S; Seeni A; Kaus NHM; Ann LC; Bakhori SKM; Hasan H; Mohamad D, Review on Zinc Oxide Nanoparticles: Antibacterial Activity and Toxicity Mechanism. *Nano-Micro Lett* 2015, 7 (3), 219–242.
76. Davoodi E; Zhianmanesh M; Montazerian H; Milani AS; Hoorfar M, Nano-Porous Anodic Alumina: Fundamentals and Applications in Tissue Engineering. *J. Mater. Sci.: Mater. Med* 2020, 31 (7), 60, 1–16. [PubMed: 32642974]
77. Narayan R; Nayak UY; Raichur AM; Garg S, Mesoporous Silica Nanoparticles: A Comprehensive Review on Synthesis and Recent Advances. *Pharmaceutics* 2018, 10 (3), 118, 1–49.
78. Stöber W; Fink A; Bohn E, Controlled Growth of Monodisperse Silica Spheres in the Micron Size Range. *J. Colloid Interface Sci* 1968, 26 (1), 62–69.
79. Wu S-H; Mou C-Y; Lin H-P, Synthesis of Mesoporous Silica Nanoparticles. *Chem. Soc. Rev* 2013, 42 (9), 3862–3875. [PubMed: 23403864]
80. Hernández Montoto A; Montes R; Samadi A; Gorbe M; Terrés JM; Cao-Milán R; Aznar E; Ibañez J; Masot R; Marcos MD; Orzáez M; Sancenón F; Oddershede LB; Martínez-Mañez R, Gold Nanostars Coated with Mesoporous Silica Are Effective and Nontoxic Photothermal Agents Capable of Gate Keeping and Laser-Induced Drug Release. *ACS Appl. Mater. Interfaces* 2018, 10 (33), 27644–27656. [PubMed: 30040374]
81. Shao L; Li Y; Huang F; Wang X; Lu J; Jia F; Pan Z; Cui X; Ge G; Deng X; Wu Y, Complementary Autophagy Inhibition and Glucose Metabolism with Rattle-Structured Polydopamine@Mesoporous Silica Nanoparticles for Augmented Low-Temperature Photothermal Therapy and *in Vivo* Photoacoustic Imaging. *Theranostics* 2020, 10 (16), 7273–7286. [PubMed: 32641992]
82. Howarth AJ; Peters AW; Vermeulen NA; Wang TC; Hupp JT; Farha OK, Best Practices for the Synthesis, Activation, and Characterization of Metal-Organic Frameworks. *Chem. Mater* 2017, 29 (1), 26–39.
83. Safaei M; Foroughi MM; Ebrahimipour N; Jahani S; Omid A; Khatami M, A Review on Metal-Organic Frameworks: Synthesis and Applications. *TrAC, Trends Anal. Chem* 2019, 118, 401–425.
84. Zhu W; Chen M; Liu Y; Tian Y; Song Z; Song G; Zhang X, A Dual Factor Activated Metal-Organic Framework Hybrid Nanoplatfor for Photoacoustic Imaging and Synergetic Photo-Chemotherapy. *Nanoscale* 2019, 11 (43), 20630–20637. [PubMed: 31641722]

85. Lei Z; Tang Q; Ju Y; Lin Y; Bai X; Luo H; Tong Z, Block Copolymer@ZIF-8 Nanocomposites as a pH-Responsive Multi-Steps Release System for Controlled Drug Delivery. *J. Biomater. Sci., Polym. Ed* 2020, 31 (6), 695–711. [PubMed: 31914358]
86. Wang L; Zheng M; Xie Z, Nanoscale Metal-Organic Frameworks for Drug Delivery: A Conventional Platform with New Promise. *J. Mater. Chem. B* 2018, 6 (5), 707–717. [PubMed: 32254257]
87. Krupa A; Descamps M; Willart J-F; Strach B; Wyska E. b.; Jachowicz R; Danede F, High-Energy Ball Milling as Green Process to Vitrify Tadalafil and Improve Bioavailability. *Mol. Pharm* 2016, 13 (11), 3891–3902. [PubMed: 27618666]
88. Raji M; Mekhroum MEM; Bouhfid R, Nanoclay Modification and Functionalization for Nanocomposites Development: Effect on the Structural, Morphological, Mechanical and Rheological Properties. In *Nanoclay Reinforced Polymer Composites*, Springer: 2016; pp 1–34.
89. Kotal M; Bhowmick AK, Polymer Nanocomposites from Modified Clays: Recent Advances and Challenges. *Prog. Polym. Sci* 2015, 51, 127–187.
90. Nguyen QT; Baird DG, Preparation of Polymer-Clay Nanocomposites and Their Properties. *Adv. Polym. Technol* 2006, 25 (4), 270–285.
91. Cui Z-K; Kim S; Baljon JJ; Wu BM; Aghaloo T; Lee M, Microporous Methacrylated Glycol Chitosan-Montmorillonite Nanocomposite Hydrogel for Bone Tissue Engineering. *Nat. Commun* 2019, 10 (1), 1–10. [PubMed: 30602773]
92. Rajabi N; Kharaziha M; Emadi R; Zarrabi A; Mokhtari H; Salehi S, An Adhesive and Injectable Nanocomposite Hydrogel of Thiolated Gelatin/Gelatin Methacrylate/Laponite® as a Potential Surgical Sealant. *J. Colloid Interface Sci* 2020, 564, 155–169. [PubMed: 31911221]
93. Muthiah Pillai NS; Eswar K; Amirthalingam S; Mony U; Kerala Varma P; Jayakumar R, Injectable Nano Whitlockite Incorporated Chitosan Hydrogel for Effective Hemostasis. *ACS Appl. Bio Mater* 2019, 2 (2), 865–873.
94. Gao G; Du G; Sun Y; Fu J, Self-Healable, Tough, and Ultrastretchable Nanocomposite Hydrogels Based on Reversible Polyacrylamide/Montmorillonite Adsorption. *ACS Appl. Mater. Interfaces* 2015, 7 (8), 5029–5037. [PubMed: 25668063]
95. Bonifacio MA; Cochis A; Cometa S; Scalzone A; Gentile P; Procino G; Milano S; Scalia AC; Rimondini L; De Giglio E, Advances in Cartilage Repair: The Influence of Inorganic Clays to Improve Mechanical and Healing Properties of Antibacterial Gellan Gum-Manuka Honey Hydrogels. *Mater. Sci. Eng., C* 2020, 108, 110444, 1–7.
96. Oliveira GC; Moccelini SK; Castilho M; Terezo AJ; Possavatz J; Magalhães MR; Dores EF, Biosensor Based on Atemoya Peroxidase Immobilised on Modified Nanoclay for Glyphosate Biomonitoring. *Talanta* 2012, 98, 130–136. [PubMed: 22939138]
97. Khatoun N; Chu MQ; Zhou CH, Nanoclay-Based Drug Delivery Systems and Their Therapeutic Potentials. *J. Mater. Chem. B* 2020, 8 (33), 7335–7351. [PubMed: 32687134]
98. Bugatti V; Sorrentino A; Gorrasi G, Encapsulation of Lysozyme into Halloysite Nanotubes and Dispersion in PLA: Structural and Physical Properties and Controlled Release Analysis. *Eur. Polym. J* 2017, 93, 495–506.
99. Gaharwar AK; Avery RK; Assmann A; Paul A; McKinley GH; Khademhosseini A; Olsen BD, Shear-Thinning Nanocomposite Hydrogels for the Treatment of Hemorrhage. *ACS Nano* 2014, 8 (10), 9833–9842. [PubMed: 25221894]
100. Yook S; Es-haghi SS; Yildirim A; Mutlu Z; Cakmak M, Anisotropic Hydrogels Formed by Magnetically-Oriented Nanoclay Suspensions for Wound Dressings. *Soft Matter* 2019, 15 (47), 9733–9741. [PubMed: 31742299]
101. Page DJ; Clarkin CE; Mani R; Khan NA; Dawson JI; Evans ND, Injectable Nanoclay Gels for Angiogenesis. *Acta Biomater.* 2019, 100, 378–387. [PubMed: 31541735]
102. Avery RK; Albadawi H; Akbari M; Zhang YS; Duggan MJ; Sahani DV; Olsen BD; Khademhosseini A; Oklu R, An Injectable Shear-Thinning Biomaterial for Endovascular Embolization. *Sci. Transl. Med* 2016, 8 (365), 365ra156, 1–12.
103. Carrado KA, Synthetic Organo-and Polymer-Clays: Preparation, Characterization, and Materials Applications. *Appl. Clay Sci* 2000, 17 (1–2), 1–23.



104. Guo F; Aryana S; Han Y; Jiao Y, A Review of the Synthesis and Applications of Polymer-Nanoclay Composites. *Appl. Sci* 2018, 8 (9), 1696, 1–29.
105. Rafiee R; Shahzadi R, Mechanical Properties of Nanoclay and Nanoclay Reinforced Polymers: A Review. *Polym. Compos* 2019, 40 (2), 431–445.
106. Peña-Parás L; Sánchez-Fernández JA; Vidaltamayo R, Nanoclays for Biomedical Applications. In *Handbook of Ecomaterials*, Martínez LMT; Kharissova OV; Kharisov BI, Eds. Springer International Publishing: Cham, 2017; pp 1–19.
107. Shi J; Wang B; Chen Z; Liu W; Pan J; Hou L; Zhang Z, A Multi-Functional Tumor Theranostic Nanoplatfrom for MRI Guided Photothermal-Chemotherapy. *Pharm. Res* 2016, 33 (6), 1472–1485. [PubMed: 26984128]
108. Wu C; Guan X; Xu J; Zhang Y; Liu Q; Tian Y; Li S; Qin X; Yang H; Liu Y, Highly Efficient Cascading Synergy of Cancer Photo-Immunotherapy Enabled by Engineered Graphene Quantum Dots/Photosensitizer/CPG Oligonucleotides Hybrid Nanotheranostics. *Biomaterials* 2019, 205, 106–119. [PubMed: 30913486]
109. Lee J; Morita M; Takemura K; Park EY, A Multi-Functional Gold/Iron-Oxide Nanoparticle-CNT Hybrid Nanomaterial as Virus DNA Sensing Platform. *Biosens. Bioelectron* 2018, 102, 425–431. [PubMed: 29175218]
110. Du B; Han S; Li H; Zhao F; Su X; Cao X; Zhang Z, Multi-Functional Liposomes Showing Radiofrequency-Triggered Release and Magnetic Resonance Imaging for Tumor Multi-Mechanism Therapy. *Nanoscale* 2015, 7 (12), 5411–5426. [PubMed: 25731982]
111. Lim DG; Rajasekaran N; Lee D; Kim NA; Jung HS; Hong S; Shin YK; Kang E; Jeong SH, Polyamidoamine-Decorated Nanodiamonds as a Hybrid Gene Delivery Vector and siRNA Structural Characterization at the Charged Interfaces. *ACS Appl. Mater. Interfaces* 2017, 9 (37), 31543–31556. [PubMed: 28853284]
112. Tang L; Ji R; Cao X; Lin J; Jiang H; Li X; Teng KS; Luk CM; Zeng S; Hao J; Lau SP, Deep Ultraviolet Photoluminescence of Water-Soluble Self-Passivated Graphene Quantum Dots. *ACS Nano* 2012, 6 (6), 5102–5110. [PubMed: 22559247]
113. Xiang MH; Li N; Liu JW; Yu RQ; Jiang JH, A Tumour mRNA-Triggered Nanoassembly for Enhanced Fluorescence Imaging-Guided Photodynamic Therapy. *Nanoscale* 2020, 12 (16), 8727–8731. [PubMed: 32296802]
114. Davoodi E; Montazerian H; Haghniaz R; Rashidi A; Ahadian S; Sheikhi A; Chen J; Khademhosseini A; Milani AS; Hoorfar M; Toyserkani E, 3D-Printed Ultra-Robust Surface-Doped Porous Silicone Sensors for Wearable Biomonitoring. *ACS Nano* 2020, 14 (2), 1520–1532. [PubMed: 31904931]
115. Montazerian H; Rashidi A; Dalili A; Najjaran H; Milani AS; Hoorfar M, Graphene-Coated Spandex Sensors Embedded into Silicone Sheath for Composites Health Monitoring and Wearable Applications. *Small* 2019, 15 (17), 1804991, 1–12.
116. Smith AT; LaChance AM; Zeng S; Liu B; Sun L, Synthesis, Properties, and Applications of Graphene Oxide/Reduced Graphene Oxide and Their Nanocomposites. *Nano Mater. Sci* 2019, 1 (1), 31–47.
117. Astefanei A; Núñez O; Galceran MT, Characterisation and Determination of Fullerenes: A Critical Review. *Anal. Chim. Acta* 2015, 882, 1–21. [PubMed: 26043086]
118. Eatemadi A; Daraee H; Karimkhanloo H; Kouhi M; Zarghami N; Akbarzadeh A; Abasi M; Hanifehpour Y; Joo SW, Carbon Nanotubes: Properties, Synthesis, Purification, and Medical Applications. *Nanoscale Res. Lett* 2014, 9 (1), 393, 1–13. [PubMed: 25170330]
119. Wepasnick KA; Smith BA; Bitter JL; Howard Fairbrother D, Chemical and Structural Characterization of Carbon Nanotube Surfaces. *Anal. Bioanal. Chem* 2010, 396 (3), 1003–1014. [PubMed: 20052581]
120. Dasari Shareena TP; McShan D; Dasmahapatra AK; Tchounwou PB, A Review on Graphene-Based Nanomaterials in Biomedical Applications and Risks in Environment and Health. *Nano-Micro Lett* 2018, 10 (3), 53, 1–34.
121. Tian P; Tang L; Teng KS; Lau SP, Graphene Quantum Dots from Chemistry to Applications. *Mater. Today Chem* 2018, 10, 221–258.

122. Anzar N; Hasan R; Tyagi M; Yadav N; Narang J, Carbon Nanotube - A Review on Synthesis, Properties and Plethora of Applications in the Field of Biomedical Science. *Sens. Int* 2020, 1, 100003, 1–10.
123. Zununi Vahed S; Salehi R; Davaran S; Sharifi S, Liposome-Based Drug Co-Delivery Systems in Cancer Cells. *Mater. Sci. Eng., C* 2017, 71, 1327–1341.
124. Mochizuki S; Kanegae N; Nishina K; Kamikawa Y; Koiwai K; Masunaga H; Sakurai K, The Role of the Helper Lipid Dioleoylphosphatidylethanolamine (DOPE) for DNA Transfection Cooperating with a Cationic Lipid Bearing Ethylenediamine. *Biochim. Biophys. Acta, Biomembr* 2013, 1828 (2), 412–418.
125. Martín-Saavedra F; Ruiz-Hernández E; Escudero-Duch C; Prieto M; Arruebo M; Sadeghi N; Deckers R; Storm G; Hennink WE; Santamaría J; Vilaboa N, Lipogels Responsive to Near-Infrared Light for the Triggered Release of Therapeutic Agents. *Acta Biomater.* 2017, 61, 54–65. [PubMed: 28801266]
126. Toro-Cordova A; Flores-Cruz M; Santoyo-Salazar J; Carrillo-Nava E; Jurado R; Figueroa-Rodriguez PA; Lopez-Sanchez P; Medina LA; Garcia-Lopez P, Liposomes Loaded with Cisplatin and Magnetic Nanoparticles: Physicochemical Characterization, Pharmacokinetics, and *in Vitro* Efficacy. *Molecules* 2018, 23 (9), 2272, 1–16.
127. Wang M; Li J; Li X; Mu H; Zhang X; Shi Y; Chu Y; Wang A; Wu Z; Sun K, Magnetically and pH Dual Responsive Dendrosomes for Tumor Accumulation Enhanced Folate-Targeted Hybrid Drug Delivery. *J. Control. Release* 2016, 232, 161–174. [PubMed: 27090165]
128. Tang F; Hughes JA, Synthesis of a Single-Tailed Cationic Lipid and Investigation of Its Transfection. *J. Control. Release* 1999, 62 (3), 345–358. [PubMed: 10528072]
129. Chatterjee S; Banerjee DK, Preparation, Isolation, and Characterization of Liposomes Containing Natural and Synthetic Lipids. In *Liposome Methods and Protocols*, Basu SC; Basu M, Eds. Humana Press: Totowa, NJ, 2002; pp 3–16.
130. Zhang H, Thin-Film Hydration Followed by Extrusion Method for Liposome Preparation. *Methods Mol. Biol* 2017, 1522, 17–22. [PubMed: 27837527]
131. Akbarzadeh A; Rezaei-Sadabady R; Davaran S; Joo SW; Zarghami N; Hanifehpour Y; Samiei M; Kouhi M; Nejati-Koshki K, Liposome: Classification, Preparation, and Applications. *Nanoscale Res. Lett* 2013, 8 (1), 102, 1–9. [PubMed: 23432972]
132. Hadian Z; Sahari MA; Moghimi HR; Barzegar M, Formulation, Characterization and Optimization of Liposomes Containing Eicosapentaenoic and Docosahexaenoic Acids; A Methodology Approach. *Iran. J. Pharm. Res* 2014, 13 (2), 393–404. [PubMed: 25237335]
133. Aisha AFA; Majid AMSA; Ismail Z, Preparation and Characterization of Nano Liposomes of Orthosiphon Stamineus Ethanolic Extract in Soybean Phospholipids. *BMC Biotech.* 2014, 14, 23, 1–11.
134. Has C; Sunthar P, A Comprehensive Review on Recent Preparation Techniques of Liposomes. *J. Liposome Res* 2019, 30 (4), 1–30. [PubMed: 31010357]
135. Pattni BS; Chupin VV; Torchilin VP, New Developments in Liposomal Drug Delivery. *Chem. Rev* 2015, 115 (19), 10938–10966. [PubMed: 26010257]
136. Dhanya GR; Caroline DS; Rekha MR; Sreenivasan K, Histidine and Arginine Conjugated Starch-PEI and Its Corresponding Gold Nanoparticles for Gene Delivery. *Int. J. Biol. Macromol* 2018, 120 (Pt A), 999–1008. [PubMed: 30171946]
137. Akinyelu J; Singh M, Chitosan Stabilized Gold-Folate-Poly (Lactide-*co*-Glycolide) Nanoplexes Facilitate Efficient Gene Delivery in Hepatic and Breast Cancer Cells. *J. Nanosci. Nanotechnol* 2018, 18 (7), 4478–4486. [PubMed: 29442622]
138. Sánchez-Moreno P; de Vicente J; Nardecchia S; Marchal JA; Boulaiz H, Thermo-Sensitive Nanomaterials: Recent Advance in Synthesis and Biomedical Applications. *Nanomaterials* 2018, 8 (11), 935, 1–32.
139. Cho H; Bae J; Garripelli VK; Anderson JM; Jun H-W; Jo S, Redox-Sensitive Polymeric Nanoparticles for Drug Delivery. *Chem. Commun* 2012, 48 (48), 6043–6045.
140. Kocak G; Tuncer C; Bütün V, pH-Responsive Polymers. *Polym. Chem* 2017, 8 (1), 144–176.
141. Zhou L; Xi Y; Xue Y; Wang M; Liu Y; Guo Y; Lei B, Injectable Self-Healing Antibacterial Bioactive Polypeptide-Based Hybrid Nanosystems for Efficiently Treating Multidrug Resistant

Infection, Skin-Tumor Therapy, and Enhancing Wound Healing. *Adv. Funct. Mater* 2019, 29 (22), 1806883, 1–11.

142. Seaberg J; Flynn N; Cai A; Ramsey JD, Effect of Redox-Responsive DTSSP Crosslinking on Poly(L-Lysine)-Grafted-Poly (ethylene Glycol) Nanoparticles for Delivery of Proteins. *Biotechnol. Bioeng* 2020, 117 (8), 2504–2515. [PubMed: 32364622]
143. Nwe N; Furuike T; Tamura H, Chapter One - Isolation and Characterization of Chitin and Chitosan from Marine Origin. In *Adv. Food Nutr. Res*, Kim S-K, Ed. Academic Press: 2014; Vol. 72, pp 1–15. [PubMed: 25081074]
144. Weyts KF; Goethals EJ, New Synthesis of Linear Polyethyleneimine. *Polym. Bull* 1988, 19 (1), 13–19.
145. Van Dijk-Wolthuis WNE; van de Water L; van de Wetering P; Van Steenberghe MJ; Kettenes-van den Bosch JJ; Schuyl WJW; Hennink WE, Synthesis and Characterization of Poly-L-Lysine with Controlled Low Molecular Weight. *Macromol. Chem. Phys* 1997, 198 (12), 3893–3906.
146. Cortés MT; Vargas C; Blanco DA; Quinchaneagua ID; Cortés C; Jaramillo AM, Bioinspired Polydopamine Synthesis and Its Electrochemical Characterization. *J. Chem. Educ* 2019, 96 (6), 1250–1255.
147. Seaberg J; Kaabipour S; Hemmati S; Ramsey JD, A Rapid Millifluidic Synthesis of Tunable Polymer-Protein Nanoparticles. *Eur. J. Pharm. Biopharm* 2020, 154, 127–135. [PubMed: 32659325]
148. Hoheisel TN; Hur K; Wiesner UB, Block Copolymer-Nanoparticle Hybrid Self-Assembly. *Prog. Polym. Sci* 2015, 40, 3–32.
149. Palit S; He L; Hamilton WA; Yethiraj A; Yethiraj A, Combining Diffusion NMR and Small-Angle Neutron Scattering Enables Precise Measurements of Polymer Chain Compression in a Crowded Environment. *Phys. Rev. Lett* 2017, 118 (9), 097801, 1–6. [PubMed: 28306301]
150. Virgen-Ortiz JJ; dos Santos JCS; Berenguer-Murcia Á; Barbosa O; Rodrigues RC; Fernandez-Lafuente R, Polyethylenimine: A Very Useful Ionic Polymer in the Design of Immobilized Enzyme Biocatalysts. *J. Mater. Chem. B* 2017, 5 (36), 7461–7490. [PubMed: 32264223]
151. Taranejoo S; Liu J; Verma P; Hourigan K, A Review of the Developments of Characteristics of PEI Derivatives for Gene Delivery Applications. *J. Appl. Polym. Sci* 2015, 132 (25), 42096, 1–8.
152. Zakeri A; Kouhbanani MAJ; Beheshtkhou N; Beigi V; Mousavi SM; Hashemi SAR; Karimi Zade A; Amani AM; Savardashtaki A; Mirzaei E; Jahandideh S; Movahedpour A, Polyethylenimine-Based Nanocarriers in Co-Delivery of Drug and Gene: A Developing Horizon. *Nano Rev. Exp* 2018, 9 (1), 1488497, 1–14. [PubMed: 30410712]
153. Shukla SC; Singh A; Pandey AK; Mishra A, Review on Production and Medical Applications of  $\epsilon$ -Polylysine. *Biochem. Eng. J* 2012, 65, 70–81.
154. Xu Y; Kim C-S; Saylor DM; Koo D, Polymer Degradation and Drug Delivery in PLGA-Based Drug-Polymer Applications: A Review of Experiments and Theories. *J. Biomed. Mater. Res. Part B* 2017, 105 (6), 1692–1716.
155. Lanzalaco S; Armelin E, Poly(N-Isopropylacrylamide) and Copolymers: A Review on Recent Progresses in Biomedical Applications. *Gels* 2017, 3 (4), 36, 1–31.
156. Ali U; Karim KJBA; Buang NA, A Review of the Properties and Applications of Poly (methyl Methacrylate) (PMMA). *Polym. Rev* 2015, 55 (4), 678–705.
157. Abbasi E; Aval SF; Akbarzadeh A; Milani M; Nasrabadi HT; Joo SW; Hanifehpour Y; Nejati-Koshki K; Pashaei-Asl R, Dendrimers: Synthesis, Applications, and Properties. *Nanoscale Res. Lett* 2014, 9 (1), 247, 1–10. [PubMed: 24994950]
158. Mbatha Londiwe S; Maiyo Fiona C; Singh M, Dendrimer Functionalized Folate-Targeted Gold Nanoparticles for Luciferase Gene Silencing *in Vitro*: A Proof of Principle Study. *Acta Pharm.* 2019, 69 (1), 49–61. [PubMed: 31259716]
159. Jeong Y; Kim ST; Jiang Y; Duncan B; Kim CS; Saha K; Yeh YC; Yan B; Tang R; Hou S; Kim C; Park MH; Rotello VM, Nanoparticle-Dendrimer Hybrid Nanocapsules for Therapeutic Delivery. *Nanomedicine (London, U. K.)* 2016, 11 (12), 1571–1578.
160. Chen Z; Peng Y; Xie X; Feng Y; Li T; Li S; Qin X; Yang H; Wu C; Zheng C; Zhu J; You F; Liu Y, Dendrimer-Functionalized Superparamagnetic Nanobeacons for Real-Time Detection

and Depletion of HSP90 $\alpha$  mRNA and MR Imaging. *Theranostics* 2019, 9 (20), 5784–5796. [PubMed: 31534519]

161. Kong L; Wu Y; Alves CS; Shi X, Efficient Delivery of Therapeutic siRNA into Glioblastoma Cells Using Multifunctional Dendrimer-Entrapped Gold Nanoparticles. *Nanomedicine (London, U. K.)* 2016, 11 (23), 3103–3115.
162. Shadrack DM; Mubofu EB; Nyandoro SS, Synthesis of Polyamidoamine Dendrimer for Encapsulating Tetramethylscutellarein for Potential Bioactivity Enhancement. *Int. J. Mol. Sci* 2015, 16 (11), 26363–26377. [PubMed: 26556337]
163. Lyu Z; Ding L; Huang AYT; Kao CL; Peng L, Poly (amidoamine) Dendrimers: Covalent and Supramolecular Synthesis. *Mater. Today Chem* 2019, 13, 34–48.
164. Xiong Z; Alves CS; Wang J; Li A; Liu J; Shen M; Rodrigues J; Tomás H; Shi X, Zwitterion-Functionalized Dendrimer-Entrapped Gold Nanoparticles for Serum-Enhanced Gene Delivery to Inhibit Cancer Cell Metastasis. *Acta Biomater.* 2019, 99, 320–329. [PubMed: 31513912]
165. Li Y-F; Zhang H-T; Xin L, Hyaluronic Acid-Modified Polyamidoamine Dendrimer G5-Entrapped Gold Nanoparticles Delivering METase Gene Inhibits Gastric Tumor Growth *via* Targeting CD44+ Gastric Cancer Cells. *J. Cancer Res. Clin. Oncol* 2018, 144 (8), 1463–1473. [PubMed: 29858680]
166. Mullen DG; Desai A; van Dongen MA; Barash M; Baker JR Jr.; Banaszak Holl MM, Best Practices for Purification and Characterization of PAMAM Dendrimer. *Macromolecules* 2012, 45 (12), 5316–5320. [PubMed: 23180887]
167. Lloyd JR; Jayasekara PS; Jacobson KA, Characterization of Polyamidoamino (PAMAM) Dendrimers Using In-Line Reversed Phase LC Electrospray Ionization Mass Spectrometry. *Anal. Methods* 2016, 8 (2), 263–269. [PubMed: 26997980]
168. Sohail I; Bhatti IA; Ashar A; Sarim FM; Mohsin M; Naveed R; Yasir M; Iqbal M; Nazir A, Polyamidoamine (PAMAM) Dendrimers Synthesis, Characterization and Adsorptive Removal of Nickel Ions from Aqueous Solution. *J. Mater. Res. Technol* 2020, 9 (1), 498–506.
169. Araújo R. V. d.; Santos S. d. S.; Igne Ferreira E; Giarolla J, New Advances in General Biomedical Applications of PAMAM Dendrimers. *Molecules* 2018, 23 (11), 2849, 1–27.
170. Xuan M; Shao J; Li J, Cell Membrane-Covered Nanoparticles as Biomaterials. *Natl. Sci. Rev* 2019, 6 (3), 551–561. [PubMed: 34691904]
171. Jiang Y; Krishnan N; Zhou J; Chekuri S; Wei X; Kroll AV; Yu CL; Duan Y; Gao W; Fang RH; Zhang L, Engineered Cell-Membrane-Coated Nanoparticles Directly Present Tumor Antigens to Promote Anticancer Immunity. *Adv. Mater* 2020, 32 (30), 2001808, 1–12.
172. Vijayan V; Uthaman S; Park I-K, Cell Membrane-Camouflaged Nanoparticles: A Promising Biomimetic Strategy for Cancer Theragnostics. *Polymer* 2018, 10 (9), 983, 1–25.
173. Zhuang J; Gong H; Zhou J; Zhang Q; Gao W; Fang RH; Zhang L, Targeted Gene Silencing *in Vivo* by Platelet Membrane-Coated Metal-Organic Framework Nanoparticles. *Sci. Adv* 2020, 6 (13), eaaz6108, 1–10.
174. Fontana F; Shahbazi M-A; Liu D; Zhang H; Mäkilä E; Salonen J; Hirvonen JT; Santos HA, Multistaged Nanovaccines Based on Porous Silicon@Acetalated Dextran@Cancer Cell Membrane for Cancer Immunotherapy. *Adv. Mater* 2017, 29 (7), 1603239, 1–9.
175. Sun H; Su J; Meng Q; Yin Q; Chen L; Gu W; Zhang Z; Yu H; Zhang P; Wang S; Li Y, Cancer Cell Membrane-Coated Gold Nanocages with Hyperthermia-Triggered Drug Release and Homotypic Target Inhibit Growth and Metastasis of Breast Cancer. *Adv. Funct. Mater* 2017, 27 (3), 1604300, 1–9.
176. Rao L; Meng Q-F; Bu L-L; Cai B; Huang Q; Sun Z-J; Zhang W-F; Li A; Guo S-S; Liu W; Wang T-H; Zhao X-Z, Erythrocyte Membrane-Coated Upconversion Nanoparticles with Minimal Protein Adsorption for Enhanced Tumor Imaging. *ACS Appl. Mater. Interfaces* 2017, 9 (3), 2159–2168. [PubMed: 28050902]
177. Rao L; Cai B; Bu L-L; Liao Q-Q; Guo S-S; Zhao X-Z; Dong W-F; Liu W, Microfluidic Electroporation-Facilitated Synthesis of Erythrocyte Membrane-Coated Magnetic Nanoparticles for Enhanced Imaging-Guided Cancer Therapy. *ACS Nano* 2017, 11 (4), 3496–3505. [PubMed: 28272874]

178. Liang X; Ye X; Wang C; Xing C; Miao Q; Xie Z; Chen X; Zhang X; Zhang H; Mei L, Photothermal Cancer Immunotherapy by Erythrocyte Membrane-Coated Black Phosphorus Formulation. *J. Control. Release* 2019, 296, 150–161. [PubMed: 30682441]
179. Mu X; Li J; Yan S; Zhang H; Zhang W; Zhang F; Jiang J, siRNA Delivery with Stem Cell Membrane-Coated Magnetic Nanoparticles for Imaging-Guided Photothermal Therapy and Gene Therapy. *ACS Biomater. Sci. Eng* 2018, 4 (11), 3895–3905. [PubMed: 33429596]
180. Ren X; Zheng R; Fang X; Wang X; Zhang X; Yang W; Sha X, Red Blood Cell Membrane Camouflaged Magnetic Nanoclusters for Imaging-Guided Photothermal Therapy. *Biomaterials* 2016, 92, 13–24. [PubMed: 27031929]
181. Erfani A; Seaberg J; Aichele CP; Ramsey JD, Interactions between Biomolecules and Zwitterionic Moieties: A Review. *Biomacromolecules* 2020, 21 (7), 2557–2573. [PubMed: 32479065]
182. Chen S; Li L; Zhao C; Zheng J, Surface Hydration: Principles and Applications toward Low-Fouling/Nonfouling Biomaterials. *Polymer* 2010, 51 (23), 5283–5293.
183. Suk JS; Xu Q; Kim N; Hanes J; Ensign LM, PEGylation as a Strategy for Improving Nanoparticle-Based Drug and Gene Delivery. *Adv. Drug Deliv. Rev* 2016, 99 (Pt A), 28–51. [PubMed: 26456916]
184. Debayle M; Balloul E; Dembele F; Xu X; Hanafi M; Ribot F; Monzel C; Coppey M; Fragola A; Dahan M; Pons T; Lequeux N, Zwitterionic Polymer Ligands: An Ideal Surface Coating to Totally Suppress Protein-Nanoparticle Corona Formation? *Biomaterials* 2019, 219, 119357, 1–8. [PubMed: 31351245]
185. Harris JM; Chess RB, Effect of Pegylation on Pharmaceuticals. *Nat. Rev. Drug Discov* 2003, 2 (3), 214–221. [PubMed: 12612647]
186. Turecek PL; Bossard MJ; Schoetens F; Ivens IA, PEGylation of Biopharmaceuticals: A Review of Chemistry and Nonclinical Safety Information of Approved Drugs. *J. Pharm. Sci* 2016, 105 (2), 460–475. [PubMed: 26869412]
187. Knop K; Hoogenboom R; Fischer D; Schubert US, Poly (ethylene Glycol) in Drug Delivery: Pros and Cons as Well as Potential Alternatives. *Angew. Chem. Int. Ed* 2010, 49 (36), 6288–6308.
188. Zhang L; Zhang S; Chen H; Liang Y; Zhao B; Luo W; Xiao Q; Li J; Zhu J; Peng C; Zhang Y; Hong Z; Wang Y; Li Y, An Acoustic/Thermo-Responsive Hybrid System for Advanced Doxorubicin Delivery in Tumor Treatment. *Biomater. Sci* 2020, 8 (8), 2202–2211. [PubMed: 32100739]
189. Cho H-J; Lee S-J; Park S-J; Paik CH; Lee S-M; Kim S; Lee Y-S, Activatable iRGD-Based Peptide Monolith: Targeting, Internalization, and Fluorescence Activation for Precise Tumor Imaging. *J. Control. Release* 2016, 237, 177–184. [PubMed: 27349354]
190. Qiu J; Kong L; Cao X; Li A; Wei P; Wang L; Mignani S; Caminade AM; Majoral JP; Shi X, Enhanced Delivery of Therapeutic siRNA into Glioblastoma Cells Using Dendrimer-Entrapped Gold Nanoparticles Conjugated with  $\beta$ -Cyclodextrin. *Nanomaterials* 2018, 8 (3), 131, 1–11.
191. Muhamad N; Plengsuriyakarn T; Na-Bangchang K, Application of Active Targeting Nanoparticle Delivery System for Chemotherapeutic Drugs and Traditional/Herbal Medicines in Cancer Therapy: A Systematic Review. *Int. J. Nanomed* 2018, 13, 3921–3935.
192. Bazak R; Houri M; El Achy S; Kamel S; Refaat T, Cancer Active Targeting by Nanoparticles: A Comprehensive Review of Literature. *J. Cancer Res. Clin. Oncol* 2015, 141 (5), 769–784. [PubMed: 25005786]
193. Zhang W; Sun Y; Zhang Z; Wang W, Designing Aptamer-Gold Nanoparticle-Loaded pH-Sensitive Liposomes Encapsulate Morin for Treating Cancer. *Nanoscale Res. Lett* 2020, 15 (1), 68, 1–17. [PubMed: 32232589]
194. Li B; Li B; He D; Feng C; Luo Z; He M, Preparation, Characterization, and *in Vitro* pH-Sensitivity Evaluation of Superparamagnetic Iron Oxide Nanoparticle- Misonidazole pH-Sensitive Liposomes. *Curr. Drug Deliv* 2019, 16 (3), 254–267. [PubMed: 30426901]
195. Illes B; Wuttke S; Engelke H, Liposome-Coated Iron Fumarate Metal-Organic Framework Nanoparticles for Combination Therapy. *Nanomaterials* 2017, 7 (11), 351, 1–11.
196. Sajeesh S; Choe JY; Lee DK, Core-Shell Hybrid Nanostructured Delivery Platforms for Advanced RNAi Therapeutics. *Nanomedicine (London, U. K.)* 2017, 12 (19), 2271–2286.

197. Mahalunkar S; Yadav AS; Gorain M; Pawar V; Braathen R; Weiss S; Bogen B; Gosavi SW; Kundu GC, Functional Design of pH-Responsive Folate-Targeted Polymer-Coated Gold Nanoparticles for Drug Delivery and *in Vivo* Therapy in Breast Cancer. *Int. J. Nanomed* 2019, 14, 8285–8302.
198. Lei Q; Hu JJ; Rong L; Cheng H; Sun YX; Zhang XZ, Gold Nanocluster Decorated Polypeptide/DNA Complexes for NIR Light and Redox Dual-Responsive Gene Transfection. *Molecules* 2016, 21 (8), 1103, 1–15.
199. Bishop CJ; Liu AL; Lee DS; Murdock RJ; Green JJ, Layer-by-Layer Inorganic/Polymeric Nanoparticles for Kinetically Controlled Multigene Delivery. *J. Biomed. Mater. Res. Part A* 2016, 104 (3), 707–713.
200. Chen X; Zhang Q; Li J; Yang M; Zhao N; Xu FJ, Rattle-Structured Rough Nanocapsules with *in Situ*-Formed Gold Nanorod Cores for Complementary Gene/Chemo/Photothermal Therapy. *ACS Nano* 2018, 12 (6), 5646–5656. [PubMed: 29870655]
201. Dávila JL; d'Ávila MA, Laponite as a Rheology Modifier of Alginate Solutions: Physical Gelation and Aging Evolution. *Carbohydr. Polym* 2017, 157, 1–8. [PubMed: 27987800]
202. Ye H; Tong J; Liu J; Lin W; Zhang C; Chen K; Zhao J; Zhu W, Combination of Gemcitabine-Containing Magnetoliposome and Oxaliplatin-Containing Magnetoliposome in Breast Cancer Treatment: A Possible Mechanism with Potential for Clinical Application. *Oncotarget* 2016, 7 (28), 43762–43778. [PubMed: 27248325]
203. Meng Q-F; Rao L; Zan M; Chen M; Yu G-T; Wei X; Wu Z; Sun Y; Guo S-S; Zhao X-Z; Wang F-B; Liu W, Macrophage Membrane-Coated Iron Oxide Nanoparticles for Enhanced Photothermal Tumor Therapy. *Nanotechnology* 2018, 29 (13), 134004, 1–11. [PubMed: 29334363]
204. Shao J; Abdelghani M; Shen G; Cao S; Williams DS; van Hest JCM, Erythrocyte Membrane Modified Janus Polymeric Motors for Thrombus Therapy. *ACS Nano* 2018, 12 (5), 4877–4885. [PubMed: 29733578]
205. Wang Y; Shahi PK; Xie R; Zhang H; Abdeen AA; Yodsanit N; Ma Z; Saha K; Pattnaik BR; Gong S, A pH-Responsive Silica-Metal-Organic Framework Hybrid Nanoparticle for the Delivery of Hydrophilic Drugs, Nucleic Acids, and CRISPR-Cas9 Genome-Editing Machineries. *J. Control. Release* 2020, 324, 194–203. [PubMed: 32380204]
206. Zahiri M; Babaei M; Abnous K; Taghdisi SM; Ramezani M; Alibolandi M, Hybrid Nanoreservoirs Based on Dextran-Capped Dendritic Mesoporous Silica Nanoparticles for CD133-Targeted Drug Delivery. *J. Cell. Physiol* 2020, 235 (2), 1036–1050. [PubMed: 31276199]
207. Jones CH; Chen C-K; Ravikrishnan A; Rane S; Pfeifer BA, Overcoming Nonviral Gene Delivery Barriers: Perspective and Future. *Mol. Pharm* 2013, 10 (11), 4082–4098. [PubMed: 24093932]
208. Xu F; Bandara A; Akiyama H; Eshaghi B; Stelter D; Keyes T; Straub JE; Gummuluru S; Reinhard BM, Membrane-Wrapped Nanoparticles Probe Divergent Roles of GM3 and Phosphatidylserine in Lipid-Mediated Viral Entry Pathways. *Proc. Natl. Acad. Sci. U.S.A* 2018, 115 (39), 9041–9050.
209. Du B; Gu X; Han X; Ding G; Wang Y; Li D; Wang E; Wang J, Lipid-Coated Gold Nanoparticles Functionalized by Folic Acid as Gene Vectors for Targeted Gene Delivery *in Vitro* and *in Vivo*. *ChemMedChem* 2017, 12 (21), 1768–1775. [PubMed: 28967206]
210. Grafals-Ruiz N; Rios-Vicil CI; Lozada-Delgado EL; Quiñones-Díaz BI; Noriega-Rivera RA; Martínez-Zayas G; Santana-Rivera Y; Santiago-Sánchez GS; Valiyeva F; Vivas-Mejía PE, Brain Targeted Gold Liposomes Improve RNAi Delivery for Glioblastoma. *Int. J. Nanomed* 2020, 15, 2809–2828.
211. Wang P; Zhang L; Xie Y; Wang N; Tang R; Zheng W; Jiang X, Genome Editing for Cancer Therapy: Delivery of Cas9 Protein/sgRNA Plasmid *via* a Gold Nanocluster/Lipid Core-Shell Nanocarrier. *Adv. Sci* 2017, 4 (11), 1700175, 1–10.
212. Wang P; Zhang L; Zheng W; Cong L; Guo Z; Xie Y; Wang L; Tang R; Feng Q; Hamada Y; Gonda K; Hu Z; Wu X; Jiang X, Thermo-Triggered Release of CRISPR-Cas9 System by Lipid-Encapsulated Gold Nanoparticles for Tumor Therapy. *Angew. Chem. Int. Ed* 2018, 130 (6), 1507–1512.
213. Fitzgerald KA; Rahme K; Guo J; Holmes JD; O'Driscoll CM, Anisamide-Targeted Gold Nanoparticles for siRNA Delivery in Prostate Cancer Synthesis, Physicochemical

- Characterisation and *in Vitro* Evaluation. *J. Mater. Chem. B* 2016, 4 (13), 2242–2252. [PubMed: 32263220]
214. Daniels AN; Singh M, Sterically Stabilized siRNA:Gold Nanocomplexes Enhance *c-MYC* Silencing in a Breast Cancer Cell Model. *Nanomedicine (London, U. K.)* 2019, 14 (11), 1387–1401.
215. Shaat H; Mostafa A; Moustafa M; Gamal-Eldeen A; Emam A; El-Hussieny E; Elhefnawi M, Modified Gold Nanoparticles for Intracellular Delivery of Anti-Liver Cancer siRNA. *Int. J. Pharm* 2016, 504 (1), 125–133. [PubMed: 27036397]
216. Niu J; Chu Y; Huang Y-F; Chong Y-S; Jiang Z-H; Mao Z-W; Peng L-H; Gao J-Q, Transdermal Gene Delivery by Functional Peptide-Conjugated Cationic Gold Nanoparticle Reverses the Progression and Metastasis of Cutaneous Melanoma. *ACS Appl. Mater. Interfaces* 2017, 9 (11), 9388–9401. [PubMed: 28252938]
217. Kong L; Qiu J; Sun W; Yang J; Shen M; Wang L; Shi X, Multifunctional PEI-Entrapped Gold Nanoparticles Enable Efficient Delivery of Therapeutic siRNA into Glioblastoma Cells. *Biomater. Sci* 2017, 5 (2), 258–266. [PubMed: 27921110]
218. Li Z; Liu Y; Huang X; Hu C; Wang H; Yuan L; Brash JL; Chen H, One-Step Preparation of Gold Nanovectors Using Folate Modified Polyethylenimine and Their Use in Target-Specific Gene Transfection. *Colloids Surf., B* 2019, 177, 306–312.
219. Ramchandani D; Lee SK; Yomtoubian S; Han MS; Tung C-H; Mittal V, Nanoparticle Delivery of miR-708 Mimetic Impairs Breast Cancer Metastasis. *Mol. Cancer Ther* 2019, 18 (3), 579–591. [PubMed: 30679387]
220. Yi Y; Kim HJ; Zheng M; Mi P; Naito M; Kim BS; Min HS; Hayashi K; Perche F; Toh K; Liu X; Mochida Y; Kinoh H; Cabral H; Miyata K; Kataoka K, Glucose-Linked Sub-50-nm Unimer Polyion Complex-Assembled Gold Nanoparticles for Targeted siRNA Delivery to Glucose Transporter 1-Overexpressing Breast Cancer Stem-Like Cells. *J. Control. Release* 2019, 295, 268–277. [PubMed: 30639386]
221. Takanche JS; Kim J-E; Kim J-S; Lee M-H; Jeon J-G; Park I-S; Yi H-K, Chitosan-Gold Nanoparticles Mediated Gene Delivery of *c-MYB* Facilitates Osseointegration of Dental Implants in Ovariectomized Rat. *Artif. Cells Nanomed. Biotechnol* 2018, 46 (S3), S807–S817. [PubMed: 30307328]
222. Labala S; Jose A; Venuganti VVK, Transcutaneous Iontophoretic Delivery of STAT3 siRNA Using Layer-by-Layer Chitosan Coated Gold Nanoparticles to Treat Melanoma. *Colloids Surf., B* 2016, 146, 188–197.
223. Yu F; Huang J; Yu Y; Lu Y; Chen Y; Zhang H; Zhou G; Sun Z; Liu J; Sun D; Zhang G; Zou H; Zhong Y, Glutathione-Responsive Multilayer Coated Gold Nanoparticles for Targeted Gene Delivery. *J. Biomed. Nanotechnol* 2016, 12 (3), 503–515. [PubMed: 27280248]
224. Haladjova E; Rangelov S; Tsvetanov CB; Posheva V; Peycheva E; Maximova V; Momekova D; Mountrichas G; Pispas S; Bakandritsos A, Enhanced Gene Expression Promoted by Hybrid Magnetic/Cationic Block Copolymer Micelles. *Langmuir* 2014, 30 (27), 8193–8200. [PubMed: 24945823]
225. Ben Djemaa S; David S; Hervé-Aubert K; Falanga A; Galdiero S; Allard-Vannier E; Chourpa I; Munnier E, Formulation and *in Vitro* Evaluation of a siRNA Delivery Nanosystem Decorated with gH625 Peptide for Triple Negative Breast Cancer Theranosis. *Eur. J. Pharm. Biopharm* 2018, 131, 99–108. [PubMed: 30063968]
226. Salah Z; Abd El Azeem EM; Youssef HF; Gamal-Eldeen AM; Farrag AR; El-Meliegy E; Soliman B; Elhefnawi M, Effect of Tumor Suppressor MiR-34a Loaded on ZSM-5 Nanozeolite in Hepatocellular Carcinoma: *In Vitro* and *in Vivo* Approach. *Curr. Gene Ther* 2019, 19 (5), 342–354. [PubMed: 31701846]
227. Alexander ST; Albert RM; Aleksandra VP; Kirill VL; Maria VO; Andrey VV; Boris VA; Gleb BS, Hybrid Inorganic-Organic Capsules for Efficient Intracellular Delivery of Novel siRNAs against Influenza A (H1N1) Virus Infection. *Sci. Rep* 2017, 7, 102, 1–12. [PubMed: 28273907]
228. Chen P; Liu Y; Zhao J; Pang X; Zhang P; Hou X; Chen P; He C-Y; Wang Z; Chen Z-Y, The Synthesis of Amphiphilic Polyethyleneimine/Calcium Phosphate Composites for Bispecific T-Cell Engager Based Immunogene Therapy. *Biomater. Sci* 2018, 6 (3), 633–641. [PubMed: 29411792]

229. Ahadian S; Finbloom JA; Mofidfar M; Diltemiz SE; Nasrollahi F; Davoodi E; Hosseini V; Mylonaki I; Sangabathuni S; Montazerian H; Fetah K; Nasiri R; Dokmeci MR; Stevens MM; Desai TA; Khademhosseini A, Micro and Nanoscale Technologies in Oral Drug Delivery. *Adv. Drug Deliv. Rev* 2020, 157, 37–62. [PubMed: 32707147]
230. Karimi Zarchi AA; Amini SM; Salimi A; Kharazi S, Synthesis and Characterisation of Liposomal Doxorubicin with Loaded Gold Nanoparticles. *IET Nanobiotechnol.* 2018, 12 (6), 846–849. [PubMed: 30104461]
231. Zhang N; Chen H; Liu A-Y; Shen J-J; Shah V; Zhang C; Hong J; Ding Y, Gold Conjugate-Based Liposomes with Hybrid Cluster Bomb Structure for Liver Cancer Therapy. *Biomaterials* 2016, 74, 280–291. [PubMed: 26461120]
232. Kanwa N; De SK; Adhikari C; Chakraborty A, Spectroscopic Study of the Interaction of Carboxyl-Modified Gold Nanoparticles with Liposomes of Different Chain Lengths and Controlled Drug Release by Layer-by-Layer Technology. *J. Phys. Chem. B* 2017, 121 (50), 11333–11343. [PubMed: 29148780]
233. Szuplewska A; R korajska Joniec A; Poczta ska E; Krysi ski P; Dybko A; Chudy M, Magnetic Field-Assisted Selective Delivery of Doxorubicin to Cancer Cells Using Magnetoliposomes as Drug Nanocarriers. *Nanotechnology* 2019, 30 (31), 315101, 1–11. [PubMed: 30991371]
234. Behnam B; Rezazadehkermani M; Ahmadzadeh S; Mokhtarzadeh A; Nematollahi-Mahani SN; Pardakhty A, Microniosomes for Concurrent Doxorubicin and Iron Oxide Nanoparticles Loading; Preparation, Characterization and Cytotoxicity Studies. *Artif. Cells Nanomed. Biotechnol* 2018, 46 (1), 118–125. [PubMed: 28375753]
235. Skouras A; Papadia K; Mourtas S; Klepetsanis P; Antimisariis SG, Multifunctional Doxorubicin-Loaded Magnetoliposomes with Active and Magnetic Targeting Properties. *Eur. J. Pharm. Sci* 2018, 123, 162–172. [PubMed: 30041027]
236. Aadinath W; Bhushani A; Anandharamkrishnan C, Synergistic Radical Scavenging Potency of Curcumin-in- $\beta$ -Cyclodextrin-in-Nanomagnetoliposomes. *Mater. Sci. Eng., C* 2016, 64, 293–302.
237. Cruz N; Pinho JO; Soveral G; Ascensão L; Matela N; Reis C; Gaspar MM, A Novel Hybrid Nanosystem Integrating Cytotoxic and Magnetic Properties as a Tool to Potentiate Melanoma Therapy. *Nanomaterials* 2020, 10 (4), 693, 1–13.
238. Halevas E; Mavroidi B; Swanson CH; Smith GC; Moschona A; Hadjispyrou S; Salifoglou A; Pantazaki AA; Pelecanou M; Litsardakis G, Magnetic Cationic Liposomal Nanocarriers for the Efficient Drug Delivery of a Curcumin-Based Vanadium Complex with Anticancer Potential. *J. Inorg. Biochem* 2019, 199, 110778, 1–17. [PubMed: 31442839]
239. Li L; Wang Q; Zhang X; Luo L; He Y; Zhu R; Gao D, Dual-Targeting Liposomes for Enhanced Anticancer Effect in Somatostatin Receptor II-Positive Tumor Model. *Nanomedicine (London, U. K.)* 2018, 13 (17), 2155–2169.
240. Wang X; Yang R; Yuan C; An Y; Tang Q; Chen D, Preparation of Folic Acid-Targeted Temperature-Sensitive Magnetoliposomes and their Antitumor Effects *in Vitro* and *in Vivo*. *Target. Oncol* 2018, 13 (4), 481–494. [PubMed: 29992403]
241. Nguyen VD; Zheng S; Han J; Le VH; Park JO; Park S, Nanohybrid Magnetic Liposome Functionalized with Hyaluronic Acid for Enhanced Cellular Uptake and Near-Infrared-Triggered Drug Release. *Colloids Surf., B* 2017, 154, 104–114.
242. Ploetz E; Zimpel A; Cauda V; Bauer D; Lamb DC; Haisch C; Zahler S; Vollmar AM; Wuttke S; Engelke H, Metal-Organic Framework Nanoparticles Induce Pyroptosis in Cells Controlled by the Extracellular pH. *Adv. Mater* 2020, 32 (19), 1907267, 1–8.
243. Su Q; Pu X; Bai H; Chen X; Liao X; Huang Z; Yin G, Improvement of Thermosensitive Liposome Stability by Cerasome Forming Lipid with Si-O-Si Network Structure. *Curr. Drug Deliv* 2018, 15 (4), 585–593. [PubMed: 28721817]
244. Mebrouk K; Ciancone M; Vives T; Cammas-Marion S; Benvegna T; Le Goff-Gaillard C; Arlot-Bonnemains Y; Fourmigué M; Camerel F, Fine and Clean Photothermally Controlled NIR Drug Delivery from Biocompatible Nickel-Bis (dithiolene)-Containing Liposomes. *ChemMedChem* 2017, 12 (21), 1753–1758. [PubMed: 28902984]



245. Wehbe N; Patra D; Abdel-Massih RM; Baydoun E, Modulation of Membrane Properties by Silver Nanoparticles Probed by Curcumin Embedded in 1,2-Dimyristoyl-Sn-Glycero-3-Phosphocholine Liposomes. *Colloids Surf., B* 2019, 173, 94–100.
246. Ramalingam V; Varunkumar K; Ravikumar V; Rajaram R, Target Delivery of Doxorubicin Tethered with PVP Stabilized Gold Nanoparticles for Effective Treatment of Lung Cancer. *Sci. Rep* 2018, 8 (1), 3815, 1–12. [PubMed: 29491463]
247. Maney V; Singh M, The Synergism of Platinum-Gold Bimetallic Nanoconjugates Enhances 5-Fluorouracil Delivery *in Vitro*. *Pharmaceutics* 2019, 11 (9), 439, 1–19.
248. Ahmadkhani L; Baghban A; Mohammadpoor S; Khalilov R; Akbarzadeh A; Kavetskiy T; Saghi S; Nasibova AN, Synthesis and Evaluation of a Triblock Copolymer/ZnO Nanoparticles from Poly( $\epsilon$ -Caprolactone) and Poly(Acrylic Acid) as a Potential Drug Delivery Carrier. *Drug Res. (Stuttgart, Ger.)* 2017, 67 (4), 228–238.
249. Cortese B; D'Amone S; Testini M; Ratano P; Palamà IE, Hybrid Clustered Nanoparticles for Chemo-Antibacterial Combinatorial Cancer Therapy. *Cancers* 2019, 11 (9), 1338, 1–18.
250. Parlanti P; Boni A; Signore G; Santi M, Targeted Dendrimer-Coated Magnetic Nanoparticles for Selective Delivery of Therapeutics in Living Cells. *Molecules* 2020, 25 (9), 2252, 1–12.
251. Michlewska S; Ionov M; Szwed A; Rogalska A; Sanz Del Olmo N; Ortega P; Denel M; Jacenik D; Shcharbin D; de la Mata FJ; Bryszewska M, Ruthenium Dendrimers against Human Lymphoblastic Leukemia 1301 Cells. *Int. J. Mol. Sci* 2020, 21 (11), 4119, 1–13.
252. Zhuang J; Duan Y; Zhang Q; Gao W; Li S; Fang RH; Zhang L, Multimodal Enzyme Delivery and Therapy Enabled by Cell Membrane-Coated Metal-Organic Framework Nanoparticles. *Nano Lett.* 2020, 20 (5), 4051–4058. [PubMed: 32352801]
253. Rao L; Meng Q-F; Huang Q; Wang Z; Yu G-T; Li A; Ma W; Zhang N; Guo S-S; Zhao X-Z; Liu K; Yuan Y; Liu W, Platelet-Leukocyte Hybrid Membrane-Coated Immunomagnetic Beads for Highly Efficient and Highly Specific Isolation of Circulating Tumor Cells. *Adv. Funct. Mater* 2018, 28 (34), 1803531, 1–9.
254. Limban C; Missir AV; Caproiu MT; Grumezescu AM; Chifiriuc MC; Bleotu C; Marutescu L; Papacocea MT; Nuta DC, Novel Hybrid Formulations Based on Thiourea Derivatives and Core@Shell Fe<sub>3</sub>O<sub>4</sub>@C<sub>18</sub> Nanostructures for the Development of Antifungal Strategies. *Nanomaterials* 2018, 8 (1), 47, 1–14.
255. Rahmatolahzadeh R; Hamadani M; Ma'mani L; Shafiee A, Aspartic Acid Functionalized PEGylated MSN@GO Hybrid as an Effective and Sustainable Nano-System for *in Vitro* Drug Delivery. *Adv. Med. Sci* 2018, 63 (2), 257–264. [PubMed: 29486375]
256. Smith AM; Mancini MC; Nie S, Second Window for *in Vivo* Imaging. *Nat. Nanotechnol* 2009, 4 (11), 710–711. [PubMed: 19898521]
257. He S; Song J; Qu J; Cheng Z, Crucial Breakthrough of Second Near-Infrared Biological Window Fluorophores: Design and Synthesis Toward Multimodal Imaging and Theranostics. *Chem. Soc. Rev* 2018, 47 (12), 4258–4278. [PubMed: 29725670]
258. Hemmer E; Benayas A; Légaré F; Vetrone F, Exploiting the Biological Windows: Current Perspectives on Fluorescent Bioprobes Emitting Above 1000 Nm. *Nanoscale Horiz.* 2016, 1 (3), 168–184. [PubMed: 32260620]
259. Huang P; Liu J; Wang W; Zhang Y; Zhao F; Kong D; Liu J; Dong A, Zwitterionic Nanoparticles Constructed from Bioreducible RAFT-ROP Double Head Agent for Shell Shedding Triggered Intracellular Drug Delivery. *Acta Biomater.* 2016, 40, 263–272. [PubMed: 26607767]
260. Saini R; Lee NV; Liu KY; Poh CF, Prospects in the Application of Photodynamic Therapy in Oral Cancer and Premalignant Lesions. *Cancers* 2016, 8 (9), 83, 1–14.
261. Ma Y; Zhang Y; Li X; Zhao Y; Li M; Jiang W; Tang X; Dou J; Lu L; Wang F; Wang Y, Near-Infrared II Phototherapy Induces Deep Tissue Immunogenic Cell Death and Potentiates Cancer Immunotherapy. *ACS Nano* 2019, 13 (10), 11967–11980. [PubMed: 31553168]
262. Qian RC; Cao Y; Long YT, Binary System for MicroRNA-Targeted Imaging in Single Cells and Photothermal Cancer Therapy. *Anal. Chem* 2016, 88 (17), 8640–8647. [PubMed: 27482754]
263. Rio ISR; Rodrigues ARO; Rodrigues CP; Almeida BG; Pires A; Pereira AM; Araújo JP; Castanheira EMS; Coutinho PJG, Development of Novel Magnetoliposomes Containing Nickel

- Ferrite Nanoparticles Covered with Gold for Applications in Thermotherapy. *Materials* 2020, 13 (4), 815, 1–19.
264. He W; Frueh J; Wu Z; He Q, Leucocyte Membrane-Coated Janus Microcapsules for Enhanced Photothermal Cancer Treatment. *Langmuir* 2016, 32 (15), 3637–3644. [PubMed: 27023433]
265. Xing Y; Li L; Ai X; Fu L, Polyaniline-Coated Upconversion Nanoparticles with Upconverting Luminescent and Photothermal Conversion Properties for Photothermal Cancer Therapy. *Int. J. Nanomed* 2016, 11, 4327–4338.
266. Basoglu H; Bilgin MD; Demir MM, Protoporphyrin IX-Loaded Magnetoliposomes as a Potential Drug Delivery System for Photodynamic Therapy: Fabrication, Characterization and *in Vitro* Study. *Photodiagn. Photodyn. Ther* 2016, 13, 81–90.
267. Zhang Y; Wang F; Liu C; Wang Z; Kang L; Huang Y; Dong K; Ren J; Qu X, Nanozyme Decorated Metal-Organic Frameworks for Enhanced Photodynamic Therapy. *ACS Nano* 2018, 12 (1), 651–661. [PubMed: 29290107]
268. Zuo H; Tao J; Shi H; He J; Zhou Z; Zhang C, Platelet-Mimicking Nanoparticles Co-Loaded with W<sub>18</sub>O<sub>49</sub> and Metformin Alleviate Tumor Hypoxia for Enhanced Photodynamic Therapy and Photothermal Therapy. *Acta Biomater.* 2018, 80, 296–307. [PubMed: 30223092]
269. Xu L; Gao F; Fan F; Yang L, Platelet Membrane Coating Coupled with Solar Irradiation Endows a Photodynamic Nanosystem with Both Improved Antitumor Efficacy and Undetectable Skin Damage. *Biomaterials* 2018, 159, 59–67. [PubMed: 29309994]
270. Zhou Z; Peng S; Sui M; Chen S; Huang L; Xu H; Jiang T, Multifunctional Nanocomplex for Surface-Enhanced Raman Scattering Imaging and Near-Infrared Photodynamic Antimicrobial Therapy of Vancomycin-Resistant Bacteria. *Colloids Surf., B* 2018, 161, 394–402.
271. Youssef Z; Jouan-Hureaux V; Colombeau L; Arnoux P; Moussaron A; Baros F; Toufaily J; Hamieh T; Roques-Carmes T; Frochet C, Titania and Silica Nanoparticles Coupled to Chlorin e6 for Anti-Cancer Photodynamic Therapy. *Photodiagn. Photodyn. Ther* 2018, 22, 115–126.
272. Lan S; Lin Z; Zhang D; Zeng Y; Liu X, Photocatalysis Enhancement for Programmable Killing of Hepatocellular Carcinoma through Self-Compensation Mechanisms Based on Black Phosphorus Quantum-Dot-Hybridized Nanocatalysts. *ACS Appl. Mater. Interfaces* 2019, 11 (10), 9804–9813. [PubMed: 30773883]
273. Feng L; Dong Z; Liang C; Chen M; Tao D; Cheng L; Yang K; Liu Z, Iridium Nanocrystals Encapsulated Liposomes as Near-Infrared Light Controllable Nanozymes for Enhanced Cancer Radiotherapy. *Biomaterials* 2018, 181, 81–91. [PubMed: 30077139]
274. Liu J; Song L; Liu S; Zhao S; Jiang Q; Ding B, A Tailored DNA Nanoplatform for Synergistic RNAi-/Chemotherapy of Multidrug-Resistant Tumors. *Angew. Chem. Int. Ed* 2018, 57 (47), 15486–15490.
275. Zhang L; Jean SR; Li X; Sack T; Wang Z; Ahmed S; Chan G; Das J; Zaragoza A; Sargent EH; Kelley SO, Programmable Metal/Semiconductor Nanostructures for mRNA-Modulated Molecular Delivery. *Nano Lett.* 2018, 18 (10), 6222–6228. [PubMed: 30188727]
276. Skalickova S; Nejdil L; Kudr J; Ruttikay-Nedecky B; Jimenez AM; Kopel P; Kremplova M; Masarik M; Stiborova M; Eckschlager T; Adam V; Kizek R, Fluorescence Characterization of Gold Modified Liposomes with Antisense *N-myc* DNA Bound to the Magnetisable Particles with Encapsulated Anticancer Drugs (Doxorubicin, Ellipticine and Etoposide). *Sensors* 2016, 16 (3), 290, 1–11. [PubMed: 26927112]
277. Zhu H; Han W; Gan Y; Li Q; Li X; Shao L; Zhu D; Guo H, Combined Modality Therapy Based on Hybrid Gold Nanostars Coated with Temperature Sensitive Liposomes to Overcome Paclitaxel-Resistance in Hepatic Carcinoma. *Pharmaceutics* 2019, 11 (12), 683, 1–20.
278. Xuexiang H; Yiye L; Ying X; Xiao Z; Yinlong Z; Xiao Y; Yongwei W; Ruifang Z; Gregory JA; Yuliang Z; Guangjun N, Reversal of Pancreatic Desmoplasia by Re-Educating Stellate Cells with a Tumour Microenvironment-Activated Nanosystem. *Nat. Commun* 2018, 9 (1), 1–18. [PubMed: 29317637]
279. Wang F; Huang Q; Wang Y; Zhang W; Lin R; Yu Y; Shen Y; Cui H; Guo S, Rational Design of Multimodal Therapeutic Nanosystems for Effective Inhibition of Tumor Growth and Metastasis. *Acta Biomater.* 2018, 77, 240–254. [PubMed: 30012354]

280. Gilam A; Conde J; Weissglas-Volkov D; Oliva N; Friedman E; Artzi N; Shomron N, Local MicroRNA Delivery Targets Palladin and Prevents Metastatic Breast Cancer. *Nat. Commun* 2016, 7, 12868, 1–14. [PubMed: 27641360]
281. Kotcherlakota R; Srinivasan DJ; Mukherjee S; Haroon MM; Dar GH; Venkatraman U; Patra CR; Gopal V, Engineered Fusion Protein-Loaded Gold Nanocarriers for Targeted Co-Delivery of Doxorubicin and Erbb2-siRNA in Human Epidermal Growth Factor Receptor-2+ Ovarian Cancer. *J. Mater. Chem. B* 2017, 5 (34), 7082–7098. [PubMed: 32263899]
282. He ZM; Zhang PH; Li X; Zhang JR; Zhu JJ, A Targeted DNzyme-Nanocomposite Probe Equipped with Built-In Zn(2+) Arsenal for Combined Treatment of Gene Regulation and Drug Delivery. *Sci. Rep* 2016, 6, 22737, 1–10. [PubMed: 26956167]
283. Lin L; Fan Y; Gao F; Jin L; Li D; Sun W; Li F; Qin P; Shi Q; Shi X; Du L, UTMD-Promoted Co-Delivery of Gemcitabine and miR-21 Inhibitor by Dendrimer-Entrapped Gold Nanoparticles for Pancreatic Cancer Therapy. *Theranostics* 2018, 8 (7), 1923–1939. [PubMed: 29556365]
284. Zhang J; Zhao T; Han F; Hu Y; Li Y, Photothermal and Gene Therapy Combined with Immunotherapy to Gastric Cancer by the Gold Nanoshell-Based System. *J. Nanobiotechnol* 2019, 17 (1), 80, 1–11.
285. Liu B; Cao W; Qiao G; Yao S; Pan S; Wang L; Yue C; Ma L; Liu Y; Cui D, Effects of Gold Nanoprism-Assisted Human PD-L1 siRNA on Both Gene Down-Regulation and Photothermal Therapy on Lung Cancer. *Acta Biomater.* 2019, 99, 307–319. [PubMed: 31513911]
286. Jia HZ; Chen WH; Wang X; Lei Q; Yin WN; Wang Y; Zhuo RX; Feng J; Zhang XZ, Virus-Surface-Mimicking Surface Clustering of AuNPs onto DNAEntrapped Polymeric Nanoparticle for Enhanced Cellular Internalization and Nanocluster-Induced NIR Photothermal Therapy. *Adv. Sci* 2015, 2 (12), 1500108, 1–6.
287. Liu Y; Xu M; Zhao Y; Chen X; Zhu X; Wei C; Zhao S; Liu J; Qin X, Flower-Like Gold Nanoparticles for Enhanced Photothermal Anticancer Therapy by the Delivery of Pooled siRNA to Inhibit Heat Shock Stress Response. *J. Mater. Chem. B* 2019, 7 (4), 586–597. [PubMed: 32254792]
288. Wang Z; Wang L; Prabhakar N; Xing Y; Rosenholm JM; Zhang J; Cai K, CaP Coated Mesoporous Polydopamine Nanoparticles with Responsive Membrane Permeation Ability for Combined Photothermal and siRNA Therapy. *Acta Biomater.* 2019, 86, 416–428. [PubMed: 30611792]
289. Liu Y; Zhang X; Liu Z; Wang L; Luo L; Wang M; Wang Q; Gao D, Gold Nanoshell-Based Betulinic Acid Liposomes for Synergistic Chemo-Photothermal Therapy. *Nanomed. Nanotechnol. Biol. Med* 2017, 13 (6), 1891–1900.
290. Luo L; Bian Y; Liu Y; Zhang X; Wang M; Xing S; Li L; Gao D, Combined Near Infrared Photothermal Therapy and Chemotherapy Using Gold Nanoshells Coated Liposomes to Enhance Antitumor Effect. *Small* 2016, 12 (30), 4103–4112. [PubMed: 27294601]
291. Rodrigues ARO; Matos JOG; Nova Dias AM; Almeida BG; Pires A; Pereira AM; Araújo JP; Queiroz MRP; Castanheira EMS; Coutinho PJG, Development of Multifunctional Liposomes Containing Magnetic/Plasmonic MnFe<sub>2</sub>O<sub>4</sub>/Au Core/Shell Nanoparticles. *Pharmaceutics* 2018, 11 (1), 10, 1–19.
292. Li Y; He D; Tu J; Wang R; Zu C; Chen Y; Yang W; Shi D; Webster TJ; Shen Y, The Comparative Effect of Wrapping Solid Gold Nanoparticles and Hollow Gold Nanoparticles with Doxorubicin-Loaded Thermosensitive Liposomes for Cancer Thermo-Chemotherapy. *Nanoscale* 2018, 10 (18), 8628–8641. [PubMed: 29697100]
293. Xing S; Zhang X; Luo L; Cao W; Li L; He Y; An J; Gao D, Doxorubicin/Gold Nanoparticles Coated with Liposomes for Chemo-Photothermal Synergetic Antitumor Therapy. *Nanotechnology* 2018, 29 (40), 405101, 1–11. [PubMed: 30004030]
294. Sun Y; Wang Q; Chen J; Liu L; Ding L; Shen M; Li J; Han B; Duan Y, Temperature-Sensitive Gold Nanoparticle-Coated Pluronic-PLL Nanoparticles for Drug Delivery and Chemo-Photothermal Therapy. *Theranostics* 2017, 7 (18), 4424–4444. [PubMed: 29158837]
295. Song L; Jiang Q; Liu J; Li N; Liu Q; Dai L; Gao Y; Liu W; Liu D; Ding B, DNA Origami/Gold Nanorod Hybrid Nanostructures for the Circumvention of Drug Resistance. *Nanoscale* 2017, 9 (23), 7750–7754. [PubMed: 28581004]

296. Zang Y; Wei Y; Shi Y; Chen Q; Xing D, Chemo/Photoacoustic Dual Therapy with mRNA-Triggered DOX Release and Photoinduced Shockwave Based on a DNA-Gold Nanoplatform. *Small* 2016, 12 (6), 756–769. [PubMed: 26683002]
297. Cao Y; Li S; Chen C; Wang D; Wu T; Dong H; Zhang X, Rattle-Type Au@Cu<sub>2</sub>-xS Hollow Mesoporous Nanocrystals with Enhanced Photothermal Efficiency for Intracellular Oncogenic MicroRNA Detection and Chemo-Photothermal Therapy. *Biomaterials* 2018, 158, 23–33. [PubMed: 29274527]
298. Wang S; Yang L; Cho HY; Dean Chueng ST; Zhang H; Zhang Q; Lee KB, Programmed Degradation of a Hierarchical Nanoparticle with Redox and Light Responsivity for Self-Activated Photo-Chemical Enhanced Chemodynamic Therapy. *Biomaterials* 2019, 224, 119498, 1–12. [PubMed: 31557590]
299. Zhang H; Li Y; Pan Z; Chen Y; Fan Z; Tian H; Zhou S; Zhang Y; Shang J; Jiang B; Wang F; Luo F; Hou Z, Multifunctional Nanosystem Based on Graphene Oxide for Synergistic Multistage Tumor-Targeting and Combined Chemo-Photothermal Therapy. *Mol. Pharm* 2019, 16 (5), 1982–1998. [PubMed: 30892898]
300. Zaharie-Butucel D; Potara M; Suarasan S; Licarete E; Astilean S, Efficient Combined Near-Infrared-Triggered Therapy: Phototherapy over Chemotherapy in Chitosan-Reduced Graphene Oxide-IR820 Dye-Doxorubicin Nanoplatforms. *J. Colloid Interface Sci* 2019, 552, 218–229. [PubMed: 31128402]
301. Deng W; Chen W; Clement S; Guller A; Zhao Z; Engel A; Goldys EM, Controlled Gene and Drug Release from a Liposomal Delivery Platform Triggered by X-Ray Radiation. *Nat. Commun* 2018, 9 (1), 2713, 1–11. [PubMed: 30006596]
302. Liu Q; Zhou Y; Li M; Zhao L; Ren J; Li D; Tan Z; Wang K; Li H; Hussain M; Zhang L; Shen G; Zhu J; Tao J, Polyethylenimine Hybrid Thin-Shell Hollow Mesoporous Silica Nanoparticles as Vaccine Self-Adjuvants for Cancer Immunotherapy. *ACS Appl. Mater. Interfaces* 2019, 11 (51), 47798–47809. [PubMed: 31773941]
303. Zhuang X; Wu T; Zhao Y; Hu X; Bao Y; Guo Y; Song Q; Li G; Tan S; Zhang Z, Lipid-Enveloped Zinc Phosphate Hybrid Nanoparticles for Codelivery of H-2K<sup>b</sup> and H-2D<sup>b</sup>-Restricted Antigenic Peptides and Monophosphoryl Lipid A to Induce Antitumor Immunity against Melanoma. *J. Control. Release* 2016, 228, 26–37. [PubMed: 26921522]
304. Sharma P; Shin JB; Park BC; Lee JW; Byun SW; Jang NY; Kim YJ; Kim Y; Kim YK; Cho NH, Application of Radially Grown ZnO Nanowires on Poly-L-Lactide Microfibers Complexed with a Tumor Antigen for Cancer Immunotherapy. *Nanoscale* 2019, 11 (10), 4591–4600. [PubMed: 30809611]
305. Štarha P; Smola D; Tušek J; Trávníček Z, Efficient Synthesis of a Maghemite/Gold Hybrid Nanoparticle System as a Magnetic Carrier for the Transport of Platinum-Based Metallotherapeutics. *Int. J. Mol. Sci* 2015, 16 (1), 2034–2051. [PubMed: 25603182]
306. Senthilkumar P; Yaswant G; Kavitha S; Chandramohan E; Kowsalya G; Vijay R; Sudhagar B; Kumar D, Preparation and Characterization of Hybrid Chitosan-Silver Nanoparticles (Chi-Ag NPs); A Potential Antibacterial Agent. *Int. J. Biol. Macromol* 2019, 141, 290–298. [PubMed: 31476395]
307. Dai M; Frezzo JA; Sharma E; Chen R; Singh N; Yuvienco C; Caglar E; Xiao S; Saxena A; Montclare JK, Engineered Protein Polymer-Gold Nanoparticle Hybrid Materials for Small Molecule Delivery. *J. Nanomed. Nanotechnol* 2016, 7 (1), 356, 1–19. [PubMed: 27081576]
308. Voulgari E; Bakandritsos A; Galtsidis S; Zoumpourlis V; Burke BP; Clemente GS; Cawthorne C; Archibald SJ; Tušek J; Zbořil R; Kantarelou V; Karydas AG; Avgoustakis K, Synthesis, Characterization and *in Vivo* Evaluation of a Magnetic Cisplatin Delivery Nanosystem Based on PMAA-Graft-PEG Copolymers. *J. Control. Release* 2016, 243, 342–356. [PubMed: 27793687]
309. Lei Y; Tang L; Xie Y; Xianyu Y; Zhang L; Wang P; Hamada Y; Jiang K; Zheng W; Jiang X, Gold Nanoclusters-Assisted Delivery of NGF siRNA for Effective Treatment of Pancreatic Cancer. *Nat. Commun* 2017, 8, 15130, 1–15. [PubMed: 28440296]
310. Huo S; Gong N; Jiang Y; Chen F; Guo H; Gan Y; Wang Z; Herrmann A; Liang X-J, Gold-DNA Nanosunflowers for Efficient Gene Silencing with Controllable Transformation. *Sci. Adv* 2019, 5 (10), eaaw6264, 1–11.

311. Davoodi E; Montazerian H; Khademhosseini A; Toyserkani E, Sacrificial 3D Printing of Shrinkable Silicone Elastomers for Enhanced Feature Resolution in Flexible Tissue Scaffolds. *Acta Biomater.* 2020, 117, 261–272. [PubMed: 33031967]
312. Montazerian H; Mohamed MGA; Montazeri MM; Kheiri S; Milani AS; Kim K; Hoorfar M, Permeability and Mechanical Properties of Gradient Porous PDMS Scaffolds Fabricated by 3D-Printed Sacrificial Templates Designed with Minimal Surfaces. *Acta Biomater.* 2019, 96, 149–160. [PubMed: 31252172]
313. Rigo C; Ferroni L; Tocco I; Roman M; Munivrana I; Gardin C; Cairns WR; Vindigni V; Azzena B; Barbante C, Active Silver Nanoparticles for Wound Healing. *Int. J. Mol. Sci* 2013, 14 (3), 4817–4840. [PubMed: 23455461]
314. Chai S-H; Wang Y; Qiao Y; Wang P; Li Q; Xia C; Ju M, Bio Fabrication of Silver Nanoparticles as an Effective Wound Healing Agent in the Wound Care After Anorectal Surgery. *J. Photochem. Photobiol., B* 2018, 178, 457–462. [PubMed: 29223119]
315. Berthet M; Gauthier Y; Lacroix C; Verrier B; Monge C, Nanoparticle-Based Dressing: The Future of Wound Treatment? *Trends Biotechnol.* 2017, 35 (8), 770–784. [PubMed: 28645529]
316. Akturk O; Kismet K; Yasti AC; Kuru S; Duymus ME; Kaya F; Caydere M; Hucumenoglu S; Keskin D, Collagen/Gold Nanoparticle Nanocomposites: A Potential Skin Wound Healing Biomaterial. *J. Biomater. Appl* 2016, 31 (2), 283–301. [PubMed: 27095659]
317. Sun L; Yi S; Wang Y; Pan K; Zhong Q; Zhang M, A Bio-Inspired Approach for *in Situ* Synthesis of Tunable Adhesive. *Bioinspir. Biomim* 2013, 9 (1), 016005, 1–11. [PubMed: 24343277]
318. Chen WY; Chang HY; Lu JK; Huang YC; Harroun SG; Tseng YT; Li YJ; Huang CC; Chang HT, Self-Assembly of Antimicrobial Peptides on Gold Nanodots: against Multidrug-Resistant Bacteria and Wound-Healing Application. *Adv. Funct. Mater* 2015, 25 (46), 7189–7199.
319. Huang H-C; Walker CR; Nanda A; Rege K, Laser Welding of Ruptured Intestinal Tissue Using Plasmonic Polypeptide Nanocomposite Solders. *ACS Nano* 2013, 7 (4), 2988–2998. [PubMed: 23530530]
320. Gopal A; Kant V; Gopalakrishnan A; Tandan SK; Kumar D, Chitosan-Based Copper Nanocomposite Accelerates Healing in Excision Wound Model in Rats. *Eur. J. Pharmacol* 2014, 731, 8–19. [PubMed: 24632085]
321. Yadav E; Singh D; Yadav P; Verma A, Ameliorative Effect of Biofabricated ZnO Nanoparticles of *Trianthema Portulacastrum Linn.* on Dermal Wounds *via* Removal of Oxidative Stress and Inflammation. *RSC Adv.* 2018, 8 (38), 21621–21635. [PubMed: 35539937]
322. Thangavel P; Kannan R; Ramachandran B; Moorthy G; Suguna L; Muthuvijayan V, Development of Reduced Graphene Oxide (rGO)-Isabgol Nanocomposite Dressings for Enhanced Vascularization and Accelerated Wound Healing in Normal and Diabetic Rats. *J. Colloid Interface Sci* 2018, 517, 251–264. [PubMed: 29428812]
323. Quignard S; Coradin T; Powell JJ; Jugdaohsingh R, Silica Nanoparticles as Sources of Silicic Acid Favoring Wound Healing *in Vitro*. *Colloids Surf., B* 2017, 155, 530–537.
324. Khalid A; Ullah H; Ul-Islam M; Khan R; Khan S; Ahmad F; Khan T; Wahid F, Bacterial Cellulose-TiO<sub>2</sub> Nanocomposites Promote Healing and Tissue Regeneration in Burn Mice Model. *RSC Adv.* 2017, 7 (75), 47662–47668.
325. Liu C; Yao W; Tian M; Wei J; Song Q; Qiao W, Mussel-Inspired Degradable Antibacterial Polydopamine/Silica Nanoparticle for Rapid Hemostasis. *Biomaterials* 2018, 179, 83–95. [PubMed: 29980077]
326. Fan X; Wang S; Fang Y; Li P; Zhou W; Wang Z; Chen M; Liu H, Tough Polyacrylamide-Tannic Acid-Kaolin Adhesive Hydrogels for Quick Hemostatic Application. *Mater. Sci. Eng., C* 2020, 109, 110649, 1–9.
327. Lokhande G; Carrow JK; Thakur T; Xavier JR; Parani M; Bayless KJ; Gaharwar AK, Nanoengineered Injectable Hydrogels for Wound Healing Application. *Acta Biomater.* 2018, 70, 35–47. [PubMed: 29425720]
328. Pinkas O; Goder D; Noyvirt R; Peleg S; Kahlon M; Zilberman M, Structuring of Composite Hydrogel Bioadhesives and Its Effect on Properties and Bonding Mechanism. *Acta Biomater.* 2017, 51, 125–137. [PubMed: 28110072]

329. Webster TJ; Ergun C; Doremus RH; Siegel RW; Bizios R, Specific Proteins Mediate Enhanced Osteoblast Adhesion on Nanophase Ceramics. *J. Biomed. Mater. Res* 2000, 51 (3), 475–483. [PubMed: 10880091]
330. Colon G; Ward BC; Webster TJ, Increased Osteoblast and Decreased Staphylococcus Epidermidis Functions on Nanophase ZnO and TiO<sub>2</sub>. *J. Biomed. Mater. Res. Part A* 2006, 78 (3), 595–604.
331. Zhang L; Chen Y; Rodriguez J; Fenniri H; Webster TJ, Biomimetic Helical Rosette Nanotubes and Nanocrystalline Hydroxyapatite Coatings on Titanium for Improving Orthopedic Implants. *Int. J. Nanomed* 2008, 3 (3), 323–333.
332. Kisiday J; Jin M; Kurz B; Hung H; Semino C; Zhang S; Grodzinsky A, Self-Assembling Peptide Hydrogel Fosters Chondrocyte Extracellular Matrix Production and Cell Division: Implications for Cartilage Tissue Repair. *Proc. Natl. Acad. Sci. U.S.A* 2002, 99 (15), 9996–10001. [PubMed: 12119393]
333. Zhou X; Tenaglio S; Esworthy T; Hann SY; Cui H; Webster TJ; Fenniri H; Zhang LG, Three-Dimensional Printing Biologically Inspired DNA-Based Gradient Scaffolds for Cartilage Tissue Regeneration. *ACS Appl. Mater. Interfaces* 2020, 12 (29), 33219–33228. [PubMed: 32603082]
334. Sitharaman B; Shi X; Walboomers XF; Liao H; Cuijpers V; Wilson LJ; Mikos AG; Jansen JA, *In Vivo* Biocompatibility of Ultra-Short Single-Walled Carbon Nanotube/Biodegradable Polymer Nanocomposites for Bone Tissue Engineering. *Bone* 2008, 43 (2), 362–370. [PubMed: 18541467]
335. Li W-J; Tuli R; Okafor C; Derfoul A; Danielson KG; Hall DJ; Tuan RS, A Three-Dimensional Nanofibrous Scaffold for Cartilage Tissue Engineering Using Human Mesenchymal Stem Cells. *Biomaterials* 2005, 26 (6), 599–609. [PubMed: 15282138]
336. Shao W; He J; Sang F; Wang Q; Chen L; Cui S; Ding B, Enhanced Bone Formation in Electrospun Poly (L-Lactic-*co*-Glycolic Acid)-Tussah Silk Fibroin Ultrafine Nanofiber Scaffolds Incorporated with Graphene Oxide. *Mater. Sci. Eng., C* 2016, 62, 823–834.
337. Nie W; Peng C; Zhou X; Chen L; Wang W; Zhang Y; Ma PX; He C, Three-Dimensional Porous Scaffold by Self-Assembly of Reduced Graphene Oxide and Nano-Hydroxyapatite Composites for Bone Tissue Engineering. *Carbon* 2017, 116, 325–337.
338. Webster TJ; Ejiogor JU, Increased Osteoblast Adhesion on Nanophase Metals: Ti, Ti6Al4V, and CoCrMo. *Biomaterials* 2004, 25 (19), 4731–4739. [PubMed: 15120519]
339. Xu C; Xiao L; Cao Y; He Y; Lei C; Xiao Y; Sun W; Ahadian S; Zhou X; Khademhosseini A, Mesoporous Silica Rods with Cone Shaped Pores Modulate Inflammation and Deliver BMP-2 for Bone Regeneration. *Nano Res.* 2020, 13 (9), 1–9.
340. Babitha S; Annamalai M; Dykas MM; Saha S; Poddar K; Venugopal JR; Ramakrishna S; Venkatesan T; Korrapati PS, Fabrication of a Biomimetic ZeinPDA Nanofibrous During Scaffold Impregnated with BMP-2 Peptide Conjugated TiO<sub>2</sub> Nanoparticle for Bone Tissue Engineering. *J. Tissue Eng. Regen. Med* 2018, 12 (4), 991–1001.
341. Li J; Li L; Zhou J; Zhou Z; Wu X-l.; Wang, L.; Yao, Q., 3D Printed Dual-Functional Biomaterial with Self-Assembly Micro-Nano Surface and Enriched Nano Argentum for Antibacterial and Bone Regeneration. *Appl. Mater. Today* 2019, 17, 206–215.
342. Song Y; Wu H; Gao Y; Li J; Lin K; Liu B; Lei X; Cheng P; Zhang S; Wang Y, Zinc Silicate/ Nano-Hydroxyapatite/Collagen Scaffolds Promote Angiogenesis and Bone Regeneration *via* the p38 MAPK Pathway in Activated Monocytes. *ACS Appl. Mater. Interfaces* 2020, 12 (14), 16058–16075. [PubMed: 32182418]
343. Xing H; Wang X; Xiao G; Zhao Z; Zou S; Li M; Richardson JJ; Tardy BL; Xie L; Komasa S, Hierarchical Assembly of Nanostructured Coating for siRNA-Based Dual Therapy of Bone Regeneration and Revascularization. *Biomaterials* 2020, 235, 119784, 1–10. [PubMed: 31981763]
344. Lee SJ; Yoo JJ; Lim GJ; Atala A; Stitzel J, *In Vitro* Evaluation of Electrospun Nanofiber Scaffolds for Vascular Graft Application. *J. Biomed. Mater. Res. Part A* 2007, 83 (4), 999–1008.
345. Huang R; Gao X; Wang J; Chen H; Tong C; Tan Y; Tan Z, Triple-Layer Vascular Grafts Fabricated by Combined E-Jet 3D Printing and Electrospinning. *Ann. Biomed. Eng* 2018, 46 (9), 1254–1266. [PubMed: 29845412]

346. Park S; Kim J; Lee M-K; Park C; Jung H-D; Kim H-E; Jang T-S, Fabrication of Strong, Bioactive Vascular Grafts with PCL/Collagen and PCL/Silica Bilayers for Small-Diameter Vascular Applications. *Mater. Des* 2019, 181, 108079, 1–10.
347. Xue C; Xie H; Eichenbaum J; Chen Y; Wang Y; van den Dolder FW; Lee J; Lee K; Zhang S; Sun W, Synthesis of Injectable Shear-Thinning Biomaterials of Various Compositions of Gelatin and Synthetic Silicate Nanoplatelet. *Biotechnol. J* 2020, 15 (8), 1900456, 1–9.
348. Ashtari K; Nazari H; Ko H; Tebon P; Akhshik M; Akbari M; Alhosseini SN; Mozafari M; Mehravi B; Soleimani M, Electrically Conductive Nanomaterials for Cardiac Tissue Engineering. *Adv. Drug Deliv. Rev* 2019, 144, 162–179. [PubMed: 31176755]
349. Ahadian S; Yamada S; Ramón-Azcón J; Estili M; Liang X; Nakajima K; Shiku H; Khademhosseini A; Matsue T, Hybrid Hydrogel-Aligned Carbon Nanotube Scaffolds To Enhance Cardiac Differentiation of Embryoid Bodies. *Acta Biomater.* 2016, 31, 134–143. [PubMed: 26621696]
350. Ren J; Xu Q; Chen X; Li W; Guo K; Zhao Y; Wang Q; Zhang Z; Peng H; Li YG, Superaligned Carbon Nanotubes Guide Oriented Cell Growth and Promote Electrophysiological Homogeneity for Synthetic Cardiac Tissues. *Adv. Mater* 2017, 29 (44), 1702713, 1–8.
351. Shin SR; Jung SM; Zalabany M; Kim K; Zorlutuna P; Kim S. b.; Nikkhah M; Khabiry M; Azize M; Kong J, Carbon-Nanotube-Embedded Hydrogel Sheets for Engineering Cardiac Constructs and Bioactuators. *ACS Nano* 2013, 7 (3), 2369–2380. [PubMed: 23363247]
352. Roshanbinfar K; Mohammadi Z; Mesgar AS-M; Dehghan MM; Oommen OP; Hilborn J; Engel FB, Carbon Nanotube Doped Pericardial Matrix Derived Electroconductive Biohybrid Hydrogel for Cardiac Tissue Engineering. *Biomater. Sci* 2019, 7 (9), 3906–3917. [PubMed: 31322163]
353. Shevach M; Fleischer S; Shapira A; Dvir T, Gold Nanoparticle-Decellularized Matrix Hybrids for Cardiac Tissue Engineering. *Nano Lett.* 2014, 14 (10), 5792–5796. [PubMed: 25176294]
354. Ganji Y; Li Q; Quabius ES; Böttner M; Selhuber-Unkel C; Kasra M, Cardiomyocyte Behavior on Biodegradable Polyurethane/Gold Nanocomposite Scaffolds Under Electrical Stimulation. *Mater. Sci. Eng., C* 2016, 59, 10–18.
355. Navaei A; Saini H; Christenson W; Sullivan RT; Ros R; Nikkhah M, Gold Nanorod-Incorporated Gelatin-Based Conductive Hydrogels for Engineering Cardiac Tissue Constructs. *Acta Biomater.* 2016, 41, 133–146. [PubMed: 27212425]
356. Koh H; Yong T; Chan C; Ramakrishna S, Enhancement of Neurite Outgrowth Using Nano-Structured Scaffolds Coupled with Laminin. *Biomaterials* 2008, 29 (26), 3574–3582. [PubMed: 18533251]
357. Lee S-J; Asheghali D; Blevins B; Timsina R; Esworthy T; Zhou X; Cui H; Hann SY; Qiu X; Tokarev A, Touch-Spun Nanofibers for Nerve Regeneration. *ACS Appl. Mater. Interfaces* 2019, 12 (2), 2067–2075.
358. Hu H; Ni Y; Montana V; Haddon RC; Parpura V, Chemically Functionalized Carbon Nanotubes as Substrates for Neuronal Growth. *Nano Lett.* 2004, 4 (3), 507–511. [PubMed: 21394241]
359. Kim HJ; Lee JS; Park JM; Lee S; Hong SJ; Park JS; Park K-H, Fabrication of Nanocomposites Complexed with Gold Nanoparticles on Polyaniline and Application to Their Nerve Regeneration. *ACS Appl. Mater. Interfaces* 2020, 12 (27), 30750–30760. [PubMed: 32539331]
360. Chen X; Ge X; Qian Y; Tang H; Song J; Qu X; Yue B; Yuan WE, Electrospinning Multilayered Scaffolds Loaded with Melatonin and Fe<sub>3</sub>O<sub>4</sub> Magnetic Nanoparticles for Peripheral Nerve Regeneration. *Adv. Funct. Mater* 2020, 30 (38), 2004537, 1–12.
361. Park S; Park HH; Ko YS; Lee SJ; Le TS; Woo K; Ko G, Disinfection of Various Bacterial Pathogens Using Novel Silver Nanoparticle-Decorated Magnetic Hybrid Colloids. *Sci. Total Environ* 2017, 609, 289–296. [PubMed: 28753503]
362. Shankar S; Oun AA; Rhim JW, Preparation of Antimicrobial Hybrid Nano-Materials Using Regenerated Cellulose and Metallic Nanoparticles. *Int. J. Biol. Macromol* 2018, 107 (Pt A), 17–27. [PubMed: 28855135]
363. Elashnikov R; Radocha M; Panov I; Rimpelova S; Ulbrich P; Michalcova A; Svorcik V; Lyutakov O, Porphyrin–Silver Nanoparticles Hybrids: Synthesis, Characterization and Antibacterial Activity. *Mater. Sci. Eng., C* 2019, 102, 192–199.

364. Zhang C; Du C; Liao JY; Gu Y; Gong Y; Pei J; Gu H; Yin D; Gao L; Pan Y, Synthesis of Magnetite Hybrid Nanocomplexes to Eliminate Bacteria and Enhance Biofilm Disruption. *Biomater. Sci* 2019, 7 (7), 2833–2840. [PubMed: 31066733]
365. Tung le M; Cong NX; Huy le T; Lan NT; Phan VN; Hoa NQ; Vinh le K; Thinh NV; Tai le T; Ngo DT; Mølhave K; Huy TQ; Le AT, Synthesis, Characterizations of Superparamagnetic Fe<sub>3</sub>O<sub>4</sub>-Ag Hybrid Nanoparticles and Their Application for Highly Effective Bacteria Inactivation. *J. Nanosci. Nanotechnol* 2016, 16 (6), 5902–5912. [PubMed: 27427651]
366. Ullah S; Ahmad A; Subhan F; Jan A; Raza M; Khan AU; Rahman AU; Khan UA; Tariq M; Yuan Q, Tobramycin Mediated Silver Nanospheres/Graphene Oxide Composite for Synergistic Therapy of Bacterial Infection. *J. Photochem. Photobiol., B* 2018, 183, 342–348. [PubMed: 29763756]
367. Al-Obaidi H; Kalgudi R; Zariwala MG, Fabrication of Inhaled Hybrid Silver/Ciprofloxacin Nanoparticles with Synergetic Effect against *Pseudomonas Aeruginosa*. *Eur. J. Pharm. Biopharm* 2018, 128, 27–35. [PubMed: 29654885]
368. Kim D; Kwon SJ; Wu X; Sauve J; Lee I; Nam J; Kim J; Dordick JS, Selective Killing of Pathogenic Bacteria by Antimicrobial Silver Nanoparticle-Cell Wall Binding Domain Conjugates. *ACS Appl. Mater. Interfaces* 2018, 10 (16), 13317–13324. [PubMed: 29619821]
369. Palmieri G; Tatè R; Gogliettino M; Balestrieri M; Rea I; Terracciano M; Proroga YT; Capuano F; Anastasio A; De Stefano L, Small Synthetic Peptides Bioconjugated to Hybrid Gold Nanoparticles Destroy Potentially Deadly Bacteria at Submicromolar Concentrations. *Bioconjug. Chem* 2018, 29 (11), 3877–3885. [PubMed: 30352512]
370. Monti S; Jose J; Sahajan A; Kalarikkal N; Thomas S, Structure and Dynamics of Gold Nanoparticles Decorated with Chitosan-Gentamicin Conjugates: ReaxFF Molecular Dynamics Simulations to Disclose Drug Delivery. *Phys. Chem. Chem. Phys* 2019, 21 (24), 13099–13108. [PubMed: 31169276]
371. Wang C; Cui Q; Wang X; Li L, Preparation of Hybrid Gold/Polymer Nanocomposites and Their Application in a Controlled Antibacterial Assay. *ACS Appl. Mater. Interfaces* 2016, 8 (42), 29101–29109. [PubMed: 27700040]
372. Esteban-Fernández de Ávila B; Angsantikul P; Ramírez-Herrera DE; Soto F; Teymourian H; Dehaini D; Chen Y; Zhang L; Wang J, Hybrid Biomembrane-Functionalized Nanorobots for Concurrent Removal of Pathogenic Bacteria and Toxins. *Sci. Rob* 2018, 3 (18), eaat0485, 1–9.
373. Kalita S; Kandimalla R; Bhowal AC; Kotoky J; Kundu S, Functionalization of  $\beta$ -Lactam Antibiotic on Lysozyme Capped Gold Nanoclusters Retrogress MRSA and Its Persists Following Awakening. *Sci. Rep* 2018, 8 (1), 5778, 1–13. [PubMed: 29636496]
374. Zheng Y; Liu W; Chen Y; Li C; Jiang H; Wang X, Conjugating Gold Nanoclusters and Antimicrobial Peptides: From Aggregation-Induced Emission to Antibacterial Synergy. *J. Colloid Interface Sci* 2019, 546, 1–10. [PubMed: 30901687]
375. Covarrubias C; Trepiana D; Corral C, Synthesis of Hybrid Copper-Chitosan Nanoparticles with Antibacterial Activity against Cariogenic *Streptococcus Mutans*. *Dent. Mater. J* 2018, 37 (3), 379–384. [PubMed: 29415972]
376. Elfeky AS; Salem SS; Elzaref AS; Owda ME; Eladawy HA; Saeed AM; Awad MA; Abou-Zeid RE; Fouda A, Multifunctional Cellulose Nanocrystal/Metal Oxide Hybrid, Photo-Degradation, Antibacterial and Larvicidal Activities. *Carbohydr. Polym* 2020, 230, 115711, 1–11. [PubMed: 31887890]
377. Senthilkumar RP; Bhuvaneshwari V; Ranjithkumar R; Sathiyavimal S; Malayaman V; Chandarshekar B, Synthesis, Characterization and Antibacterial Activity of Hybrid Chitosan-Cerium Oxide Nanoparticles: As a Bionanomaterials. *Int. J. Biol. Macromol* 2017, 104 (Pt B), 1746–1752. [PubMed: 28359891]
378. Li Y; Liu X; Tan L; Cui Z; Yang X; Yeung KWK; Pan H; Wu S, Construction of *N*-Halamine Labeled Silica/Zinc Oxide Hybrid Nanoparticles for Enhancing Antibacterial Ability of Ti Implants. *Mater. Sci. Eng., C* 2017, 76, 50–58.
379. Orenstein WA; Ahmed R, Simply Put: Vaccination Saves Lives. *Proc. Natl. Acad. Sci. U.S.A* 2017, 114 (16), 4031–4033. [PubMed: 28396427]



380. Kang S; Ahn S; Lee J; Kim JY; Choi M; Gujrati V; Kim H; Kim J; Shin EC; Jon S, Effects of Gold Nanoparticle-Based Vaccine Size on Lymph Node Delivery and Cytotoxic T-Lymphocyte Responses. *J. Control. Release* 2017, 256, 56–67. [PubMed: 28428066]
381. Sanchez-Villamil JI; Tapia D; Torres AG, Development of a Gold Nanoparticle Vaccine against Enterohemorrhagic *Escherichia coli* O157:H7. *Mbio* 2019, 10 (4), e01869–19, 1–16. [PubMed: 31409688]
382. Quach QH; Ang SK; Chu JJ; Kah JCY, Size-Dependent Neutralizing Activity of Gold Nanoparticle-Based Subunit Vaccine against Dengue Virus. *Acta Biomater.* 2018, 78, 224–235. [PubMed: 30099200]
383. Gregory AE; Judy BM; Qazi O; Blumentritt CA; Brown KA; Shaw AM; Torres AG; Titball RW, A Gold Nanoparticle-Linked Glycoconjugate Vaccine against *Burkholderia Mallei*. *Nanomed. Nanotechnol. Biol. Med* 2015, 11 (2), 447–56.
384. Al-Deen FN; Ho J; Selomulya C; Ma C; Coppel R, Superparamagnetic Nanoparticles for Effective Delivery of Malaria DNA Vaccine. *Langmuir* 2011, 27 (7), 3703–3712. [PubMed: 21361304]
385. Wang G; Zhou H; Nian QG; Yang Y; Qin CF; Tang R, Robust Vaccine Formulation Produced by Assembling a Hybrid Coating of Polyethyleneimine-Silica. *Chem. Sci* 2016, 7 (3), 1753–1759. [PubMed: 28936324]
386. Amin MK; Boateng JS, Comparison and Process Optimization of PLGA, Chitosan and Silica Nanoparticles for Potential Oral Vaccine Delivery. *Ther. Deliv* 2019, 10 (8), 493–514. [PubMed: 31496377]
387. Yang Y; Chen Q; Wu JP; Kirk TB; Xu J; Liu Z; Xue W, Reduction-Responsive Codelivery System Based on a Metal-Organic Framework for Eliciting Potent Cellular Immune Response. *ACS Appl. Mater. Interfaces* 2018, 10 (15), 12463–12473. [PubMed: 29595246]
388. Ibrahim M; Hazhirkarzar B; Dublin A, Magnetic Resonance Imaging (MRI) Gadolinium. StatPearls Publishing: Treasure Island (FL), 2020.
389. Erdogan S; Torchilin VP, Gadolinium-Loaded Polychelating Polymer-Containing Tumor-Targeted Liposomes. *Methods Mol. Biol* 2017, 1522, 179–192. [PubMed: 27837539]
390. Palma SI; Rodrigues CA; Carvalho A; Morales Mdel P; Freitas F; Fernandes AR; Cabral JM; Roque AC, A Value-Added Exopolysaccharide as a Coating Agent for MRI Nanoparticles. *Nanoscale* 2015, 7 (34), 14272–14283. [PubMed: 26186402]
391. Kim MH; Son HY; Kim GY; Park K; Huh YM; Haam S, Redoxable Heteronanocrystals Functioning Magnetic Relaxation Switch for Activatable T1 and T2 Dual-Mode Magnetic Resonance Imaging. *Biomaterials* 2016, 101, 121–130. [PubMed: 27281684]
392. Hsu BYW; Ng M; Tan A; Connell J; Roberts T; Lythgoe M; Zhang Y; Wong SY; Bhakoo K; Seifalian AM; Li X; Wang J, pH-Activatable MnO-Based Fluorescence and Magnetic Resonance Bimodal Nanoprobe for Cancer Imaging. *Adv. Healthc. Mater* 2016, 5 (6), 721–729. [PubMed: 26895111]
393. Guan T; Shang W; Li H; Yang X; Fang C; Tian J; Wang K, From Detection to Resection: Photoacoustic Tomography and Surgery Guidance with Indocyanine Green Loaded Gold Nanorod@Liposome Core-Shell Nanoparticles in Liver Cancer. *Bioconjug. Chem* 2017, 28 (4), 1221–1228. [PubMed: 28345887]
394. Sardarabadi H; Chafai DE; Gheybi F; Sasanpour P; Raffi-Tabar H; Cifra M, Enhancement of the Biological Autoluminescence by Mito-Liposomal Gold Nanoparticle Nanocarriers. *J. Photochem. Photobiol., B* 2020, 204, 111812, 1–7. [PubMed: 32062391]
395. Tang J; Ma D; Pecic S; Huang C; Zheng J; Li J; Yang R, Noninvasive and Highly Selective Monitoring of Intracellular Glucose *via* a Two-Step Recognition-Based Nanokit. *Anal. Chem* 2017, 89 (16), 8319–8327. [PubMed: 28707883]
396. Sabzehparvar F; Rahmani Cherati T; Mohsenifar A; Roodbar Shojaei T; Tabatabaei M, Immobilization of Gold Nanoparticles with Rhodamine to Enhance the Fluorescence Resonance Energy Transfer Between Quantum Dots and Rhodamine; New Method for Downstream Sensing of Infectious Bursal Disease Virus. *Spectrochim. Acta, Part A* 2019, 212, 173–179.

397. Chechetka SA; Yuba E; Kono K; Yudasaka M; Bianco A; Miyako E, Magnetically and Near-Infrared Light-Powered Supramolecular Nanotransporters for the Remote Control of Enzymatic Reactions. *Angew. Chem. Int. Ed* 2016, 55 (22), 6476–6481.
398. Cao L; Han G-C; Xiao H; Chen Z; Fang C, A Novel 3D Paper-Based Microfluidic Electrochemical Glucose Biosensor Based on rGO-TEPA/PB Sensitive Film. *Anal. Chim. Acta* 2020, 1096, 34–43. [PubMed: 31883589]
399. Kim S-K; Jeon C; Lee G-H; Koo J; Cho SH; Han S; Shin M-H; Sim J-Y; Hahn SK, Hyaluronate-Gold Nanoparticle/Glucose Oxidase Complex for Highly Sensitive Wireless Noninvasive Glucose Sensors. *ACS Appl. Mater. Interfaces* 2019, 11 (40), 37347–37356. [PubMed: 31502433]
400. Adeniyi O; Sicwetsha S; Mashazi P, Nanomagnet-Silica Nanoparticles Decorated with Au@ Pd for Enhanced Peroxidase-Like Activity and Colorimetric Glucose Sensing. *ACS Appl. Mater. Interfaces* 2019, 12 (2), 1973–1987.
401. Kim H; Rim YS; Kwon J-Y, Evaluation of Metal Oxide Thin-Film Electrolyte-Gated Field Effect Transistors for Glucose Monitoring in Small Volume of Body Analytes. *IEEE Sens. J* 2020, 20 (16), 9004–9010.
402. Toloza CAT; Almeida JMS; Khan S; Dos Santos YG; da Silva AR; Romani EC; Larrude DG; Freire FL Jr.; Aucélio RQ, Gold Nanoparticles Coupled with Graphene Quantum Dots in Organized Medium to Quantify Aminoglycoside Anti-Biotics in Yellow Fever Vaccine after Solid Phase Extraction Using a Selective Imprinted Polymer. *J. Pharm. Biomed. Anal* 2018, 158, 480–493. [PubMed: 29960239]
403. Zeng R; Zhang L; Su L; Luo Z; Zhou Q; Tang D, Photoelectrochemical Bioanalysis of Antibiotics on rGO-Bi<sub>2</sub>WO<sub>6</sub>-Au Based on Branched Hybridization Chain Reaction. *Biosens. Bioelectron* 2019, 133, 100–106. [PubMed: 30913509]
404. Li Z; Liu C; Sarpong V; Gu Z, Multisegment Nanowire/Nanoparticle Hybrid Arrays as Electrochemical Biosensors for Simultaneous Detection of Antibiotics. *Biosens. Bioelectron* 2019, 126, 632–639. [PubMed: 30513482]
405. Cui J; Chen S; Ma X; Shao H; Zhan J, Galvanic Displacement-Induced Codeposition of Reduced-Graphene-Oxide/Silver on Alloy Fibers for Non-Destructive SPME@SERS Analysis of Antibiotics. *Microchim. Acta* 2018, 186 (1), 19, 1–8.
406. Chen TW; Rajaji U; Chen SM; Muthumariyappan A; Mogren MMA; Jothi Ramalingam R; Hochlaf M, Facile Synthesis of Copper(II) Oxide Nanospheres Covered on Functionalized Multiwalled Carbon Nanotubes Modified Electrode as Rapid Electrochemical Sensing Platform for Super-Sensitive Detection of Antibiotic. *Ultrason. Sonochem* 2019, 58, 104596, 1–9. [PubMed: 31450358]
407. Jimenez Jimenez AM; Moulick A; Bhowmick S; Strmiska V; Gagic M; Horakova Z; Kostrica R; Masarik M; Heger Z; Adam V, One-Step Detection of Human Papilloma Viral Infection Using Quantum Dot-Nucleotide Interaction Specificity. *Talanta* 2019, 205, 120111, 1–8. [PubMed: 31450441]
408. Achilleos DS; Hatton TA; Vamvakaki M, Photoreponsive Hybrid Nanoparticles with Inherent FRET Activity. *Langmuir* 2016, 32 (23), 5981–5989. [PubMed: 27222922]
409. Perdikaki A; Galeou A; Pilatos G; Prombona A; Karanikolos GN, Ion-Based Metal/Graphene Antibacterial Agents Comprising Mono-Ionic and Bi-Ionic Silver and Copper Species. *Langmuir* 2018, 34 (37), 11156–11166. [PubMed: 30145895]
410. Atiyah AA; Haider AJ; Dhahi RM, Cytotoxicity Properties of Functionalised Carbon Nanotubes on Pathogenic Bacteria. *IET Nanobiotechnol.* 2019, 13 (6), 597, 1–5. [PubMed: 31432792]
411. Kakavandi B; Bahari N; Rezaei Kalantary R; Dehghani Fard E, Enhanced Sono-Photocatalysis of Tetracycline Antibiotic Using TiO<sub>2</sub> Decorated on Magnetic Activated Carbon (MAC@T) Coupled with US and UV: A New Hybrid System. *Ultrason. Sonochem* 2019, 55, 75–85. [PubMed: 31084793]
412. Viswanathan K; Bharathi BD; Karuppanan C; Sanjeevi T; Nithyanantham M; Arul Kumar K; Murugaiyan LMP; Gopal D; Muthusamy R, Studies on Antimicrobial and Wound Healing Applications of Gauze Coated with CHX-Ag Hybrid NPs. *IET Nanobiotechnol.* 2020, 14 (1), 14–18. [PubMed: 31935672]

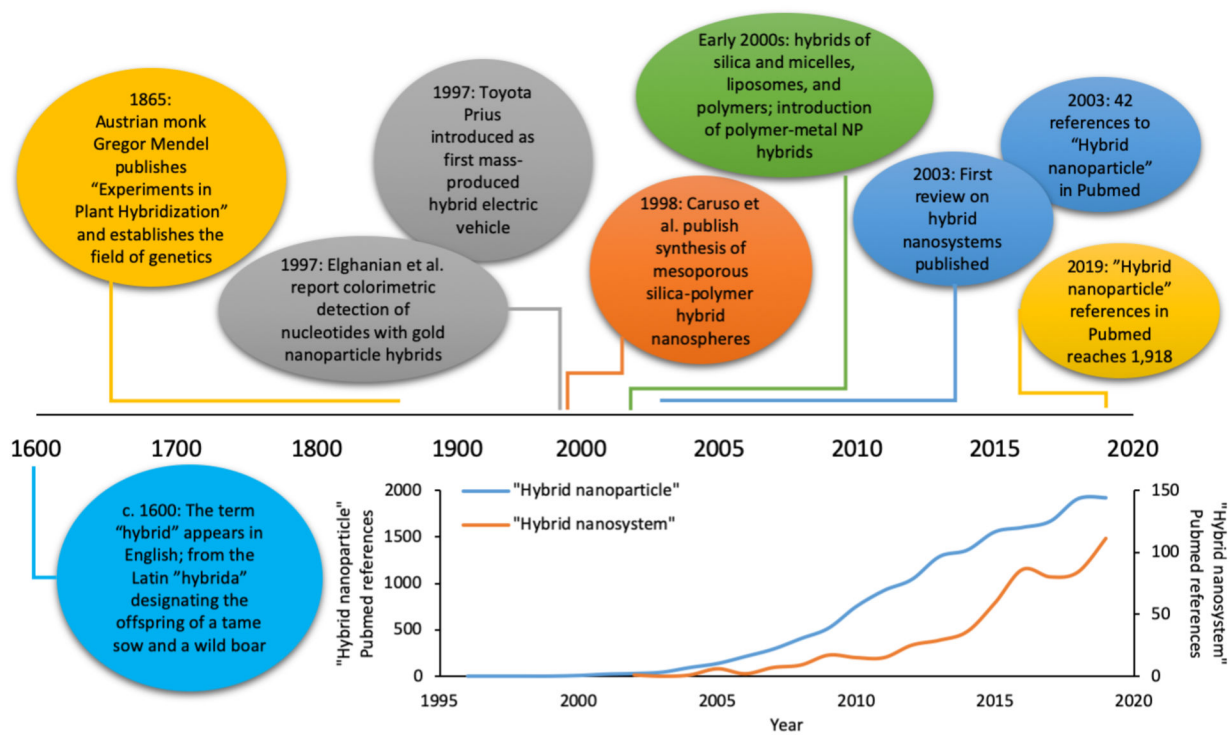
413. Le Thi P; Lee Y; Hoang Thi TT; Park KM; Park KD, Catechol-Rich Gelatin Hydrogels *in Situ* Hybridizations with Silver Nanoparticle for Enhanced Antibacterial Activity. *Mater. Sci. Eng., C* 2018, 92, 52–60.
414. Indira Devi MP; Nallamuthu N; Rajini N; Varada Rajulu A; Hari Ram N; Siengchin S, Cellulose Hybrid Nanocomposites Using Napier Grass Fibers with *in Situ* Generated Silver Nanoparticles as Fillers for Antibacterial Applications. *Int. J. Biol. Macromol* 2018, 118 (Pt A), 99–106. [PubMed: 29883698]
415. Fu F; Gu J; Zhang R; Xu X; Yu X; Liu L; Liu X; Zhou J; Yao J, Three-Dimensional Cellulose Based Silver-Functionalized ZnO Nanocomposite with Controlled Geometry: Synthesis, Characterization and Properties. *J. Colloid Interface Sci* 2018, 530, 433–443. [PubMed: 29990779]
416. Errokh A; Magnin A; Putaux JL; Boufi S, Hybrid Nanocellulose Decorated with Silver Nanoparticles as Reinforcing Filler with Antibacterial Properties. *Mater. Sci. Eng., C* 2019, 105, 110044, 1–9.
417. Jankauskait V; Lazauskas A; Griškonis E; Lisauskait A; Žukien K, UV-Curable Aliphatic Silicone Acrylate Organic-Inorganic Hybrid Coatings with Antibacterial Activity. *Molecules* 2017, 22 (6), 964, 1–13.
418. Wang X; Su K; Tan L; Liu X; Cui Z; Jing D; Yang X; Liang Y; Li Z; Zhu S; Yeung KWK; Zheng D; Wu S, Rapid and Highly Effective Noninvasive Disinfection by Hybrid Ag/CS@MnO<sub>2</sub> Nanosheets Using Near-Infrared Light. *ACS Appl. Mater. Interfaces* 2019, 11 (16), 15014–15027. [PubMed: 30933472]
419. Li M; Liu X; Xu Z; Yeung KW; Wu S, Dopamine Modified Organic-Inorganic Hybrid Coating for Antimicrobial and Osteogenesis. *ACS Appl. Mater. Interfaces* 2016, 8 (49), 33972–33981. [PubMed: 27960367]
420. Antonoglou O; Giannousi K; Arvanitidis J; Mourdikoudis S; Pantazaki A; Dendrinou-Samara C, Elucidation of One Step Synthesis of PEGylated CuFe Bimetallic Nanoparticles. Antimicrobial Activity of CuFe@PEG vs Cu@PEG. *J. Inorg. Biochem* 2017, 177, 159–170. [PubMed: 28964993]
421. Onnainty R; Onida B; Páez P; Longhi M; Barresi A; Granero G, Targeted Chitosan-Based Bionanocomposites for Controlled Oral Mucosal Delivery of Chlorhexidine. *Int. J. Pharm* 2016, 509 (1–2), 408–418. [PubMed: 27282538]
422. Marchant MJ; Guzmán L; Corvalán AH; Kogan MJ, Gold@Silica Nanoparticles Functionalized with Oligonucleotides: A Prominent Tool for the Detection of the Methylated Reprimo Gene in Gastric Cancer by Dynamic Light Scattering. *Nanomaterials* 2019, 9 (9), 1333.
423. Zhong X; Zhang Y; Tan L; Zheng T; Hou Y; Hong X; Du G; Chen X; Zhang Y; Sun X, An Aluminum Adjuvant-Integrated Nano-MOFs Antigen Delivery System to Induce Strong Humoral and Cellular Immune Responses. *J. Control. Release* 2019, 300, 81–92. [PubMed: 30826373]
424. Ruiz-de-Angulo A; Zabaleta A; Gómez-Vallejo V; Llop J; Mareque-Rivas JC, Microdosed Lipid-Coated <sup>67</sup>Ga-Magnetite Enhances Antigen-Specific Immunity by Image Tracked Delivery of Antigen and CpG to Lymph Nodes. *ACS Nano* 2016, 10 (1), 1602–1618. [PubMed: 26678549]
425. Liu Y; Zhu X; Lu Y; Wang X; Zhang C; Sun H; Ma G, Antigen-Inorganic Hybrid Flowers-Based Vaccines with Enhanced Room Temperature Stability and Effective Anticancer Immunity. *Adv. Healthc. Mater* 2019, 8 (21), e1900660, 1–10. [PubMed: 31583853]
426. Wang X; Deng YQ; Yang D; Xiao Y; Zhao H; Nian QG; Xu X; Li XF; Tang R; Qin CF, Biomimetic Inorganic Camouflage Circumvents Antibody-Dependent Enhancement of Infection. *Chem. Sci* 2017, 8 (12), 8240–8246. [PubMed: 29568472]
427. Prasad R; Jain NK; Yadav AS; Chauhan DS; Devrukhkar J; Kumawat MK; Shinde S; Gorain M; Thakor AS; Kundu GC; Conde J; Srivastava R, Liposomal Nanotheranostics for Multimode Targeted *in Vivo* Bioimaging and Near-Infrared Light Mediated Cancer Therapy. *Commun. Biol* 2020, 3 (1), 284, 1–14. [PubMed: 32504032]
428. Zhang N; Li J; Hou R; Zhang J; Wang P; Liu X; Zhang Z, Bubble-Generating Nano-Lipid Carriers for Ultrasound/CT Imaging-Guided Efficient Tumor Therapy. *Int. J. Pharm* 2017, 534 (1–2), 251–262. [PubMed: 28803939]

429. Zhao F; Zhou J; Su X; Wang Y; Yan X; Jia S; Du B, A Smart Responsive Dual Aptamers-Targeted Bubble-Generating Nanosystem for Cancer Triplex Therapy and Ultrasound Imaging. *Small* 2017, 13 (20), 1603990, 1–13.
430. Thébault CJ; Ramniceanu G; Michel A; Beauvineau C; Girard C; Seguin J; Mignet N; Ménager C; Doan BT, *In Vivo* Evaluation of Magnetic Targeting in Mice Colon Tumors with Ultra-Magnetic Liposomes Monitored by MRI. *Mol. Imaging Biol* 2019, 21 (2), 269–278. [PubMed: 29942990]
431. Liu KC; Arivajigane A; Wu SJ; Tzou SC; Chen CY; Wang YM, Development of a Novel Thermal-Sensitive Multifunctional Liposome with Antibody Conjugation to Target EGFR-Expressing Tumors. *Nanomed. Nanotechnol. Biol. Med* 2019, 15 (1), 285–294.
432. Saesoo S; Sathornsumetee S; Anekwiang P; Treetidnipa C; Thuwajit P; Bunthot S; Maneeprakorn W; Maurizi L; Hofmann H; Rungsardthong RU; Saengkrit N, Characterization of Liposome-Containing SPIONS Conjugated with Anti-CD20 Developed As a Novel Theranostic Agent for Central Nervous System Lymphoma. *Colloids Surf., B* 2018, 161, 497–507.
433. Xu HL; Yang JJ; ZhuGe DL; Lin MT; Zhu QY; Jin BH; Tong MQ; Shen BX; Xiao J; Zhao YZ, Glioma-Targeted Delivery of a Theranostic Liposome Integrated with Quantum Dots, Superparamagnetic Iron Oxide, and Cilengitide for Dual-Imaging Guiding Cancer Surgery. *Adv. Healthc. Mater* 2018, 7 (9), e1701130, 1–18. [PubMed: 29350498]
434. Zheng XC; Ren W; Zhang S; Zhong T; Duan XC; Yin YF; Xu MQ; Hao YL; Li ZT; Li H; Liu M; Li ZY; Zhang X, The Theranostic Efficiency of Tumor-Specific, pH-Responsive, Peptide-Modified, Liposome-Containing Paclitaxel and Superparamagnetic Iron Oxide Nanoparticles. *Int. J. Nanomed* 2018, 13, 1495–1504.
435. Liu Y; Yang F; Yuan C; Li M; Wang T; Chen B; Jin J; Zhao P; Tong J; Luo S; Gu N, Magnetic Nanoliposomes as *in Situ* Microbubble Bombers for Multimodality Image-Guided Cancer Theranostics. *ACS Nano* 2017, 11 (2), 1509–1519. [PubMed: 28045496]
436. Wei P; Chen J; Hu Y; Li X; Wang H; Shen M; Shi X, Dendrimer-Stabilized Gold Nanostars as a Multifunctional Theranostic NanoplatforM for CT Imaging, Photothermal Therapy, and Gene Silencing of Tumors. *Adv. Healthc. Mater* 2016, 5 (24), 3203–3213. [PubMed: 27901317]
437. Wang P; Lin L; Guo Z; Chen J; Tian H; Chen X; Yang H, Highly Fluorescent Gene Carrier Based on Ag-Au Alloy Nanoclusters. *Macromol. Biosci* 2016, 16 (1), 160–167. [PubMed: 26287567]
438. Wang X; Yu X; Wang X; Qi M; Pan J; Wang Q, One-Step Nanosurface Self-Assembly of D-Peptides Renders Bubble-Free Ultrasound Theranostics. *Nano Lett.* 2019, 19 (4), 2251–2258. [PubMed: 30868886]
439. Duan S; Yang Y; Zhang C; Zhao N; Xu FJ, NIR-Responsive Polycationic Gatekeeper-Cloaked Hetero-Nanoparticles for Multimodal Imaging-Guided Triple-Combination Therapy of Cancer. *Small* 2017, 13 (9), 1603133, 1–10.
440. Yang Z; Fan W; Zou J; Tang W; Li L; He L; Shen Z; Wang Z; Jacobson O; Aronova MA; Rong P; Song J; Wang W; Chen X, Precision Cancer Theranostic Platform by *in Situ* Polymerization in Perylene Diimide-Hybridized Hollow Mesoporous Organosilica Nanoparticles. *J. Am. Chem. Soc* 2019, 141 (37), 14687–14698. [PubMed: 31466436]
441. Bocanegra Gordan AI; Ruiz-de-Angulo A; Zabaleta A; Gómez Blanco N; Cobaleda-Siles BM; García-Granda MJ; Padro D; Llop J; Arnaiz B; Gato M; Escors D; Mareque-Rivas JC, Effective Cancer Immunotherapy in Mice by PolyICImiquimod Complexes and Engineered Magnetic Nanoparticles. *Biomaterials* 2018, 170, 95–115. [PubMed: 29656235]
442. Yao MH; Ma M; Chen Y; Jia XQ; Xu G; Xu HX; Chen HR; Wu R, Multifunctional Bi2S3/PLGA Nanocapsule for Combined HIFU/Radiation Therapy. *Biomaterials* 2014, 35 (28), 8197–8205. [PubMed: 24973300]
443. Croissant JG; Zhang D; Alsaïari S; Lu J; Deng L; Tamanai F; AlMalik AM; Zink JJ; Khashab NM, Protein-Gold Clusters-Capped Mesoporous Silica Nanoparticles for High Drug Loading, Autonomous Gemcitabine/Doxorubicin Co-Delivery, and *in Vivo* Tumor Imaging. *J. Control. Release* 2016, 229, 183–191. [PubMed: 27016140]
444. Zhan C; Huang Y; Lin G; Huang S; Zeng F; Wu S, A Gold Nanocage/Cluster Hybrid Structure for Whole-Body Multispectral Optoacoustic Tomography Imaging, EGFR Inhibitor Delivery, and Photothermal Therapy. *Small* 2019, 15 (33), e1900309, 1–14. [PubMed: 31245925]

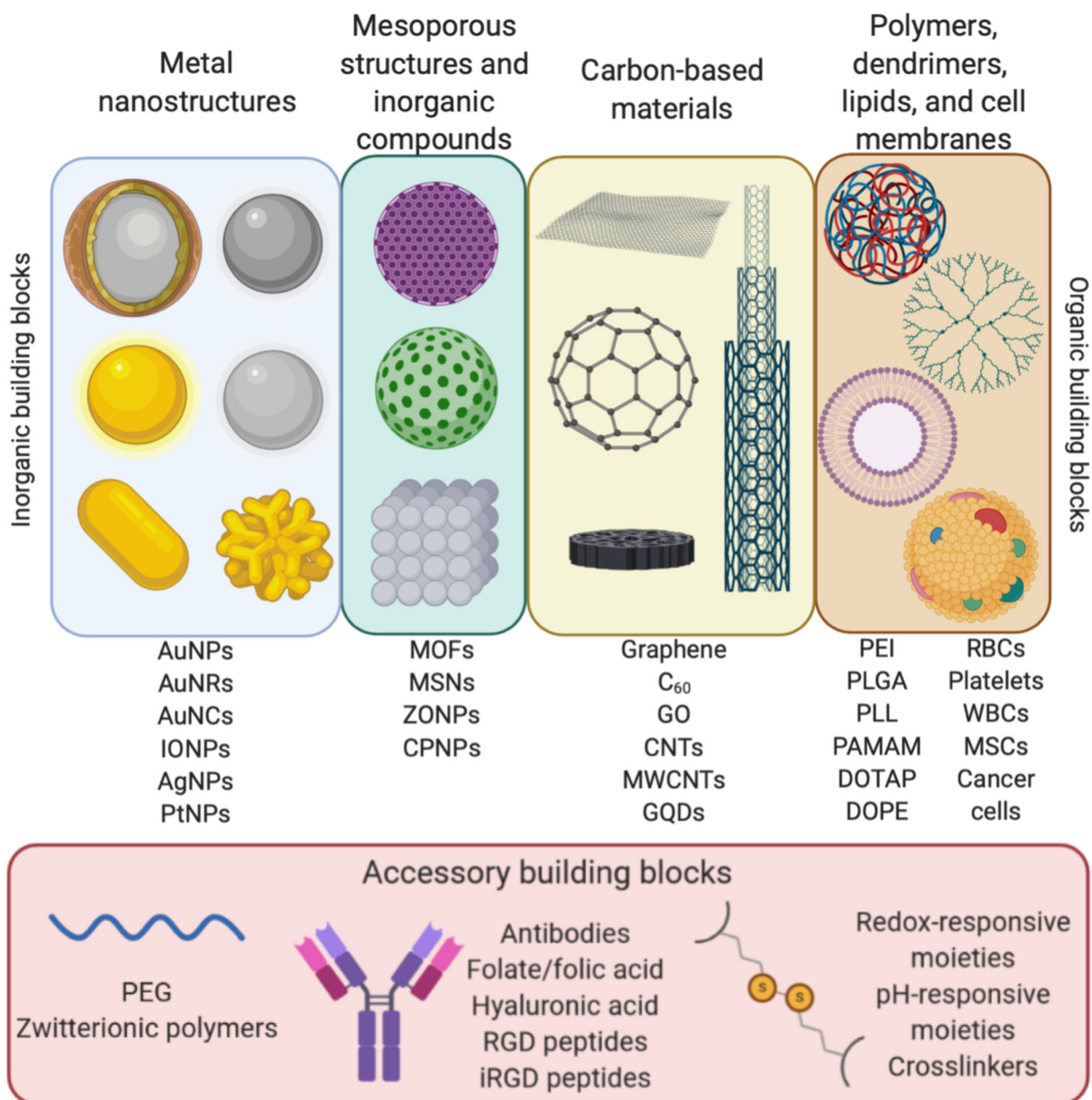
445. Zhou L; Chen Z; Dong K; Yin M; Ren J; Qu X, DNA-Mediated Biomineralization of Rare-Earth Nanoparticles for Simultaneous Imaging and Stimuli-Responsive Drug Delivery. *Biomaterials* 2014, 35 (30), 8694–8702. [PubMed: 25002259]
446. Zhang X; Ong'achwa Machuki J; Pan W; Cai W; Xi Z; Shen F; Zhang L; Yang Y; Gao F; Guan M, Carbon Nitride Hollow Theranostic Nanoregulators Executing Laser-Activatable Water Splitting for Enhanced Ultrasound/Fluorescence Imaging and Cooperative Phototherapy. *ACS Nano* 2020, 14 (4), 4045–4060. [PubMed: 32255341]
447. Shi J; Chen Z; Wang L; Wang B; Xu L; Hou L; Zhang Z, A Tumor-Specific Cleavable Nanosystem of PEG-Modified C60@Au Hybrid Aggregates for Radio Frequency-Controlled Release, Hyperthermia, Photodynamic Therapy and X-Ray Imaging. *Acta Biomater.* 2016, 29, 282–297. [PubMed: 26485168]
448. Shi J; Wang L; Gao J; Liu Y; Zhang J; Ma R; Liu R; Zhang Z, A Fullerene-Based Multi-Functional Nanoplatform for Cancer Theranostic Applications. *Biomaterials* 2014, 35 (22), 5771–5784. [PubMed: 24746227]
449. Zheng T; Zhou T; Feng X; Shen J; Zhang M; Sun Y, Enhanced Plasmon-Induced Resonance Energy Transfer (PIRET)-Mediated Photothermal and Photodynamic Therapy Guided by Photoacoustic and Magnetic Resonance Imaging. *ACS Appl. Mater. Interfaces* 2019, 11 (35), 31615–31626. [PubMed: 31359757]
450. Du Y; Jiang Q; Beziere N; Song L; Zhang Q; Peng D; Chi C; Yang X; Guo H; Diot G; Ntziachristos V; Ding B; Tian J, DNA-Nanostructure-Gold-Nanorod Hybrids for Enhanced *in Vivo* Photoacoustic Imaging and Photothermal Therapy. *Adv. Mater* 2016, 28 (45), 10000–10007. [PubMed: 27679425]
451. Song J; Yang X; Jacobson O; Huang P; Sun X; Lin L; Yan X; Niu G; Ma Q; Chen X, Ultrasmall Gold Nanorod Vesicles with Enhanced Tumor Accumulation and Fast Excretion from the Body for Cancer Therapy. *Adv. Mater* 2015, 27 (33), 4910–4917. [PubMed: 26198622]
452. Huang W-T; Chan M-H; Chen X; Hsiao M; Liu R-S, Theranostic Nanobubble Encapsulating a Plasmon-Enhanced Upconversion Hybrid Nanosystem for Cancer Therapy. *Theranostics* 2020, 10 (2), 782–796. [PubMed: 31903150]
453. Li J; Wang X; Zheng D; Lin X; Wei Z; Zhang D; Li Z; Zhang Y; Wu M; Liu X, Cancer Cell Membrane-Coated Magnetic Nanoparticles for MR/NIR Fluorescence Dual-Modal Imaging and Photodynamic Therapy. *Biomater. Sci* 2018, 6 (7), 1834–1845. [PubMed: 29786715]
454. Sun Y; Liang Y; Dai W; He B; Zhang H; Wang X; Wang J; Huang S; Zhang Q, Peptide-Drug Conjugate-Based Nanocombination Actualizes Breast Cancer Treatment by Maytansinoid and Photothermia with the Assistance of Fluorescent and Photoacoustic Images. *Nano Lett.* 2019, 19 (5), 3229–3237. [PubMed: 30957499]

### Vocabulary

- Hybrid nanosystem
  - A nano-scale device, complex, or assembly containing both inorganic and organic components.
- Inorganic/organic building blocks
  - The fundamental materials that make up a hybrid nanosystem. Hybrid nanosystems are formed through combination of one or more inorganic building blocks with one or more organic building blocks.
- Hybrid architecture
  - The structural and material organization of a hybrid nanosystem; directly associated with the function of a hybrid nanosystem.
- Combination therapy
  - Application of two or more distinct types of treatment (*i.e.* chemotherapy, gene therapy, phototherapy, *etc.*) *via* a single hybrid nanosystem.
- Theranostics
  - The integration of therapeutic properties with diagnostic or imaging properties in a single nanosystem.

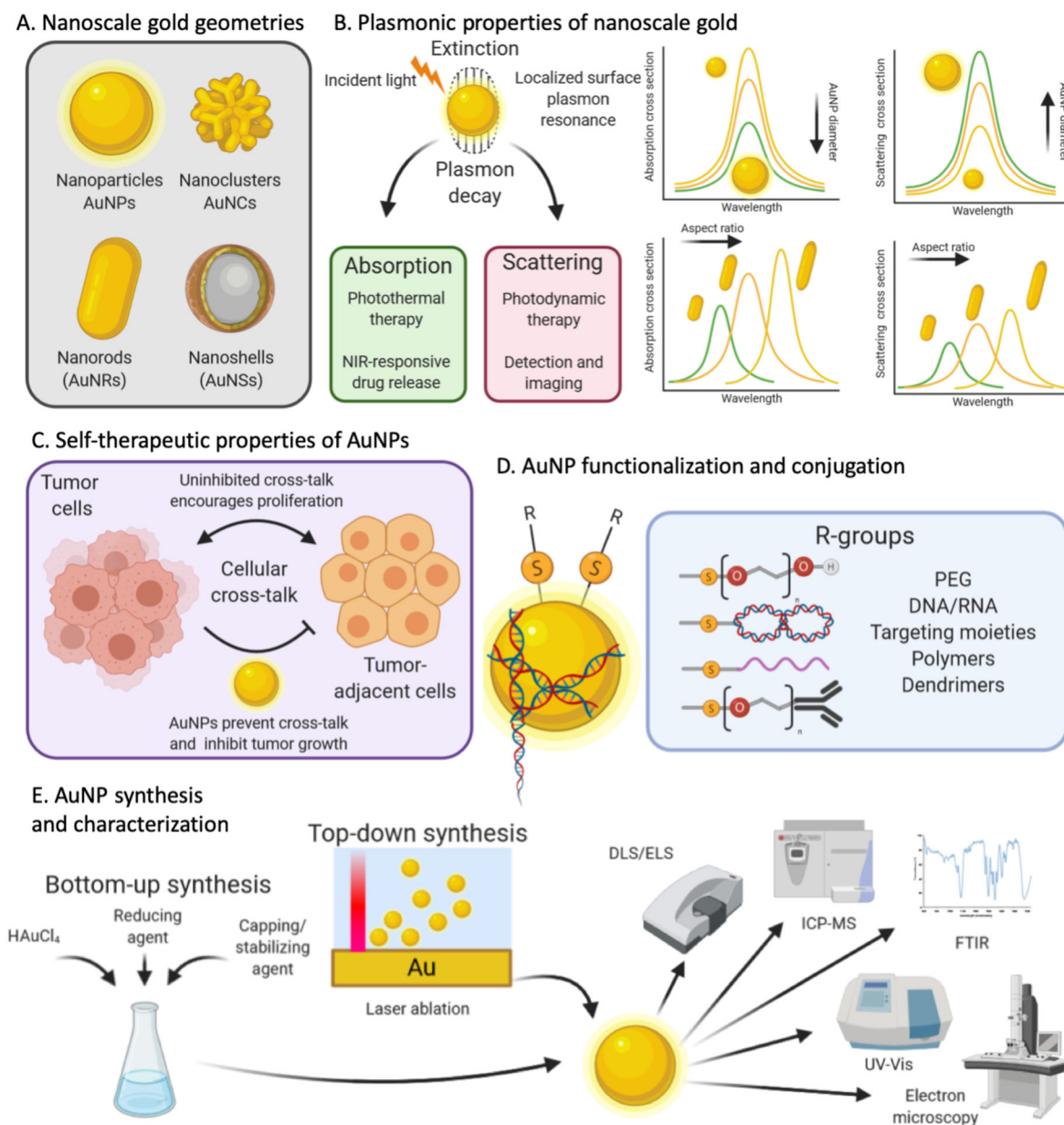


**Figure 1:**  
Timeline of biomedical hybridization milestones<sup>3, 4</sup>

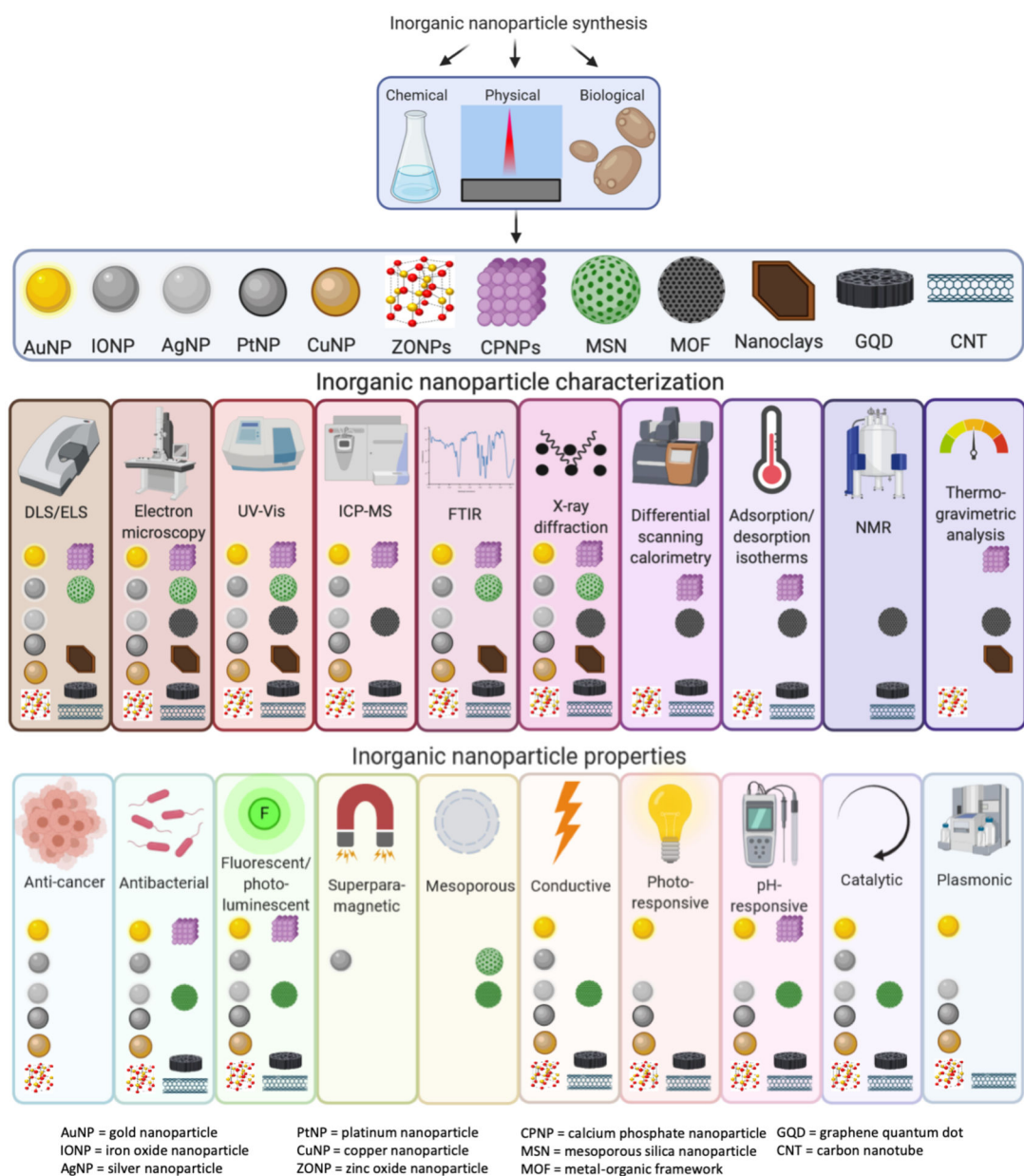


**Figure 2:** Building blocks for hybrid nanosystems. Created with [BioRender.com](https://www.biorender.com/).

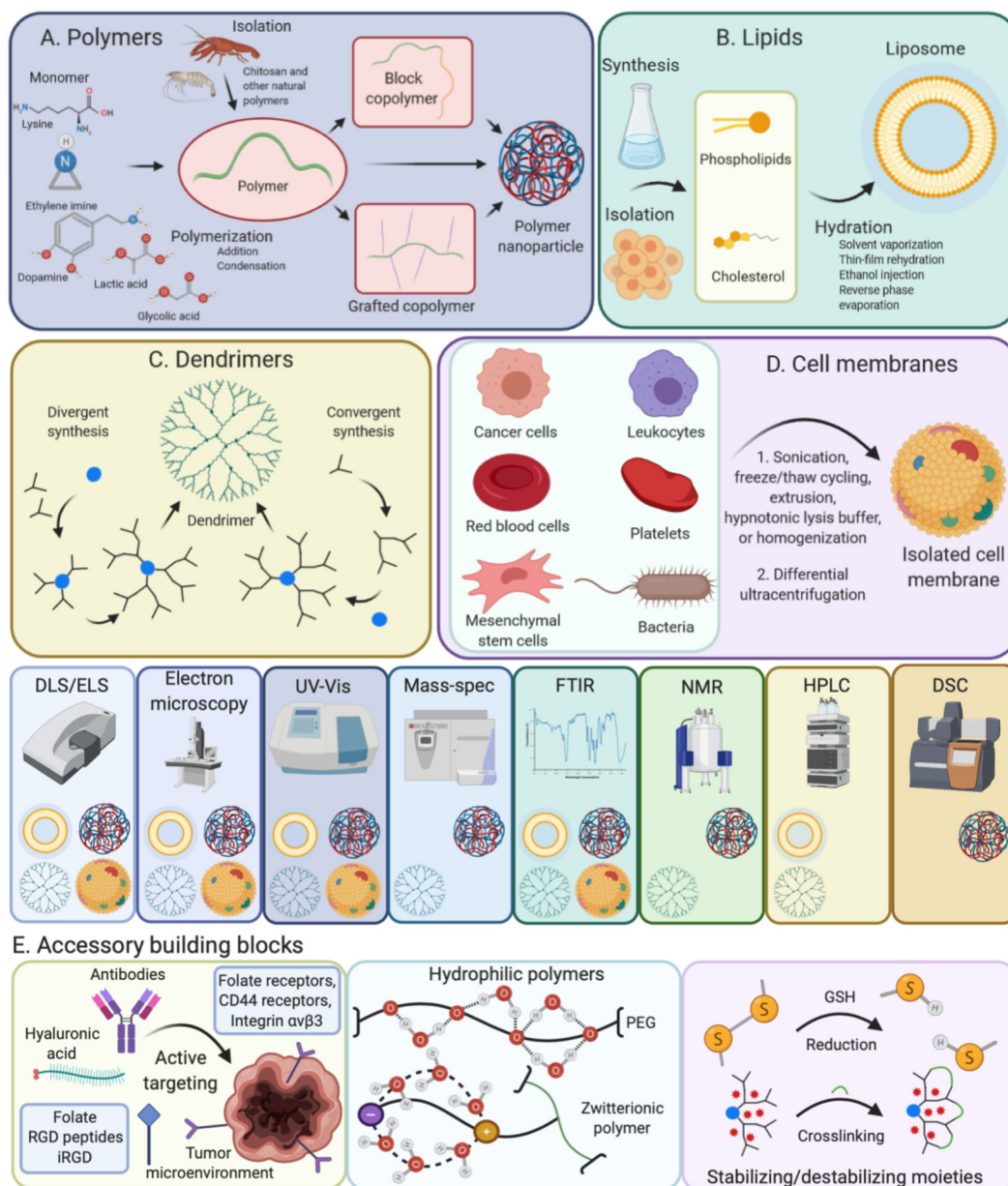




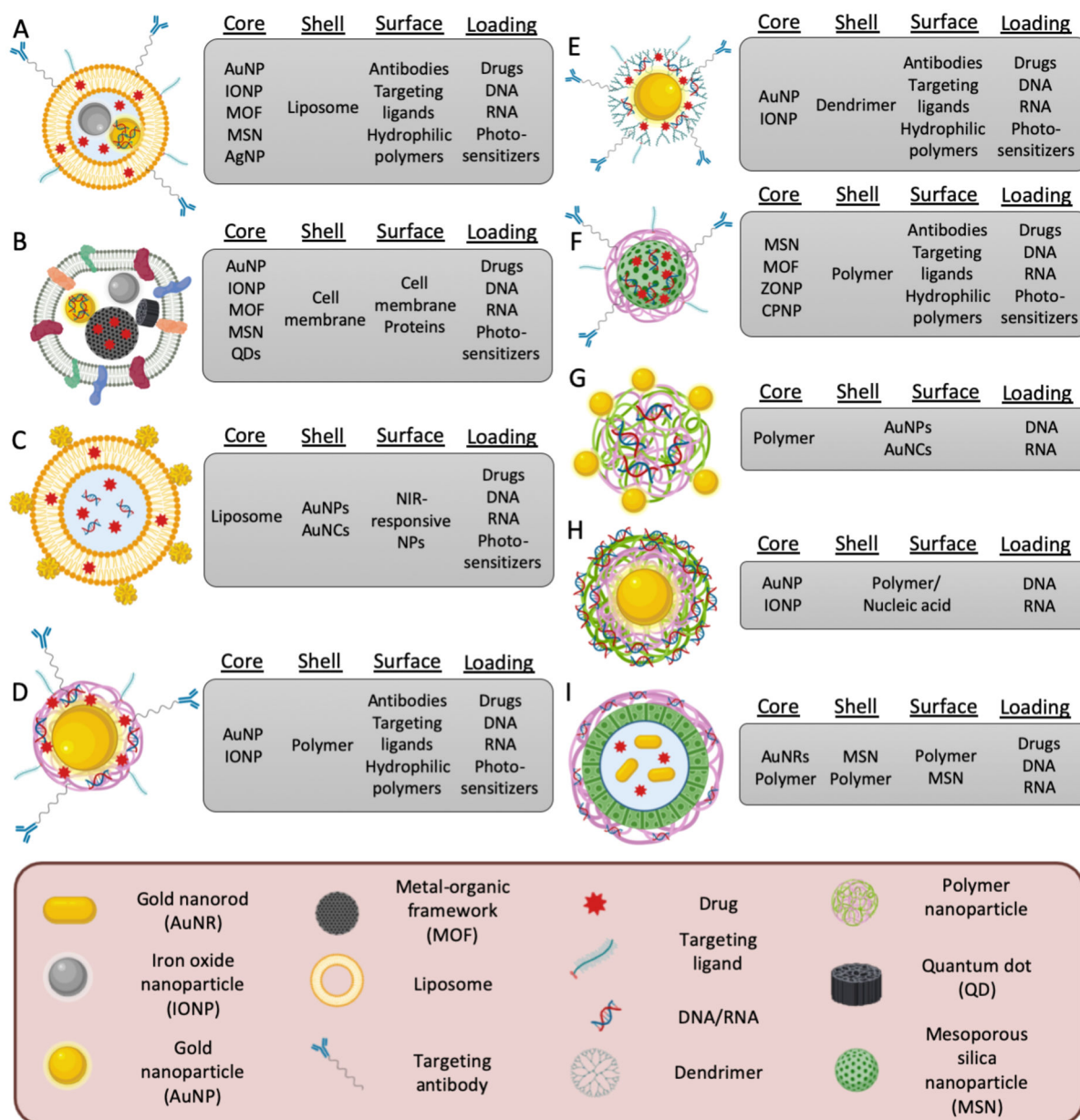
**Figure 3:** Nanoscale gold for biomedical applications. A) Geometries for nanoscale gold. B) Plasmonic properties of nanoscale gold. C) Self-therapeutic properties of AuNPs. D) AuNP functionalization and conjugation. E) AuNP synthesis and characterization.<sup>11, 27, 43, 46</sup>  
Created with [BioRender.com](https://www.biorender.com).



**Figure 4:** Characterization and properties of various inorganic components of hybrid nanosystems. Created with [BioRender.com](https://www.biorender.com).



**Figure 5:** Organic and accessory building blocks for hybrid nanosystems. Created with [BioRender.com](https://www.biorender.com/).

**Figure 6:**

Architectures for hybrid nanosystems. A) Inorganic-liposome hybrid with nanoparticles incorporated within the liposome.<sup>125, 193–195, 202</sup> B) Cell membrane-coated nanoparticles.<sup>173, 179, 203, 204</sup> C) Liposome with surface-associated nanoscale metals.<sup>28</sup> D) Functionalized polymer-coated metal nanoparticle.<sup>197</sup> E) Dendrimer-conjugated metallic nanoparticles.<sup>165</sup> F) Mesoporous nanostructure with a polymer coating.<sup>205, 206</sup> G) Polymer-nucleic acid complex with metallic nanoparticles on the surface.<sup>198</sup> H) Metallic nanoparticle core coated in sequential layers of polymer and nucleic acid.<sup>199</sup> I) Rattle-type nanostructure of metal nanoparticles within a polymer-coated mesoporous shell.<sup>200</sup> Created with [BioRender.com](https://www.biorender.com).

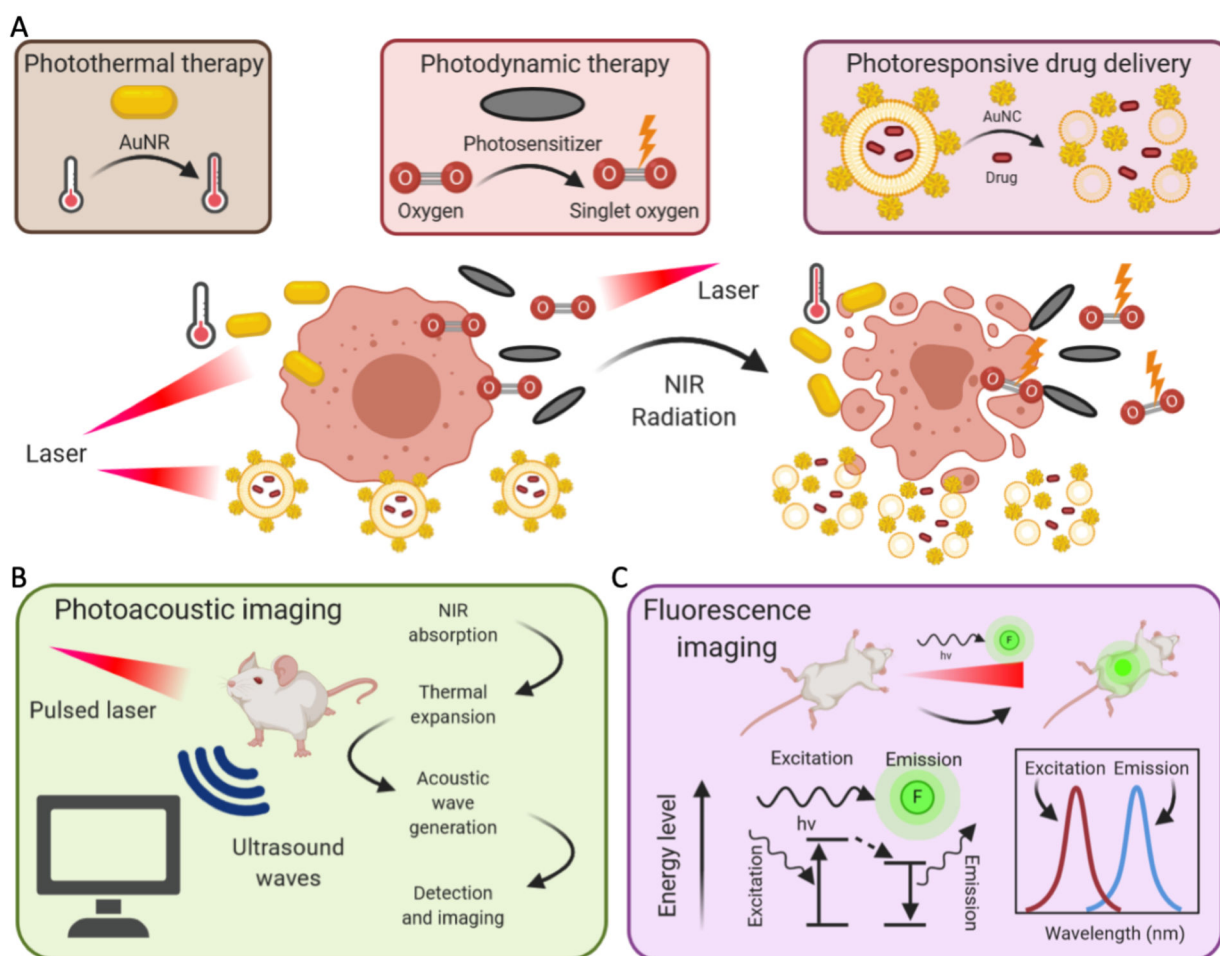


**Figure 7:** A) Phototherapy, photoresponsive drug delivery, and photoimaging. B) Photoacoustic imaging. C) Fluorescence imaging. Created with [BioRender.com](https://www.biorender.com/).

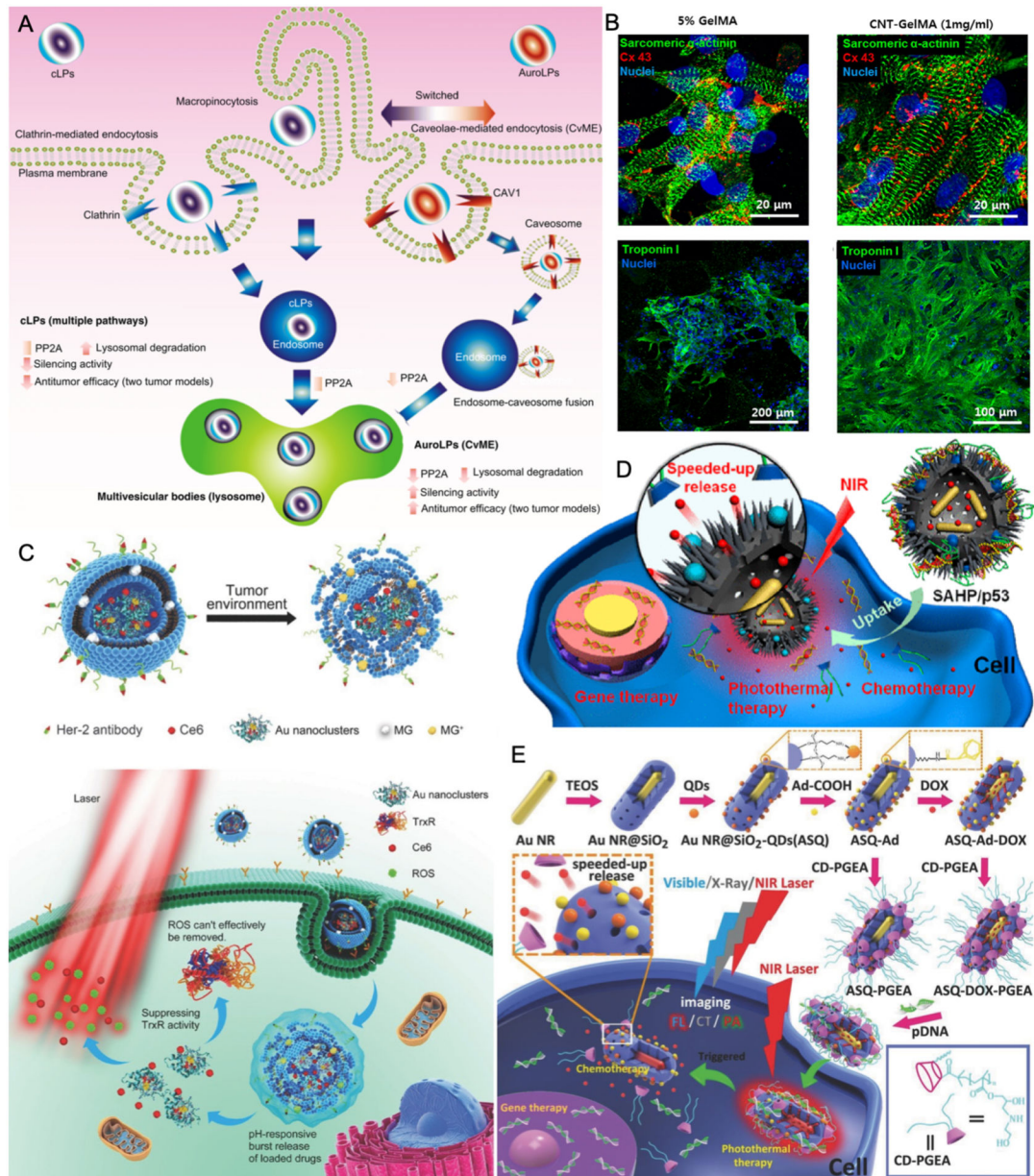


**Figure 8:** Select hybrid nanosystems of various applications. A) Auroliposomes shift the gene delivery uptake pathway. From Hossen, M. N. *et al.* Switching the intracellular pathway and enhancing the therapeutic efficacy of small interfering RNA by auroliposome. *Science Advances* 6, eaba5379, doi:10.1126/sciadv.aba5379 (2020). Reprinted with permission from AAAS.<sup>22</sup> B) CNT-embedded hydrogels create multifunctional cardiac scaffolds. Reprinted with permission from Shin, S. R.; Jung, S. M.; Zalabany, M.; Kim, K.; Zorlutuna, P.; Kim, S. b.; Nikkhah, M.; Khabiry, M.; Azize, M.; Kong, J., Carbon-nanotube-embedded hydrogel sheets for engineering cardiac constructs and bioactuators. *ACS Nano* 2013, 7 (3), 2369–2380. Copyright 2013 American Chemical Society.<sup>351</sup> C) Dual-loaded liposomal nanocomposite enhances phototherapy by inhibiting thioredoxin reductase. Reprinted by

permission from John Wiley and Sons: Advanced Healthcare Materials. Au Nanoclusters and Photosensitizer Dual Loaded Spatiotemporal Controllable Liposomal Nanocomposites Enhance Tumor Photodynamic Therapy Effect by Inhibiting Thioredoxin Reductase, Gao, F. *et al.* (2017)<sup>16</sup> D) Rattle-structured nanocapsules for gene/chemo/phototherapy. Reprinted by permission from Chen, X. *et al.* Rattle-Structured Rough Nanocapsules with *in-Situ*-Formed Gold Nanorod Cores for Complementary Gene/Chemo/Photothermal Therapy. ACS Nano 12, 5646–5656, doi:[10.1021/acsnano.8b01440](https://doi.org/10.1021/acsnano.8b01440) (2018). Copyright 2018 American Chemical Society.<sup>200</sup> E) NIR-responsive nanoparticles for imaging-guided triple-combination therapy. Reprinted by permission from Wiley-VHC: Small. NIR-Responsive Polycationic Gatekeeper-Cloaked Hetero-Nanoparticles for Multimodal Imaging-Guided Triple-Combination Therapy of Cancer, Duan, S. *et al.* (2017)<sup>439</sup>

**Table 1:**

Recent hybrid nanosystems for cancer therapy.

<i>Therapy</i>	<b>Inorganic component</b>	<b>Organic component</b>	<b>Therapeutic compound</b>	<b>Targeting ligand</b>	<b>Stimulus sensitivity</b>	<b>Reference</b>
<i>Cancer immunotherapy</i>	MSN	Dextran, membrane (cancer cell)	Antigen	N/A	N/A	174
<i>Cancer immunotherapy</i>	MSN	Polymer	Antigen	N/A	N/A	302
<i>Cancer immunotherapy</i>	Inorganic compound (zinc phosphate)	Lipid	Antigen	N/A	N/A	303
<i>Cancer immunotherapy</i>	Inorganic compound (zinc oxide)	Polymer	Antigen	N/A	N/A	304
<i>Chemotherapy</i>	Metal (gold)	Lipid	DOX	N/A	NIR	28
<i>Chemotherapy</i>	Metal (gold)	Lipid	DOX	N/A	NIR, temperature	125
<i>Chemotherapy</i>	Metal (gold)	Lipid	DOX	Mucin-1 aptamer	NIR, temperature	17
<i>Chemotherapy</i>	Metal (gold)	Lipid	DOX	Hyaluronic acid	NIR	14
<i>Chemotherapy</i>	Metal (gold)	Lipid	Temozolomide	N/A	N/A	12
<i>Chemotherapy</i>	Metal (gold)	Lipid	DOX	N/A	pH	232
<i>Chemotherapy</i>	Metal (gold)	Lipid	Morin	AS1411 DNA aptamer	pH	193
<i>Chemotherapy</i>	Metal (gold)	Lipid	DOX	N/A	N/A	230
<i>Chemotherapy</i>	Metal (gold)	Lipid	PTX	N/A	N/A	231
<i>Chemotherapy</i>	Metal (gold, iron oxide)	Lipid	Cisplatin	N/A	pH, magnetic field	305
<i>Chemotherapy</i>	Metal (iron oxide)	Lipid	Misonidazole	N/A	pH, magnetic field	306
<i>Chemotherapy</i>	Metal (iron oxide)	Lipid	Curcumin	N/A	magnetic field	236
<i>Chemotherapy</i>	Metal (iron oxide)	Lipid	Cisplatin	N/A	magnetic field	126
<i>Chemotherapy</i>	Metal (iron oxide)	Lipid	DOX	Apolipoprotein E, anti-rat CD71 IgG2a monoclonal antibody	magnetic field	235
<i>Chemotherapy</i>	Metal (iron oxide)	Surfactant	DOX	N/A	magnetic field	234
<i>Chemotherapy</i>	Metal (iron oxide)	Lipid	DOX	N/A	magnetic field	233
<i>Chemotherapy</i>	Metal (iron oxide)	Lipid	Curcumin	N/A	magnetic field	238
<i>Chemotherapy</i>	Metal (iron oxide)	Lipid	Gemcitabine/oxaliplatin	N/A	magnetic field	202
<i>Chemotherapy</i>	Metal (iron oxide)	Lipid	7-Allylamio-17-desmethoxygeldanamycin (17-AAG)	Folic acid	magnetic field, temperature	240



<i>Therapy</i>	<b>Inorganic component</b>	<b>Organic component</b>	<b>Therapeutic compound</b>	<b>Targeting ligand</b>	<b>Stimulus sensitivity</b>	<b>Reference</b>
<i>Chemotherapy</i>	Metal (iron oxide)	Lipid	DTX	Hyaluronic acid	NIR	241
<i>Chemotherapy</i>	Metal (silver)	Lipid	Curcumin	N/A	N/A	245
<i>Chemotherapy</i>	MOF	Lipid	Irinotecan, floxuridine	N/A	N/A	195
<i>Chemotherapy</i>	MSN	Lipid	DOX	N/A	Temperature	243
<i>Chemotherapy</i>	Metal (gold)	Polymer	Curcumin	N/A	N/A	307
<i>Chemotherapy</i>	Metal (gold)	Polymer	Sunitib malate	c(RGDfK) peptide	N/A	21
<i>Chemotherapy</i>	Metal (gold)	Polymer	DOX	N/A	N/A	246
<i>Chemotherapy</i>	Metal (gold, platinum)	Polymer	5-FU	N/A	pH	247
<i>Chemotherapy</i>	Metal (gold)	Dendrimer	PTX	N/A	N/A	159
<i>Chemotherapy</i>	Metal (iron oxide)	Polymer	Cisplatin	N/A	Magnetic field	308
<i>Chemotherapy</i>	Metal (silver)	Polymer	Imatinib mesylate	N/A	pH, enzyme	249
<i>Chemotherapy</i>	MSN	Polymer	DOX	CD133 RNA aptamer	pH	206
<i>Chemotherapy</i>	Inorganic compound (zinc oxide)	Polymer	DOX	N/A	pH	248
<i>Chemotherapy</i>	MOF	Polymer	DOX	N/A	pH	85
<i>Chemotherapy</i>	Metal (platinum)	Polymer	Gemcitabine	N/A	pH/redox	57
<i>Chemotherapy</i>	Inorganic compound (CaP)	Polymer	verapamil, novatrone	RGD peptide	pH	66
<i>Chemotherapy</i>	Inorganic compound (zinc oxide)	Nucleic acid	DOX	N/A	pH, enzyme	67
<i>Chemotherapy</i>	MSN	Carbon	Curcumin	N/A	pH	255
<i>Chemotherapy</i>	Metal (iron oxide)	Lipid	Cuphen	N/A	pH, magnetic field	237
<i>Chemotherapy</i>	Metal (iron oxide)	Lipid	Fe ions	N/A	pH, redox	242
<i>Chemotherapy</i>	Metal (iron oxide)	Dendrimer	DOX	T7 peptide	pH	250
<i>Chemotherapy</i>	Metal (gold)	Polymer	Curcumin	Folic acid	pH	197
<i>Drug+phototherapy</i>	Metal (gold)	Lipid	Au nanoshell, betulinic acid	N/A	NIR	289
<i>Drug+phototherapy</i>	Metal (gold)	Lipid	Au nanoshell, oleanoic acid	N/A	pH, NIR	290
<i>Drug+phototherapy</i>	Metal (gold)	Lipid	Au nanoshell, thienopyridine	N/A	NIR, magnetic field	291
<i>Drug+phototherapy</i>	Metal (gold)	Nucleic acid	AuNRs, DOX	Folic acid	NIR	296
<i>Drug+phototherapy</i>	Metal (gold)	Polymer	AuNP, PTX	N/A	NIR, temperature	294

<i>Therapy</i>	<b>Inorganic component</b>	<b>Organic component</b>	<b>Therapeutic compound</b>	<b>Targeting ligand</b>	<b>Stimulus sensitivity</b>	<b>Reference</b>
<i>Drug+phototherapy</i>	Metal (gold)	Lipid	AuNPs, DOX	N/A	NIR, temperature	292
<i>Drug+phototherapy</i>	Metal (gold)	Lipid	AuNPs, DOX	N/A	NIR	293
<i>Drug+phototherapy</i>	Metal (gold)	Nucleic acid	AuNR, DOX	MUC-1 DNA aptamer	NIR	295
<i>Drug+phototherapy</i>	Metal (gold)	Membrane (cancer cell)	Au nanocage, DOX	N/A	NIR	175
<i>Gene therapy</i>	Metal (gold)	Lipid	DNA	monosialodihexosylganglioside	N/A	208
<i>Gene therapy</i>	Metal (gold)	Lipid	DNA	Folic acid	pH	209
<i>Gene therapy</i>	Metal (gold)	Lipid	RNA	Apolipoprotein E, RVG peptide	N/A	210
<i>Gene therapy</i>	Metal (gold)	Lipid	DNA, protein	N/A	NIR, temperature	212
<i>Gene therapy</i>	Metal (gold)	Lipid	RNA, protein	TAT peptide	N/A	211
<i>Gene therapy</i>	Metal (gold)	Nucleic acid	RNA	N/A	N/A	309 215, 219 39
<i>Gene therapy</i>	Metal (gold)	Nucleic acid	DNA	N/A	NIR	310
<i>Gene therapy</i>	Metal (gold)	Polymer	DNA	TAT peptide	N/A	216
<i>Gene therapy</i>	Metal (gold)	Polymer	RNA	Folic acid	N/A	24
<i>Gene therapy</i>	Metal (gold)	Polymer	DNA	Histidine, arginine	N/A	136
<i>Gene therapy</i>	Metal (gold)	Polymer	DNA	Folic acid	N/A	137
<i>Gene therapy</i>	Metal (gold)	Polymer	RNA	N/A	N/A	Above
<i>Gene therapy</i>	Metal (gold)	Polymer	DNA	TAT peptide, hyaluronic acid	Redox	223
<i>Gene therapy</i>	Metal (gold)	Polymer	RNA	N/A	N/A	Above
<i>Gene therapy</i>	Metal (gold)	Polymer	RNA	N/A	N/A	Above
<i>Gene therapy</i>	Metal (gold)	Polymer	RNA	RGD peptide	N/A	217
<i>Gene therapy</i>	Metal (gold)	Polymer	DNA	Folic acid	N/A	218
<i>Gene therapy</i>	Metal (gold)	Polymer	DNA	N/A	NIR	38
<i>Gene therapy</i>	Metal (gold)	Polymer	RNA	2-deoxyglucose	pH	40
<i>Gene therapy</i>	Metal (gold)	Polymer	RNA	Anisamide	N/A	213
<i>Gene therapy</i>	Metal (gold)	Polymer	RNA	N/A	N/A	214
<i>Gene therapy</i>	Metal (gold)	Polymer	DNA	NLS peptide	NIR, redox	198
<i>Gene therapy</i>	Metal (gold)	Polymer	RNA	N/A	N/A	196
<i>Gene therapy</i>	Metal (gold)	Polymer	RNA	Glucose	N/A	220
<i>Gene therapy</i>	Metal (gold)	Polymer	RNA	N/A	Electrical potential	222
<i>Gene therapy</i>	Metal (gold)	Polymer	DNA	N/A	N/A	199
<i>Gene therapy</i>	Metal (gold)	Dendrimer	DNA	N/A	N/A	164
<i>Gene therapy</i>	Metal (gold)	Dendrimer	RNA	Folic acid	N/A	158
<i>Gene therapy</i>	Metal (gold)	Dendrimer	RNA	N/A	N/A	190

<i>Therapy</i>	<b>Inorganic component</b>	<b>Organic component</b>	<b>Therapeutic compound</b>	<b>Targeting ligand</b>	<b>Stimulus sensitivity</b>	<b>Reference</b>
<i>Gene therapy</i>	Metal (gold)	Dendrimer	RNA	RGD peptide	N/A	161
<i>Gene therapy</i>	Metal (gold)	Dendrimer	DNA	Hyaluronic acid	N/A	165
<i>Gene therapy</i>	Metal (iron oxide)	Polymer	RNA	gh625 peptide	magnetic field	225
<i>Gene therapy</i>	Metal (iron oxide)	Polymer	DNA	N/A	magnetic field	224
<i>Gene therapy</i>	Inorganic compound (CaP)	Polymer	DNA	Stearic acid	N/A	228
<i>Gene therapy</i>	MOF	Polymer	RNA	N/A	N/A	228
<i>Gene therapy</i>	MOF	Membrane (platelet)	RNA	N/A	pH	173
<i>Gene+chemo+phototherapy</i>	Metal (gold)	Lipid	Verteporfin, calcein, RNA	N/A	X-ray	301
<i>Gene+chemo+phototherapy</i>	Metal (gold), MSN	Polymer	AuNRs, DNA, sorafenib	N/A	NIR	200
<i>Gene+chemotherapy</i>	Metal (gold)	Lipid	RNA, PTX	N/A	NIR, temperature	277
<i>Gene+chemotherapy</i>	Metal (gold)	Polymer	AuNR, RNA	RGD peptide	Redox	279
<i>Gene+chemotherapy</i>	Metal (gold)	Polymer	RNA, cisplatin	N/A	N/A	280
<i>Gene+chemotherapy</i>	Metal (gold)	Protein	RNA, DOX	N/A	N/A	281
<i>Gene+chemotherapy</i>	Metal (gold)	DNA	DNA, DOX	AS1411 DNA aptamer	pH	282
<i>Gene+chemotherapy</i>	Metal (gold)	Dendrimer	RNA, gemcitabine	N/A	Ultrasound	283
<i>Gene+chemotherapy</i>	MOF, MSN	Polymer	DNA, DOX, proteins	N/A	pH	205
<i>Gene+chemotherapy</i>	Metal (gold)	Lipid	DNA, DOX	N/A	Magnetic field	276
<i>Gene+phototherapy</i>	Metal (gold)	Nucleic acid	Au nanoshell, RNA	N/A	NIR	284
<i>Gene+phototherapy</i>	Metal (gold)	Nucleic acid	Au nanoflower, siRNA	N/A	NIR	287
<i>Gene+phototherapy</i>	Metal (gold)	Polymer	AuNP, DNA	N/A	NIR	286
<i>Gene+phototherapy</i>	Metal (gold)	Polymer	Au nanoprism, RNA	N/A	NIR	285
<i>Gene+phototherapy</i>	Inorganic compound (CaP)	Polymer	Polydopamine, RNA	N/A	NIR, pH	288
<i>Photodynamic therapy</i>	Metal (gold)	Lipid	Chlorin e6	N/A	pH, NIR	16
<i>Photodynamic therapy</i>	Metal (iron oxide)	Lipid	Photoporphyrin IX	N/A	NIR	266
<i>Photodynamic therapy</i>	MOF	DNA	MOF	N/A	NIR	267
<i>Photodynamic therapy</i>	Metal (titanium oxide), MSN	Polymer	Chlorin e6	N/A	NIR	271
<i>Photodynamic therapy</i>	Inorganic compound (W18O49)	Membrane (platelet)	Metformin, W18O49	N/A	NIR	268

<i>Therapy</i>	<b>Inorganic component</b>	<b>Organic component</b>	<b>Therapeutic compound</b>	<b>Targeting ligand</b>	<b>Stimulus sensitivity</b>	<b>Reference</b>
<i>Photothermal therapy</i>	Metal (gold)	Lipid	AuNPs	N/A	NIR	261
<i>Photothermal therapy</i>	Metal (gold)	Lipid	AuNPs	Cy5 marked molecular beacon	NIR	262
<i>Photothermal therapy</i>	Metal (gold)	Lipid	AuNPs	N/A	NIR	263
<i>Photothermal therapy</i>	Metal (lanthanides)	Polymer	Polyaniline	N/A	NIR	265
<i>Photothermal therapy</i>	Metal (gold)	Polymer	AuNRs, polyaniline	N/A	NIR	13
<i>Photothermal therapy</i>	Metal (gold)	Membrane (leukocyte)	Janus AuNP	N/A	NIR	264
<i>Photothermal therapy</i>	Inorganic compound (phosphorus)	Membrane (RBC)	Black phosphorus nanoparticle	N/A	NIR	178

**Table 2:**

Hybrid nanosystems for non-cancer applications.

<i>Category</i>	<b>Application</b>	<b>Inorganic component</b>	<b>Organic component</b>	<b>Active compound</b>	<b>Reference</b>
<i>Antimicrobial</i>	Antibacterial	Metal (AgNPs)	Carbon	AgNPs	409
<i>Antimicrobial</i>	Antibiotic	Metal (AgNPs)	Carbon	Tobramycin	366
<i>Antimicrobial</i>	Antibacterial	Metal (AgNPs)	Carbon	AgNPs	410
<i>Antimicrobial</i>	Antibiotic deactivation	Inorganic compound (TiO <sub>2</sub> )	Carbon	TiO <sub>2</sub>	411
<i>Antimicrobial</i>	Antibacterial	Metal (AgNPs), MOF	Carbon	AgNPs	58
<i>Antimicrobial</i>	Antifungal	Metal (IONPs)	Carbon	Benzamide	254
<i>Antimicrobial</i>	Antimicrobial, wound healing	Metal (AgNPs)	Polymer	Chlorhexidine	412
<i>Antimicrobial</i>	Antibacterial	Metal (AgNPs)	Polymer	AgNPs	306
<i>Antimicrobial</i>	Antibacterial	Metal (AgNPs), inorganic compound (ZnO)	Polymer	AgNPs, ZnO	362
<i>Antimicrobial</i>	Antibacterial	Metal (AgNPs)	Polymer	AgNPs	413
<i>Antimicrobial</i>	Antibiotic	Metal (AgNPs), silica	Polymer	Ciprofloxacin	367
<i>Antimicrobial</i>	Antibacterial	Metal (AgNPs)	Polymer	Antibacterial peptides	369
<i>Antimicrobial</i>	Antibacterial	Metal (AgNPs)	Polymer	AgNPs	414
<i>Antimicrobial</i>	Antibacterial	Metal (CuNPs)	Polymer	CuNPs	375
<i>Antimicrobial</i>	Antibacterial	Inorganic compound (cerium oxide)	Polymer	Cerium oxide	377
<i>Antimicrobial</i>	Antibacterial	Metal (AuNCs)	Polymer	Antibacterial peptides, daptomycin	374
<i>Antimicrobial</i>	Antibacterial	Metal (AgNPs, ZnO)	Polymer	AgNPs	415
<i>Antimicrobial</i>	Antibacterial	Metal (AgNPs)	Polymer	AgNPs	416
<i>Antimicrobial</i>	Antibacterial	Metal (AgNPs, CuNPs)	Polymer	Polydopamine, AgNPs	59
<i>Antimicrobial</i>	Antibacterial, larvicidal	Metal (ZnO, CuO)	Polymer	ZnO, CuO	376
<i>Antimicrobial</i>	Antibiotic	Metal (AuNPs)	Polymer	Gentamicin	370
<i>Antimicrobial</i>	Antibacterial	Metal (AgNPs)	Polymer	AgNPs	417
<i>Antimicrobial</i>	Antibacterial	Metal, inorganic compound (AgNPs, MnO <sub>2</sub> )	Polymer	AgNPs, MnO <sub>2</sub>	418
<i>Antimicrobial</i>	Antibacterial	Metal (AgNPs), inorganic compound (hydroxyapatite)	Polymer	AgNPs	419
<i>Antimicrobial</i>	Antibacterial	Silica, inorganic compound (ZnO)	Polymer	ZnO	378
<i>Antimicrobial</i>	Antibacterial, antifungal	Metal (CuNPs, FeNPs)	Polymer	CuNPs	420
<i>Antimicrobial</i>	antibacterial	Silica	Polymer	Chlorhexidine	421
<i>Antimicrobial</i>	Antibacterial	Metal (AgNPs)	Protein	AgNPs	368
<i>Antimicrobial</i>	Antibiotic	Metal (AuNCs)	Protein	Ampicillin	373

<b>Category</b>	<b>Application</b>	<b>Inorganic component</b>	<b>Organic component</b>	<b>Active compound</b>	<b>Reference</b>
<i>Antimicrobial</i>	Antibacterial	Metal (AuNPs)	Protein	Rose bengal	371
<i>Antimicrobial</i>	Antibacterial, antitoxin	Metal (Au nanowire)	Membrane (RBC)	Membrane	372
<i>Detection and Imaging</i>	Antibiotic detection	Metal (AgNPs)	Carbon	AgNPs, Cu	405
<i>Detection and Imaging</i>	Antibiotic detection	Metal (AuNPs, CuS)	Carbon	CuS	403
<i>Detection and Imaging</i>	Antibiotic detection	Metal (CuNPs)	Carbon	Cu, MWCNTs	406
<i>Detection and Imaging</i>	MRI contrast, RNA detection	Metal (IONPs)	Dendrimer, polymer	Alexa Fluor 488	160
<i>Detection and Imaging</i>	Cancer detection	Metal (AuNPs), silica	DNA	AuNPs, DNA	422
<i>Detection and Imaging</i>	Bursal disease virus detection	Metal (AuNPs), quantum dots	DNA	Rhodamine	396
<i>Detection and Imaging</i>	HPV detection	Inorganic compound (glass NPs), quantum dots	DNA	Glass NPs, quantum dots, DNA	407
<i>Detection and Imaging</i>	Influenza A detection	Metal (AuNPs)	DNA	AuNPs	32
<i>Detection and Imaging</i>	Photoacoustic tomography	Metal (AuNRs)	Lipid	Indocyanine green	393
<i>Detection and Imaging</i>	Biological autoluminescence enhancement	Metal (AuNPs)	Lipid	AuNPs	394
<i>Detection and Imaging</i>	Glucose monitoring	Metal (AuNPs)	Lipid	Fluorophore	395
<i>Detection and Imaging</i>	Cancer detection	Metal (AuNCs)	Lipid	AuNCs	31
<i>Detection and Imaging</i>	Analysis of cellular functions	Metal (IONPs)	Lipid	IONPs	397
<i>Detection and Imaging</i>	MRI contrast	Metal (gadolinium)	Polymer	Gadolinium	389
<i>Detection and Imaging</i>	Biosensor	Silica	Polymer	Spiropyran	408
<i>Detection and Imaging</i>	MRI contrast	Metal (IONPs)	Polymer	IONPs	390
<i>Detection and Imaging</i>	Antibiotic detection	Metal (AuNPs), quantum dots	Polymer	AuNPs, graphene quantum dots	402
<i>Detection and Imaging</i>	MRI contrast	Metal (IONPs), inorganic compound (manganese oxide)	Surfactant	IONPs, manganese oxide	391
<i>Detection and Imaging</i>	Cancer imaging	Inorganic compound (upconversion nanoparticle)	Membrane (RBC)	Upconversion NP	176
<i>Drug Delivery</i>	Radical scavenging	Metal (IONPs)	Lipid	Curcumin	236
<i>Drug Delivery</i>	Enzyme delivery	MOF	Membrane (RBC, mesenchymal stem cell)	Uricase	252
<i>Gene Delivery</i>	Osseointegration of dental implants	Metal (AuNPs)	Polymer	pDNA	221
<i>Vaccine</i>	General vaccine	MOF	DNA	Ovalbumin	423

<i>Category</i>	<b>Application</b>	<b>Inorganic component</b>	<b>Organic component</b>	<b>Active compound</b>	<b>Reference</b>
<i>Vaccine</i>	General vaccine	MOF	DNA	Ovalbumin	387
<i>Vaccine</i>	General vaccine	Metal (IONPs)	Lipid	Ovalbumin	424
<i>Vaccine</i>	Japanese encephalitis	Silica	Polymer	Japanese encephalitis antigen	385
<i>Vaccine</i>	General vaccine	Silica	Polymer	Bovine serum albumin	386
<i>Vaccine</i>	<i>Burkholderia mallei</i>	Metal (AuNPs)	Polymer	<i>Burkholderia mallei</i> protein	383
<i>Vaccine</i>	General vaccine	Metal (IONPs)	Polymer	pDNA	384
<i>Vaccine</i>	General vaccine	Inorganic compound (Copper sulfate)	Protein	Ovalbumin	425
<i>Vaccine</i>	Dengue virus	Inorganic compound (CaP)	Protein	Dengue virus protein	426
<i>Vaccine</i>	Dengue virus	Metal (AuNPs)	Protein	Dengue virus protein	382

**Table 3:**

## Theranostic hybrid nanosystems

Application	Inorganic material	Organic material	Gene therapy	Drug therapy	Phototherapy	Imaging	Targeting	Stimulus responsivity	Source
<i><math>\alpha v\beta 3</math> integrin-expressing cancers</i>	Aunanostars	PAMAM	siRNA	N/A	PTT	CT imaging	RGD peptides	NIR	436
<i>Adenocarcinoma</i>	IONPs	Liposome	N/A	PTX	N/A	MRI	H <sub>7</sub> K(R <sub>2</sub> ) <sub>2</sub> , Magnetic targeting	pH, magnetic field	434
<i>Adenocarcinoma</i>	C60@Au	PEG	N/A	DOX	PDT, RTT	X-ray imaging	N/A	pH, radio waves	447
<i>Breast cancer</i>	AuNRs	DNA origami	N/A	N/A	PTT	Optoacoustic imaging	N/A	N/A	450
<i>Breast cancer</i>	GQDs	Polydopamine	N/A	CpG oligonucleotides	PDT/PTT	MRI, fluorescence imaging	N/A	Magnetic field, NIR	108
<i>Breast cancer</i>	IONPs	C60, PEG	N/A	N/A	PDT, RTT	MRI	Folic acid, magnetic field	Radio waves, NIR, magnetic field	448
<i>Breast cancer</i>	MSNs, CN, GQDs	CN, PEG	N/A	N/A	PDT/PTT	Ultrasound, fluorescence imaging, infrared thermal imaging	RGD peptides	Ultrasound, NIR	446
<i>Breast cancer</i>	Gadolinium NPs, GO	GO, PEG	N/A	DOX	PTT	MRI	Folic acid	Magnetic field, NIR	107
<i>Breast cancer</i>	IONPs, C60	DPPC (phospholipid)	N/A	DTX	PTT	MRI	Folate, magnetic field	Radio waves, magnetic field, temperature	110
<i>Breast cancer</i>	Hollow mesoporous copper sulfide	fPEDC copolymer	N/A	Maytansinoid	PTT	Photoacoustic, fluorescence imaging	RGD peptides	NIR	454
<i>Breast cancer</i>	Pd@ZIF-8	Polydopamine	N/A	DOX	PTT	Photoacoustic imaging	N/A	pH, NIR	84
<i>Breast cancer</i>	AuNS	Liposome	N/A	DTX	PTT	Ultrasound imaging	N/A	NIR, temperature	429
<i>Breast cancer</i>	IONPs	Membrane (RBC)	N/A	N/A	PTT	MRI	N/A	NIR, magnetic field	180
<i>Breast cancer</i>	IONPs	Membrane (RBC)	N/A	N/A	PTT	MRI	Magnetic targeting	Magnetic field	177
<i>Cervical cancer</i>	Au@Cu <sub>2</sub> O, QDs	Polyallylamine	N/A	N/A	PDT/PTT	MRI, photoacoustic imaging	N/A	NIR	449
<i>EGFR-expressing tumors</i>	AuNRs, IONPs	Liposome	N/A	DOX	PDT/PTT	MRI	Cetuximab (Anti-EGFR antibody), magnetic targeting	NIR, magnetic field	431



<i>Application</i>	<b>Inorganic material</b>	<b>Organic material</b>	<b>Gene therapy</b>	<b>Drug therapy</b>	<b>Phototherapy</b>	<b>Imaging</b>	<b>Targeting</b>	<b>Stimulus responsivity</b>	<b>Source</b>
<i>EGFR-expressing tumors</i>	AuNCs	BSA	N/A	Erlotinib	PTT	Optoacoustic, fluorescence imaging	N/A	pH, NIR	444
<i>Folate receptor-expressing cancers</i>	AuNPs, QDs	Liposome	N/A	DOX	PDT/PTT	Contrast and fluorescent imaging	Folic acid	NIR	427
<i>Folate receptor-expressing cancers</i>	AuNRs	Liposome	N/A	DOX	PDT	Ultrasound, CT imaging	Folic acid	NIR, ultrasound	428
<i>Glioblastoma</i>	AuNRs	PLGA	N/A	N/A	PTT	Photoacoustic imaging	N/A	NIR	451
<i>Glioma</i>	IONPs, QDs	Liposome	N/A	Cilengitide	N/A	MRI, fluorescence imaging	Magnetic targeting	Magnetic field, NIR	433
<i>Glioma</i>	AuNRs, mesoporous silica, QDs	PGMA	pDNA	DOX	PTT	Photoacoustic, X-ray CT, fluorescence imaging	N/A	NIR, X-ray	439
<i>Glioma</i>	MSNs	PEG-perylene diimide	N/A	SN38	PTT	Photoacoustic, fluorescence imaging, PET imaging	N/A	NIR	440
<i>Hepatocellular carcinoma</i>	IONPs	Liposome	N/A	anetholedithiolethione	N/A	MRI, ultrasound imaging	Magnetic targeting	Magnetic field	435
<i>Lymphoma</i>	IONPs	Liposome	N/A	Rituximab	N/A	MRI	Rituximab (Anti-CD20 antibodies), magnetic targeting	Magnetic field	432
<i>Melanoma, cervical cancer</i>	Ag/AuNPs	PEI	pDNA	N/A	N/A	Fluorescence imaging	N/A	NIR	437
<i>Pancreatic carcinoma</i>	AuNPs, mesoporous silica	BSA	N/A	Gemcitabine, DOX	N/A	Fluorescence imaging	N/A	Photo	443
<i>Prostate cancer</i>	Bi2S3	PLGA	N/A	N/A	RTT	Ultrasound, X-ray imaging	N/A	Ultrasound, X-ray	442
<i>Prostate cancer</i>	IONPs	Membrane (MSC)	siRNA	N/A	PTT	MRI	Magnetic targeting	Magnetic field, NIR	179

**Table 4:**Active clinical trials involving hybrid nanosystems (from [ClinicalTrials.gov](https://ClinicalTrials.gov), accessed Aug. 2020).

<i>Title</i>	<b>Phase</b>	<b>Status</b>	<b>Conditions</b>	<b>Interventions</b>	<b>Inorganic material</b>	<b>Organic material</b>	<b>Locations</b>
<i>Evaluating AGuIX-<math>\gamma</math>E Nanoparticles in Combination With Stereotactic Radiation for Brain Metastases</i>	Phase 2	Recruiting	Brain Metastases	Drug: AGuIX	Gadolinium	Polysiloxane	Centre Léon Bérard, Lyon, France; Centre Antoine Lacassagne, Nice, France
<i>AGuIX Gadolinium-based Nanoparticles in Combination With Chemoradiation and Brachytherapy</i>	Phase 1	Recruiting	Gynecologic Cancer	Drug: Polysiloxane Gd-Chelates based nanoparticles (AGuIX) Radiation: External beam radiotherapy (EBRT) Radiation: Uterovaginal brachytherapy Drug: Chemotherapy (cisplatin)	Gadolinium	Polysiloxane	Gustave Roussy, Villejuif, Val De Marne, France
<i>Enhanced Epidermal Antigen Specific Immunotherapy Trial -1</i>	Phase 1	Active, not recruiting	Type 1 Diabetes	Drug: C19-A3 GNP	AuNP	Peptide	Cardiff and Vale University Health Board, Cardiff, United Kingdom
<i>Radiosensitization of Multiple Brain Metastases Using AGuIX Gadolinium Based Nanoparticles</i>	Phase 1	Completed	Brain Metastases	Drug: AGuIX Radiation: whole brain radiation therapy	Gadolinium	Polysiloxane	University Hospital Grenoble, Grenoble, France
<i>Targeted Silica Nanoparticles for Real-Time Image-Guided Intraoperative Mapping of Nodal Metastases</i>	Phase 1, Phase 2	Recruiting	Head and Neck Melanoma Breast Cancer Colorectal Cancer	Drug: fluorescent cRGDY-PEG-Cy5.5-C dots	MSN	Peptide	Memorial Sloan Kettering Cancer Center, New York, New York, United States Weill Cornell Medical Center, New York, New York, United States
<i>Radiotherapy of Multiple Brain Metastases Using AGuIX®</i>	Phase 2	Recruiting	Brain Metastases, Adult Radiotherapy	Drug: AGuIX® Radiation: Whole Brain Radiation Therapy	Gadolinium	Polysiloxane	Centre hospitalier universitaire Grenoble-Alpes